
**Addis Ababa University**

**Addis Ababa Institute of Technology**

**School of Civil & Environmental Engineering**

**Master's program Hydraulic Engineering**

# Assessment of Flow/Discharge Variability Effects on Bridges and Culverts along the Holeta to Ambo Road, West Shewa Zone, Oromia Region

**By**

**Selamawit Banjaw**

**GSR/5337/12**

**Advisor: Dr. Asie Kemal**

***Addis Ababa, Ethiopia***
***April, 2024***

APPROVAL PAGE

The undersigned have examined the thesis entitled "Assessment of Flow/Discharge Variability Effect on Bridges and Culverts along the Holeta to Ambo Road, West Shewa Zone, Oromia Region" presented by Selamawit Banjaw (GSR/5737/12), submitted to Addis Ababa Institute of Technology, School of Graduate Studies in partial fulfilment of the requirement of the award of Degree of Masters of Science in civil and Environmental Engineering school.

Submitted by:

| | | |
|---|---|---|
| Selamawit Banjaw | | 22/4/24 |
| Student | Signature | Date |

Approved by:

| | | |
|---|---|---|
| Dr. Asie Kemal | Per/Daneal PLS | 22/4/24 |
| Advisor | Signature | Date |
| Dr. Geremew Sahilu | | 22/4/2024 |
| Internal Examiner | Signature | Date |
| Dr. Daneal Fikresilase | Daneal PLS | 22/4/24 |
| External Examiner | Signature | Date |
| Dr. Abrham Gebre | Abrham Gebre (Dr.) Dean, School of Civil & Environmental Engineering | |
| Chairperson | Signature | Date |



i

DECLARATION

This is to declare that the work I have presented in this thesis entitled "Assessment of Flow/Discharge Variability Effect on Bridges and Culverts along the Holeta to Ambo Road, West Shewa Zone, Oromia Region" is the original work of my own, has not been submitted to owe a degree from another university, and all the sources' data and materials used for this thesis have been properly acknowledged.

22/04/24

Selamawit Banjaw

GSR/5337/12

Selamb691@gmail.com

+251-913018853

Date



ii

ACKNOWLEDGEMENT

I commence by expressing my sincere gratitude to God, whose grace and direction have served as my research journey's core of support and inspiration. I am deeply grateful for the given wisdom and perseverance that sustained me.

I offer my gratitude to my advisor, Dr. Asie Kemal, for his outstanding mentorship and advice, which have imparted knowledge and insight that have been important in my research endeavour. I also acknowledge the enriching contributions of Dr. Belete Birhanu Kidanewold, whose collaborative efforts have significantly enhanced this work, driven by a shared helpful knowledge and guidance to accomplish this research study. My heartfelt appreciation extends to my family, particularly to my husband, Dr. Lelisa Fikadu, for his unwavering support.

Special thanks are due to all organizations for their support and collaboration, essential to the success of this research endeavour. Lastly, I express gratitude for the friendships and company of colleagues especially Mr. Ashenafi Chala who have shared in the challenges and joys of academic pursuit, exemplifying the interconnectedness of our academic community.

This research journey highlights the importance of family, mentorship and teamwork. The wonderful and human components that have enabled this endeavor make me feel humbled and appreciative.

# TABLE OF CONTENTS

# LIST OF TABLES

# LIST OF FIGURES

# LIST OF ACRONYMS AND ABBREVIATIONS

| | |
|---|---|
| BMS | Bridge Management System |
| **CN** | SCS-runoff curve number |
| **DC** | Design Criteria |
| **DEM** | Digital Elevation Model |
| **ERA** | Ethiopia Road Authority |
| GEV | Gumbel Extreme Value Method |
| **GIS** | Geographical Information System |
| **GPS** | Global Positioning System |
| **HEC** | Hydrologic Engineering Centre |
| **HMS** | Hydrologic Modelling System |
| HSG | Hydrologic Soil Group |
| IDF | Intensity-Duration-Frequency |
| NMAoE | National Metrology Agency of Ethiopia |
| NSE | Nash-Sutcliffe Efficiency |
| PBIAS | Percent Bias |
| **RC** | Reinforced Concrete |
| RMSE | Root mean square error |
| $R^2$ | Coefficients of determination |
| **SCS** | Soil Conservation Service |

# ABSTRACT

This study assessed the effect of variable flow on bridges and culverts along Holeta Ambo Road, West Shewa Zone, Oromia Regional State. In this study, the HEC-HMS hydrological model is used for analysing the flow variability. The simulation uses meteorological gauge stations over a period of thirty-year (1991-2020) for the catchment, which is sourced from Ethiopian metrology agency. The model was calibrated and validated using observed discharge data from three-gauge stations—Berga Nr. Addis Alem, Awash Bello (031020), and Debis Nr. Guder—that was collected by the Ministry of Water and Energy, Addis Ababa.

This study uses a calibrated HEC-HMS model to simulate daily flow in 56 drainage structures (bridges and culverts), over a period of 30-years (1991–2020). A coefficient of variance more than 40% is used as the threshold for variable flow. As a result, more than 71% of the structures exhibit a coefficient of variance of more than 40%.

The study also develops design rainfall and rainfall intensity–duration frequency using Gen. Extreme Value (GEV). The design rainfall is used as an input in flood frequency modelling in HEC-HMS to estimate the peak discharge. The estimated peak flow is compared with the discharge capacity calculated using Manning's formula, and the result showed that nearly 38% of drainage structure is prone to flooding.

The effect of sedimentation on culvert structure is assessed through comparing the estimated peak flow and discharge capacity before and after sedimentation, and around 13% of the culverts are affected by sedimentation. The scouring effect of structure is computed by comparing the permissible velocity with the velocity calculated using Manning's formula. Consequently, 25% of the structures, particularly the bridges, are affected by scouring.

This study reveals the impact of variable flow on drainage structures along the Holeta to Ambo Road, which is prone to flooding, sedimentation, and scouring. It is essential to replace the existing structures with those designed to manage variable flow, improve routine culvert maintenance and prioritizing the replacement of aging structures. These measures ensure the long-term safety, durability and functionality of the road network and structures. Additionally, this study provides the opening size and structure type of the selected drainage structures are used for other study.

**Key words**: Flow variability effect, Drainage structures, flooding, scouring, sedimentation

# 1 INTRODUCTION

## 1.1 Background

Roads and highways are essential for the growth and development of any country. They link various regions, and facilitate the movement of populations, services and goods, promotes economic growth, and strengthen social cohesion.(1) The importance of well-constructed highways cannot be overstated, they are an integral part of the overall infrastructure, ensuring access and movement for both urban and rural communities.(2) Ethiopia is one of the sub-Saharan African countries that place a high priority on enhancing its road infrastructure and system.(1)

Roads and highways are the backbone of a country's transportation system. Like other countries, Ethiopia recognizes the importance of transport system in promoting socioeconomic growth and development and social welfare.(3) A well-maintained and efficiently constructed road network provides numerous benefits. Firstly, it improves the connectivity, which enable access to markets-agricultural products, education, health service, and other essential services for urban and rural population. This results in improved livelihoods and equity in accessing essential services. Secondly, such infrastructures are crucial for transporting goods (i.e., sesame, coffee, and maize), fostering trade, supporting industrial and agricultural activities. Hence economic productivity and growth depends heavily on the road infrastructure. Furthermore, a good road infrastructure attracts investments and enhances tourism by enabling access to diverse cultural and natural attractions places in the country.(4) Moreover, highways contribute to a country's resilience and rapid response to disaster and emergency outbreaks.

Hence, the construction, expansion and maintenance of roads and highways are key priorities of the developmental agenda of Ethiopia. The Holeta to Ambo Road is one of Ethiopia's main highway sections. In particular, this segment is approximately 81 kilometers long and serves as trunk route connecting Addis Ababa, the capital city of the country to the western Oromia region major cities (e.g., Nekemte, Gimbi) and Benshangul Gumuz region (e.g., Assossa). The road plays a major role in linking agricultural, industrial and urban hubs, there by contributing to the economic activities of the region. The construction of the Holeta to Ambo Road was undertaken by the Ethiopian Roads Administration (ERA). The ERA has a major role in improving the connectivity and quality of roads. It is mandated for the planning, designing and executing road infrastructure projects in collaboration with key stakeholders in Ethiopia.

Holeta town is located around 35 kilometres west of Addis Ababa, in Oromia Region, Ethiopia. The economy of the town is mostly dependent on agriculture, like most of the towns in Ethiopia, although the industry sector is growing. For instance, Habesha Cement is constructing a new cement plant in the city. (5) The Ethiopian Institute of Agricultural Research has established a research station in the town since 1963. The national centre for agricultural research aimed at increasing the productivity of dairy products, potatoes, barley, and highland oil crops. (6) Furthermore, Holeta town is recognized as the location of one of the Military Academies in the Country.(7) Adjacent to the Holeta to Ambo road lies Ginchi administrative centre of Dendi woreda.(7) Mount Dendi, which rises it a height of 3,260 meters, is the highest point in the area and borders Wonchi woreda. Among the remarkable natural features is the 2,400-hectare Chilimo forest, located close to Ginchi.(8) Onward from Holeta, Ambo is the capital city of West Shewa zone and it is 114km far from Addis Ababa (9) and demarcates the end of the road for the study. Similar to other areas, the town is mainly dependent on agriculture for livelihood. Ambo is easily accessible and may attract tourists due to its serene Lake Ambo its attractive environs. Ambo Sparkling Water is a well-known local product that is highly regarded for its quality and supports the town's economy.(10) Nearby attractions include Mount Wenchi to the south with its crater lake, and the Guder and Huluka Falls. Furthermore, the existence of Ambo University and a hydroelectric power station along the Awash River significantly enhances the town's infrastructure and educational values.(7)

In the Holeta to Ambo Road there are about 31 bridges and 117 culverts. The proper design of the road drainage system is one of the main interventions in road construction. A well-built drainage system, with the potential of surface water collection, sloping surfaces, inlets or catch basins along the road, underground pipes and outlet structures, effectively manage the flow of water from the surface of the road and prevent flooding, and damage to the road infrastructure. However, “Any drainage installation is sized according to the possibility that an expected peak discharge will occur within the design life of the installation. This is, of course, linked to the intensity and duration of the events of rainfall occurring not only in the immediate proximity of the system, but also upstream of the structure. In the design phase, the probability of occurrence peak flows exceeding the design capability of a potential stream crossing facility should be calculated and used”.(11)

The Holeta to Ambo Road drainage structures are facing problems with the drainage systems due to their aging construction, and necessity of regular maintenance overtime. As a result, the

performance of the road is declining due to different factors, from those factors variability of flow is the one which pattern leading to structural failures.

Variable flow is the variation of flow on stream and river that occur in different time period. In the context of Holeta to Ambo Road, the variable flow is influenced by storms, natural flow patterns in the water bodies that intersect the road, and seasonal changes. During the rainy season the water levels of the rivers and streams along this road encounter a dramatic surge in water levels, increasing flow rates and potentially result in flooding. During the dry season, in contrary, the level of the water will drop, which results in decreased flow rate. Storm-related phenomena, including intense rainfall or floods, can cause sudden changes in flow that pose challenges to the stability and integrity of the road infrastructure.

The Holeta to Ambo Road bridge and culvert design, maintenance, and management face major difficulties due to the dynamic nature of variable flow. The variability in water levels and flow rates exerts hydrodynamic forces on the bridge and culvert structures, which may result in scouring around bridge abutment and culvert openings. This scouring may compromise the structural integrity and stability of the infrastructure, necessity of a design that takes the fluctuation in flow conditions into account. In addition, the variable flow may have an effect on the drainage system of the roads, requiring effective culvert design to control excess water and prevent waterlogging during high flow periods.

## 1.2 Statement of the problem

Bridges and culverts are very essential for the safety and operation of the road. However, they encounter significant challenges, this study particularly focusses on when subjected to variable flow conditions, which can compromise their structural stability and functionality. These challenges include increased risk of scouring the foundation material, erosion of river bed and bank, and cracking for the structure, among others, resulting in potential safety hazards and costly maintenance requirements. A pertinent case study is the Holeta to Ambo Road, where the effect of variable flow on bridges and culverts is notably observed. Here, specific drainage issues such as cracking and scouring have been observed, highlighting the urgent need for comprehensive research to understand the precise effects of variable flow on these infrastructures. By investigating the observed problems in the context of variable flow dynamics, this research aims to provide how many of drainage structures (bridge and culvert) are affected by this variable flow due to flooding, scouring and sedimentation along the Holeta

to Ambo Road, ultimately contributing to safer and more sustainable transportation infrastructure.

## 1.3 Relevance of the study

The effects of variable flow on culverts and bridges along the Holeta to Ambo Road need to be thoroughly investigated because of the potential implication for sedimentation, scouring, and flooding. For safe and uninterrupted transit, it is imperative to comprehend these dynamics. Ensuring the structural integrity of infrastructure over the long-term requires careful consideration of variable flow. Carefully examining this research gap, more durable roads can be built, benefiting neighboring communities and facilitating the development of greater transportation infrastructure in flood-prone areas. The purpose of this study is to evaluate flow variability and its effects on drainage structure (culvert and bridge) along the Holeta to Ambo road.

## 1.4 Scope of the study

The study road stretches around 81 kilometers from the starting point of Holeta town to the road's final endpoint, Ambo town. The purpose of the project is to look into how flow variability affects the risks of floods, sedimentation, and scouring at the drainage structure (culvert and bridge) along the Holeta to Ambo Road. This study's scope is restricted to the following: creating an IDF curve to estimate design rainfall as a means of estimating peak flows in HEC-HMS; The method used for assessing the risk of flooding will be evaluated by comparing estimated peak flow with the drainage capacity of the structure The sedimentation assessed by comparing the estimated peak flow with the drainage capacity before and after sedimented and lastly scouring will be assessed by analysed flow velocity and compared with the permissible velocity limit. The rainfall-runoff model for the chosen section (Holeta to Ambo Road) will be used to investigate flow variability.

## 1.5 Research question

The basic questions that will be answered by this research are:

- What is the major effect of variable flow/discharge on the performance of cross drainage structure (bridge and culverts) on Holeta to Ambo road?
- Are the selected existing structures (bridges and culverts) can accommodate the flow variability?

- How many of structure is affected by flooding, sedimentation and scouring due to variable flow along Holeta to Ambo road?

## 1.6 Objectives

### 1.6.1 General objectives

- The objective of this study is to assess the effect of variable flow /discharge on drainage structures (i.e. Bridges and Culverts) along Holeta to Ambo Road segment, Oromia Region, Ethiopia and to identify the crossing structure which need rehablitation.

### 1.6.2 Specific objectives

- To explore the effect of variable flow on the drainage structures (culvert and bridge).
- To calibrate and validate the models using stream flow data, and consequently utilize them to assess the impacts of variable flow on flooding, sedimentation and scouring.
- To use hydrological model to simulate various flow scenarios, predict potential flooding, sedimentation and scouring events.
- To determine the specific flow properties—discharge rates and velocities that cause flooding, sedimentation and scouring along the Holeta to Ambo Road.

## 1.7 Thesis structure

This thesis is structured in five chapters. In chapter one, a brief background description of the project, statement of the problem, objectives including the scope and significance of the study is provided. In chapter two, pertinent literature related to the study were presented. Chapter three describes the methodology employed in the study, particularly focus on the description of the project area, and data needs and sources for the thesis. In chapter four data analysis and results of the analysis were summarized and presented. Chapters five deals with the conclusion and recommendation through summarizing the major findings and implication of the study.

# 2 LITERATURE REVIEW

## 2.1 Introduction

The transportation system, such as highways, roads ensure the movement of people and goods, which plays a major role in the economic development of a country.(12) Bridges and culverts manage water flow and ensures the operation and safety of the roads.(13, 14, 15)

This literature review provides a critical evaluation of existing evidence, including strengths, challenges, and gaps in the existing research with emphasis on the effect of variable flow on bridge and culvert structures.

## 2.2 Highway Drainage Structures

Drainage structures are an essential component of a highway design. The design of drainage structure should be at reasonable cost and provide an adequate level of service.(16) Bridges and culverts are two examples of highway drainage structures and needs to be designed to withstand various hydraulic conditions and ensures the safe passage of water across highways.

Bridges span water bodies such as rivers and streams, while culverts allow water to flow beneath road embankments. These structures are essential component of transportation infrastructure, which ensure the reliability and safety of road networks, especially in areas prone to variable flow conditions.(17, 18). This study mainly focuses on the two types of highway drainage structures.

### Culvert and Bridge

1) Culvert

Culvert is a main component of the transportation system that maintain water flow, prevent flooding, and ensuring the integrity of the road.[19] Depending on the specific need, culvert are made up of steel, concrete, or plastic with various shapes and sizes as shown in the figure below.(19, 20)

Reinforced concrete pipe culvert

Corrugated steel pipe culvert

Box culvert

Slab culvert

Figure 2-1 Picture showing different type of culvert structures

2) Bridge

A bridge is a physical structure that allows passage over a road, river, railroad, or other body of water. Bridges are essential components of transportation infrastructure, allowing vehicles, pedestrians, and occasionally even utilities like power cables or pipelines to pass obstacles that would otherwise impede travel. (19, 20)

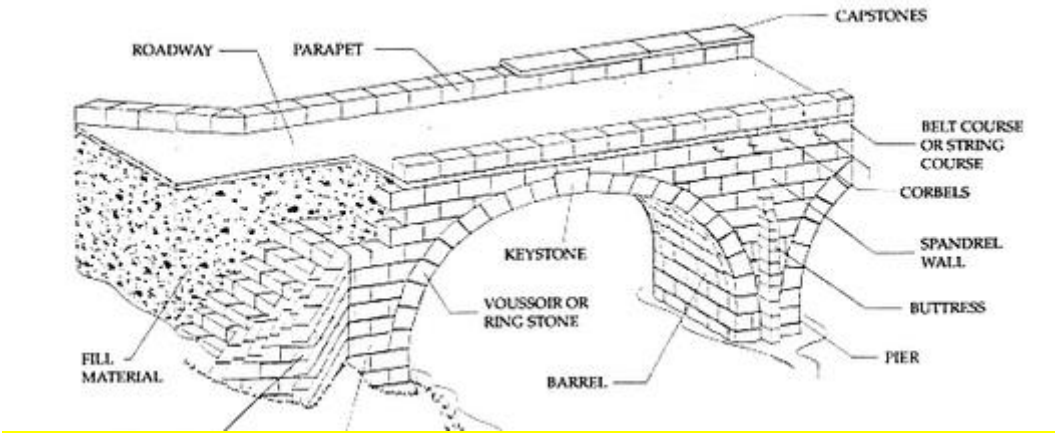


**Figure 2-2 Masonry arch bridge**

## 2.3 Review of Existing literatures

### 2.3.1 Principle of fluid mechanics or open channel flow

The fundamental principles of fluid mechanics form the cornerstone of understanding the behaviour of fluids in motion, particularly open channel flow. The flow of fluids in channels with a free surface exposed to the atmosphere is described by open channel flow. This type of flow is common in both naturally occurring water systems like rivers and streams and engineered systems like storm water drainage systems and irrigation canals. One of the fundamental principles controlling open channel flow is the conservation of mass, which stipulates that the mass flow rate into and out of a control volume must remain constant throughout time to ensure the continuation of fluid motion. This principle is important to understand the behaviour of water flow through channels in relation to the effect of flow depth, velocity distribution, and sediment transport. The concept of conservation of momentum, which is essential to open channel flow, states that unless an external force acts upon a closed system, its overall momentum stays constant. External forces like pressure gradients and gravitational pull cause changes in momentum, which in turn affect the motion of fluid particles and, in the end, shape the behaviour of flowing fluids in open channels. Energy conservation is a fundamental principle that also governs open channel flow. According to this principle, the total energy of the fluid remains constant along a streamline, neglecting losses due to dissipative processes like friction. Improved understanding and prediction of flow behaviour in open channel systems through the application of these basic concepts will facilitate the design of hydraulic structures that are both stable and efficient (21, 22).

Furthermore, a number of factors, such as channel geometry, flow depth, flow rate, and boundary roughness, affect how open channel flow behaves. Channel geometry, including shape and size of a channel, have an impact on flow characteristics like velocity distribution and flow resistance. The flow depth, which determines the flow velocity and pressure distribution, have an effect on the overall behaviour of the flow. The flow rate—the volume of water that passes through the channel per unit time affects sediment transport and flow velocity—which in turn impacts channel stability. Furthermore, flow resistance and turbulence are affected by boundary roughness (roughness of the channel bed and walls), which is eventually impact the flow velocity distribution and energy losses. Understanding these fundamental principles and factors is essential for engineers to properly build and operate open

channel systems effectively, ensuring the reliable operation of hydraulic structures and eliminate any potential flow-related concerns (21, 22).

### 2.3.2 Impact of flooding on drainage structures

Flooding poses a major risk to the structural integrity of bridge and culvert, particularly during periods of high-water flow. Elevated water levels apply hydrodynamic pressures on these structures, which may result in structural failure and damage.(23) A review of bridge failure from ten studies highlights the reasons behind bridge failures and emphasizes the necessity to of assessing flood risks and implementing resilient design measures to prevent potential damage and financial effect.(23) In addition, a review conducted by Brook L et al. (2020) and Weldegebriel B et al. (2017) on flooding in Ethiopia emphasize the need for context-specific policy approaches to address the unique challenges posed by flooding in the country. (24, 25)

According to a study by Habeeb S et al. (2022) that focuses on assessing flood risk and flow variability at drainage structures along the Ethio-Djibouti Railway Line in Ethiopia revealed that the flow variability at drainage structures has a major effect on flooding and scouring, as evidenced by high coefficients of variance at selected junction points. A comparison of the designed and simulated peak flows showed that 46% of the drainage infrastructures are susceptible to flooding once every 100 years. The study also emphasized the importance of drainage systems for transportation networks, and the need to address flood risk and flow variability along such cross country railway line. Ensuring the functionality of the railway systems can help to ensure the continued socio-economic benefits, while safeguarding lives, properties, and infrastructure from the adverse effect of flooding and flow variability.(26)

In recent years, Ethiopia has encountered a major problem with flooding related drainage structure failures, particularly during the rainy season. In 2016, a major incident occurred when heavy rainfall caused river overflows, landslides, localized flash floods, catastrophic drainage system failures, and widespread destruction and casualties in the lower Omo Valley, Diredawa, Amhara, Afar, Somali, Tigray, Gambella, Oromia, and Harari Regions.(27)

The population growth in Ethiopia have strained the existing drainage systems, many of which were not built to withstand the increased volume of water during intense rainstorms. As a result, after heavy rains, water often accumulates rapidly, overflowing drainage structures and causing flood in residential areas, streets, and agricultural land.(28, 29, 30)

The failure of drainage structure has profound effect on the communities, infrastructure, and economy. Homes and agricultural land are flooded resulting in economic losses, property destruction, and displacement. It also leads to inaccessibility of roads and transportation networks, causing disruptions to trade. Furthermore, flooding of agricultural land due to failure of drainage structure damages food products and predispose the community to food insecurity. (26, 27, 28)

The impact of flooding due to failure of drainage structure are particularly worse in disadvantaged and marginalized communities as the access to resource and infrastructure is limited in these population groups. These population groups frequently experience a major burden following floods, having difficulty of getting access to safe drinking water, shelter, and medical treatment.(24, 25)

The management of drainage structure failure in Ethiopia requires a comprehensive strategy that encompasses investment in infrastructure, better rural planning, and fostering community resilience. Specifically, the strategy needs to include improvements in land-use planning measures, upgraded and expanded drainage systems to handle more rainfall, and strengthened early warning systems to alert people to impending floods. (24, 25, 31)

Furthermore, long-term resilience against floods and drainage structure failures in Ethiopia and elsewhere–depends on measures to address climate change and mitigate its effects, such as lowering greenhouse gas emissions, deforestations and promoting sustainable development practices.(32, 33)

### 2.3.3 Sedimentation Effects on Bridge and Culvert Structures

The transport of sediment in rivers and streams exacerbate the issues with sedimentation for bridge and culverts in the Holeta to Ambo Road. Sediment buildup in culverts reduces hydraulic capacity, which causes localized floods and increased maintenance costs. In order to lessen the effects of sedimentation and ensure the functionality of drainage infrastructure, G. Mathias Kondolf et al. examined experiences from five continents and revealed the importance of sediment management strategies, such as regular dredging and erosion control measures.(34)

Drainage structure failure due to sedimentation is a major challenge worldwide, and Ethiopia is not an exception. Sedimentation is the accumulation of dirt and debris in drainage structure and streams, which cause the structure to be less or non-functional and increase the risk of flooding. (35, 36)

Sedimentation is a major problem in Ethiopia, particularly, in areas with steep slopes and high rates of soil erosion. Deforestation and excessive rainfall exacerbate soil erosion and cause large amount of sediment to be carried into rivers, streams, and drainage channels. Gradually, this sediment builds up in drainage structure such as culverts, canals, and other drainage systems that results in blockage of water flow and increased risk of flooding during rainy season.(37, 38)

Moreover, different places in the country experienced drainage structure failure as a result of sedimentation. In areas with poor land management practices will experience severe soil erosion and sedimentation in nearby streams. As a result, sediment has clogged drainage channels, resulting in water back-up and flooding of both agricultural and residential areas. (37)

The consequences of drainage structure failure due to sedimentation are multifaceted. Flooding can destroy shelter, infrastructure, and agricultural products that results in displacement of communities and financial loss. Furthermore, stagnant water brought on by clogged drainage systems can serve as a breading site for mosquitoes, increasing risk of waterborne diseases such as malaria and cholera.(39)

The drainage structure failure due to sedimentation in the country requires a multipronged approach that addresses soil erosion and improves drainage infrastructure resilience. Reforestation and soil conservation strategies would reduce the sediment entering the streams and risk of erosion. Regular maintenance and desilting are also necessary for drainage systems in order to ensure unimpeded water flow and reduce the risk of floods.(40)

Moreover, integrating nature-based solutions into country planning effort, such as green infrastructure and wetland restoration, can assist in absorbing surplus water and lessen the effect of sedimentation on drainage systems. By adopting a holistic approach that addresses the root causes of sedimentation and strengthens drainage infrastructure, the country may better address the issues of sediment-related drainage structure failure and enhance long-term resilience to floods. (41)

### 2.3.4 Scouring Vulnerability of Bridge Foundations

Scouring occurs when the force of water flow erodes and removes soil around bridge piers and foundations. This problem is common in bridges, culverts, and riverbeds, which are exposed to high-velocity water flow during heavy rainfall or flooding.(26) Scouring-related drainage

structure failure poses a serious risk to the stability and integrity of drainage systems in many parts of the world, including Ethiopia.

The scouring process is initiated by an increase in water flow around the bridge pier, leading to a localized decrease in pressure and an increase in flow velocity. As the water velocity increases, the sediment surrounding the pier gradually erodes, deepening the channel bed or leaving a scour hole around the bridge pier. Initially, the erosion may not be apparent, it may eventually deepen and spread overtime, compromising the structural integrity of the foundation and potentially leading to structural failure. (42, 43) The scouring process can be affected by factors, including the rate of water flow, sediment composition, and the channel geometry and bridge structure. For instance, high flow rates and fluctuations in water level exacerbate scouring by intensifying the erosive forces exerted on the bridge foundations. The presence of cohesive or non-cohesive materials on sediment composition affect the stability of the scour hole and the pace of erosion. Furthermore, variations in channel geometry, such as bends or constrictions, can alter flow patterns and increase the susceptibility of some areas to scouring. It is essential to understand these complex interactions in order to properly build and maintain drainage structures that are susceptible to scouring (42, 43)

Bridge foundations are vulnerable to scouring, especially during periods of variable flow and high-velocity water flow patterns. A review of bridge scour monitoring approaches by L.J. Prendergast (2014) highlights the complex relationships between flow velocity, sediment transport, and scour depth. Hence, the review highlighted the importance of complete scour counter-measure design to ensure bridge stability and safety. In addition, a regular monitoring and maintenance of bridge foundations is necessary to reduce the risks associated with scouring.(44, 45)

A study using experimental techniques on pier scour depth and related scour hole patterns for different shapes was carried out by Khan K et al. in 2024. The main objective of the study was to examine the scouring process surrounding piers of different shapes in order to identify which type of pier would be most efficient in reducing local scour. The findings of the study showed that different pier shapes have varying levels of scouring depth, with square-shaped piers having the maximum depth and diamond-shaped and elliptical-shaped piers having the lowest. Furthermore, scouring is highly influenced by pier size, as an increase in pier size will result in a rise in scour depth. Additionally, the study shows that a rise in flow corresponds to an increase in scour depth. Overall, the study sheds light on the erosive characteristics and

hydraulic behavior of water flowing around piers of various geometries, which can inform the optimization of bridge design and hydraulic engineering practices. (46)

In Ethiopia, dynamic hydrological conditions are influenced by unpredictable weather patterns and rugged terrain, making drainage infrastructure vulnerable to scouring-induced failure. The failure of a major drainage system substantially impacts the local economy, transportation networks, and access to essential services.

A study held in the Tigray region of northern Ethiopia aimed to assess scour problems at three specific bridge locations: the Tankwa, upper Geba, and Ilala bridges. The study employed various tools to assess and analysis river morphology, hydrologic, and hydraulic conditions. The results showed that the riverbanks were more unstable and degraded. Scour depths at different sections of the bridges were measured, with reductions observed when riprap was used. Overall, the hydrologic and hydraulic models demonstrated effectiveness in assessing scour problems and offering recommendations for potential mitigating strategies for bridge infrastructure in the area.(47)

The consequences of drainage structure failure due to scouring can be severe and far-reaching beyond infrastructure damage it can lead to death, property destruction, and environmental degradation. In addition, the disruption of drainage system may intensify flooding downstream, affecting communities and agricultural areas.(48, 49)

The prevention and mitigation of scouring related risk of drainage structure failure requires proactive measures such as armouring bridge foundations with materials resistant to erosion, installing scour countermeasures (e.g., riprap, gabions, or concrete aprons), and designing structures to withstand high-velocity flows.(33, 50, 51)

Moreover, routine drainage structure inspection, monitoring and maintenance are necessary to identify early sign of scour and deterioration to implement timely action. In addition to proper land management practices and lowering the risk of sediment transfer into streams, community involvement and awareness-raising campaigns can also be important in minimizing the possibility of scour-induced damage.(50, 51)

# 3 METHODOLOGY AND MATERIAL

## 3.1 Description of study area

### 3.1.1 Study setting

The Holeta to Ambo Road is found in the Oromia regional state of central Ethiopian Highlands., which is a part of the trunk road from Addis Ababa (i.e., the capital city of Ethiopia) to Gimbi. The road was constructed in 1930s by Italians, with a base that varied in width from 4 to 6 meters. Recently, international organization and the Ethiopian government rehabilitated the road projects. The road restoration was started in 2002 and completed in 2006.(52) In the rehabilitation, most of the drainage structures are not upgraded or changed.

### 3.1.2 Location of the road

The Holeta to Ambo Road connects the towns of Holeta and Ambo. Holeta is located in West Shewa zones, Oromia Region, around 35 kilometres west of Addis Ababa, Ethiopia. The road passes through a rural area and is an important transportation route in this region. Ambo is found in the same Zones of the region, and located to the west of Holeta. It has a latitude and longitude of 9°3′N 38°30′E to 9°1' N 38°9' E and an altitude of 2391m-2236m above sea level.(7)

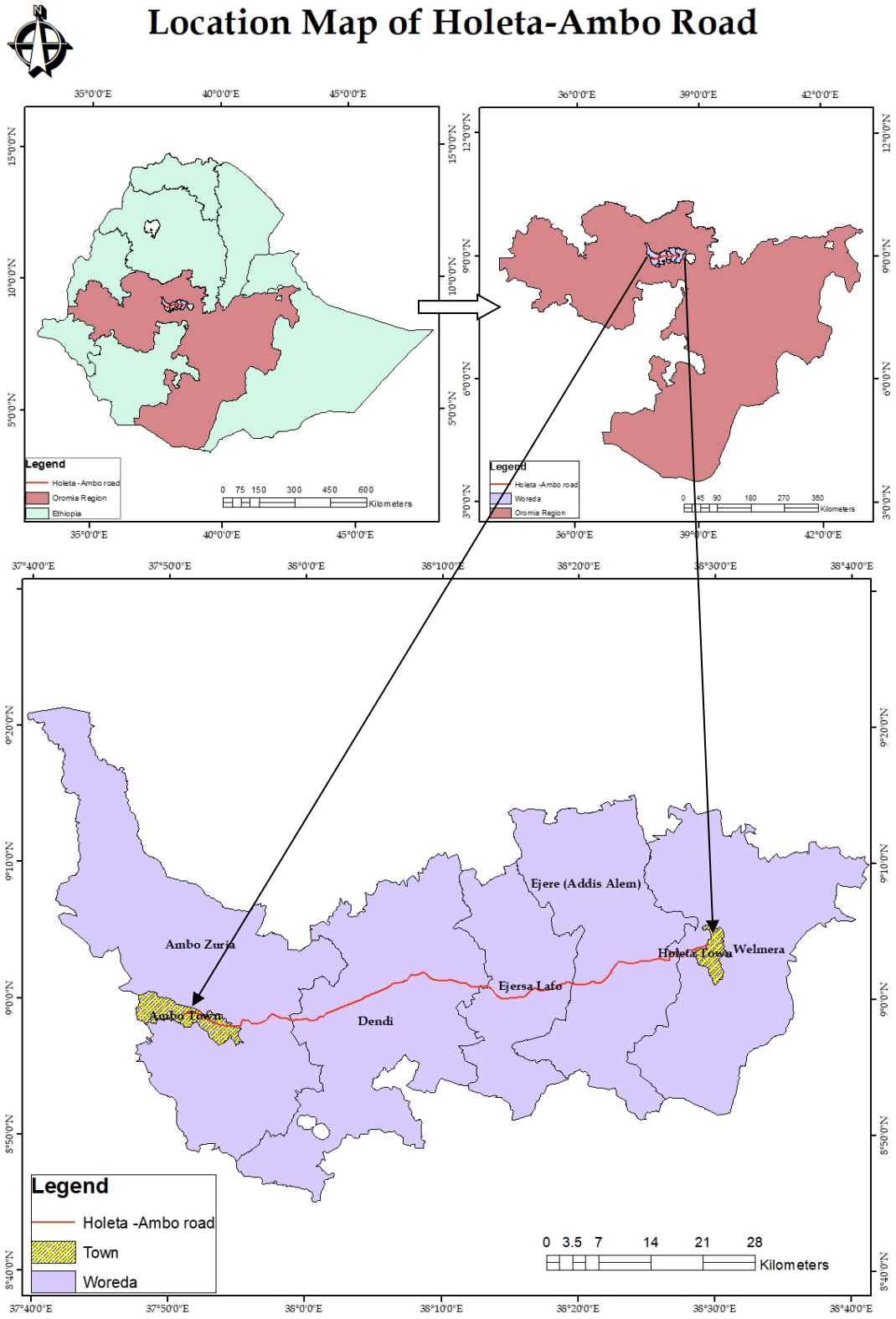


Figure 3-1: Location of the Study Road

### 3.1.3 Route selection

The Holeta to Ambo Road cross various streams and one of the main roads in the country that have drainage problems. The road is selected for the assessment of the effects of variable flow

on bridges and culverts due to its distinct mix of topographical, hydrological, and infrastructure characteristics. This road is located in an area with erratic hydrological patterns and seasonal variations in rainfall, making it a good setting for studying the effects of variable flow on drainage structures. In addition, the road is exposed to flooding due to the land scape and terrain condition of catchment area.

It is essential to study how various water flows during floods affect culverts and bridges. This study focusses on major highways that are used by peoples and business. The findings would strengthen and enhance bridge and culverts in various drainage structural defect areas and ensures important highways continue to function even in the event of flooding.

### 3.1.4 Existing Drainage structures

There are around 148 drainage structures on the Holeta to Ambo Road. Among them, thirty-one are dedicated to bridge crossings. There are eight RC Deck Girder Bridges, six RC Slab Bridges, sixteen Masonry Arch Bridges, and one Steel Girder/Composite Bridge. Beyond the bridges, the route features an array of 117 culverts, each serving a key role in managing water flow and effective water regulation. These culverts encompass various type such as Box/Slab culverts, RC pipe culverts, and corrugated steel pipe culverts. Remarkably, these engineering wonders were built across several decades, from as early as 1937 to as recent as 2008 (Source: ERA BMS).

Despite the huge number of drainage structure along the road, only 56 were analysed in this study after the stream and catchment areas were delineated. Most of the drainage structures are excluded due to the Digital Elevation Model's (DEM) resolution fails to identify the majority of streams and the number of cells selected to define the streams. The majority of this road's crossing drainage structures are intended to serve as relief crossings. They facilitate water flow off the road during rainy seasons, as opposed to crossing a clearly defined stream. This occurs when rainwater runs off accumulated the road and collects on one side. Since handling this water is the primary function of the majority of minor drainage crossings, the study concentrates on the large crossings in this manner.

The study includes sixteen masonry arch bridges, eight reinforced concrete deck girder bridges, six reinforced concrete slab bridges, one steel girder/composite bridge, and roughly nineteen box/slab culverts, four corrugated steel pipes, and two reinforced concrete pipes. The data from ERA BMS are presented in tables 3.1 and 3.2, which demonstrate the inclusion of key relevant

data of the selected drainage structures. However, the type and opening size obtained from ERA BMS are not same with the data collected from on-site visit, for example C1 and C2 are slab culvert on ERA BMS but on actual it is Double pipe with 1.06m diameter structure and additional C11 bridge length is 30m but on site it is 6m span masonry arch bridge. Therefore in order to do analysis with actual opening size of each structures visiting site and measuring was mandatory, the collected data from the site are attached in appendix 3 of this research paper.

Table 3-1: List of bridge location and geometry

| **Bridge List - ERA-BMS** | | | | | | | |
|---|---|---|---|---|---|---|---|
| New ID | **Old Bridge Id** | **X-Coord.** | **Y-Coord.** | **Bridge Name** | **Dist. From AA (Km)** | **Bridge Type** | **Bridge Length (m)** |
| C9 | A4-2-001 | 428764.2 | 997452 | Berga | 51.54 | Masonry Arch | 14 |
| C11 | A4-2-003 | 426160.2 | 997143.2 | Holuko | 54.49 | Masonry Arch | 30 |
| C13 | A4-2-005 | 425472.9 | 997252.5 | Aba Debela | 55.26 | Masonry Arch | 30 |
| C16 | A4-2-007 | 419301.8 | 995329.2 | Kella | 61.94 | Masonry Arch | 27.6 |
| C17 | A4-2-008 | 418225.98 | 995400.56 | Welonkomi | 63.34 | RC Deck Girder | 11.85 |
| C19 | A4-2-009 | 416314.3 | 995487.5 | Jemjem | 65.13 | Masonry Arch | 42 |
| C22 | A4-2-010 | 414266 | 996836.6 | Batu No 1 | 70.27 | RC Deck Girder | 19.5 |
| C23 | A4-2-011 | 413804.2 | 996811.6 | Batu No 2 | 70.72 | RC Deck Girder | 18.5 |
| C24 | A4-2-012 | 410939.8 | 997358 | Fekere 1st | 70.9 | RC Deck Girder | 12.5 |
| C25 | A4-2-013 | 410703.1 | 997403.1 | Fekere 2nd | 71.01 | RC Deck Girder | 10 |
| C26 | A4-2-014 | 409512.95 | 997693.81 | Un-named | 71.11 | RC Slab Bridge | 17.5 |
| C27 | A4-2-015 | 409115.16 | 997683.09 | Fekere 3rd | 72.97 | Masonry Arch | 49 |
| C28 | A4-2-016 | 408302.9 | 997655.7 | Ejersagiba | 73.5 | RC Slab Bridge | 4 |
| C30 | A4-2-017 | 405580.7 | 998178.9 | Aba Semar | 76.88 | Masonry Arch | 37.1 |
| C32 | A4-2-020 | 404798.7 | 998226.5 | Gurara | 77.71 | RC Deck Girder | 4.5 |
| C33 | A4-2-018 | 404248.7 | 998094.7 | Awash No 1 | 78.2 | Masonry Arch | 19.2 |
| C38 | A4-2-022 | 396838.53 | 994587.7 | Horabila | 86.86 | RC Slab Bridge | 4 |
| C39 | A4-2-025 | 394051.2 | 993388.9 | Quribe | 89.61 | RC Slab Bridge | 4 |
| C40 | A4-2-026 | 393551.1 | 993172.1 | Meti | 90.44 | RC Deck Girder | 4 |
| C41 | A4-2-019 | 392796.7 | 992744.6 | Boren N | 91.32 | Steel Girder/Composite | 15 |
| C42 | A4-2-021 | 391586.6 | 991884.9 | Derebebe | 92.94 | Masonry Arch | 65.7 |
| C43 | A4-2-029 | 390992.7 | 992001.6 | Borare (Minini1) | 93.81 | RC Deck Girder | 4 |
| C44 | A4-2-024 | 389762.9 | 992191.5 | Bollo | 95.08 | Masonry Arch | 30.9 |
| C45 | A4-2-027 | 388767.7 | 991972.6 | Amaroo | 96.21 | Masonry Arch | 8.5 |
| C46 | A4-2-028 | 385873.4 | 992922.9 | Dindila | 99.4 | Masonry Arch | 12.95 |
| C47 | A4-2-034 | 381720.5 | 991990.9 | Dunge | 104.52 | RC Slab Bridge | 4 |
| C48 | A4-2-031 | 381540.2 | 991419 | Solbe | 104.91 | Masonry Arch | 47.9 |
| C49 | - | 381066.17 | 991158.34 | - | 105.41 | Masonry Arch | 10.3 |
| C50 | A4-2-032 | 380788 | 991258.4 | Borele | 106.17 | Masonry Arch | 4 |

| Bridge List - ERA-BMS | | | | | | | |
|---|---|---|---|---|---|---|---|
| New ID | **Old Bridge Id** | **X-Coord.** | **Y-Coord.** | **Bridge Name** | **Dist. From AA (Km)** | **Bridge Type** | **Bridge Length (m)** |
| C53 | A4-2-035 | 378509.1 | 991589.4 | Shatafag | 107.5 | RC Slab Bridge | 4 |
| C56 | A4-2-036 | 374085.3 | 993066.8 | Huluka | 112.29 | Masonry Arch | 65.8 |

Table 3-2: List of Culvert location and Geometry

| Culvert List - ERA-BMS | | | | | | |
|---|---|---|---|---|---|---|
| **New ID** | **Old Culvert Id** | **X-Coord.** | **Y-Coord.** | **Dist. From AA (Km)** | **Culvert Type** | **Total Length (m)** |
| C1 | A4-2-C-004 | 443761.2 | 1002248 | 35.1 | Slab Culvert | 1.9 |
| C2 | A4-2-C-007 | 442873 | 1001947 | 36.13 | Slab Culvert | 2.2 |
| C3 | A4-2-C-008 | 442266.44 | 1001580 | 36.93 | Box Culvert | 1.2 |
| C4 | A4-2-C-009 | 441947.9 | 1001452 | 37.45 | Box Culvert | 2.1 |
| C5 | A4-2-C-012 | 440093.5 | 1001322 | 39.76 | Corrugated steel Pipe | 1 |
| C6 | A4-2-C-015 | 437868.3 | 1000658 | 41.7 | Box Culvert | 0.8 |
| C7 | A4-2-C-018 | 432269.1 | 1000122 | 47.79 | Box Culvert | 0.8 |
| C8 | A4-2-C-025 | 430032.44 | 997365.37 | 51.61 | Corrugated steel Pipe | 1.3 |
| C10 | A4-2-C-030 | 426767 | 996803.4 | 55.65 | Corrugated steel Pipe | 1.2 |
| C12 | A4-2-C-031 | 426001.3 | 997283 | 56.67 | Box Culvert | 2.6 |
| C14 | A4-2-C-036 | 423077.1 | 996317.5 | 59.6 | RC Pipe | 0.9 |
| C15 | A4-2-C-041 | 420869 | 995854.3 | 62.29 | Box Culvert | 2.2 |
| C18 | A4-2-C-048 | 417163.39 | 995154.08 | 66.38 | Slab Culvert | 2.8 |
| C20 | A4-2-C-052 | 415282.1 | 996337.3 | 69.05 | Slab Culvert | 2.4 |
| C21 | A4-2-C-054 | 414786.6 | 996800.4 | 69.7 | Corrugated steel Pipe | 1 |
| C29 | A4-2-C-062 | 406960.54 | 998091.9 | 78.1 | Slab Culvert | 1.1 |
| C31 | A4-2-C-064 | 405153.16 | 998259.2 | 77.29 | RC Pipe | 1 |
| C34 | A4-2-C-069 | 402260.93 | 997076.2 | 80.8 | Slab Culvert | 3.1 |
| C35 | A4-2-C-070 | 401398.59 | 996562.32 | 81.69 | Slab Culvert | 1.1 |
| C36 | A4-2-C-071 | 400924.97 | 996366.39 | 81.96 | Slab Culvert | 1.1 |
| C37 | A4-2-C-072 | 400570.3 | 996203.3 | 82.33 | Slab Culvert | 1.1 |
| C51 | A4-2-C-109 | 379543.1 | 991425.2 | 107.29 | Slab Culvert | 1.1 |
| C52 | A4-2-C-111 | 379035.37 | 991505.6 | 107.78 | Slab Culvert | 1.1 |
| C54 | A4-2-C-114 | 377391.9 | 992161.4 | 109.61 | Slab Culvert | 1 |
| C55 | A4-2-C-115 | 376599.3 | 992645.32 | 110.52 | Slab Culvert | 1 |

### 3.1.5 Climate condition of study area

The central highlands in Ethiopia are much colder than the country's southeast and northeast lowlands, which are subject to a tropical climate. The mean annual temperature varies in highest elevation to lowest elevation that is between 25°C and 30°Cin lowlands and 15°C and 20°C for highlands. The country has three distinct seasons due to the variation in Inter Tropical

Convergence Zone's (ITCZ). The three seasons are a lengthy rainy season (also known as Kiremt) from June to September, a short-wet season (Belg) from February to May, and a dry season (Bega) from October to January.(16)

Using the data from National Metrological Agency of Ethiopia (NMAoE) the annual average minimum and maximum temperature are graphically represented as bar chart in figures 3.2 and 3.3 as shown in the figure the minimum and maximum temperature is 9.04 and 27.08 respectively. Additionally, the average monthly minimum and maximum temperature is graphically represented in figure 3.4

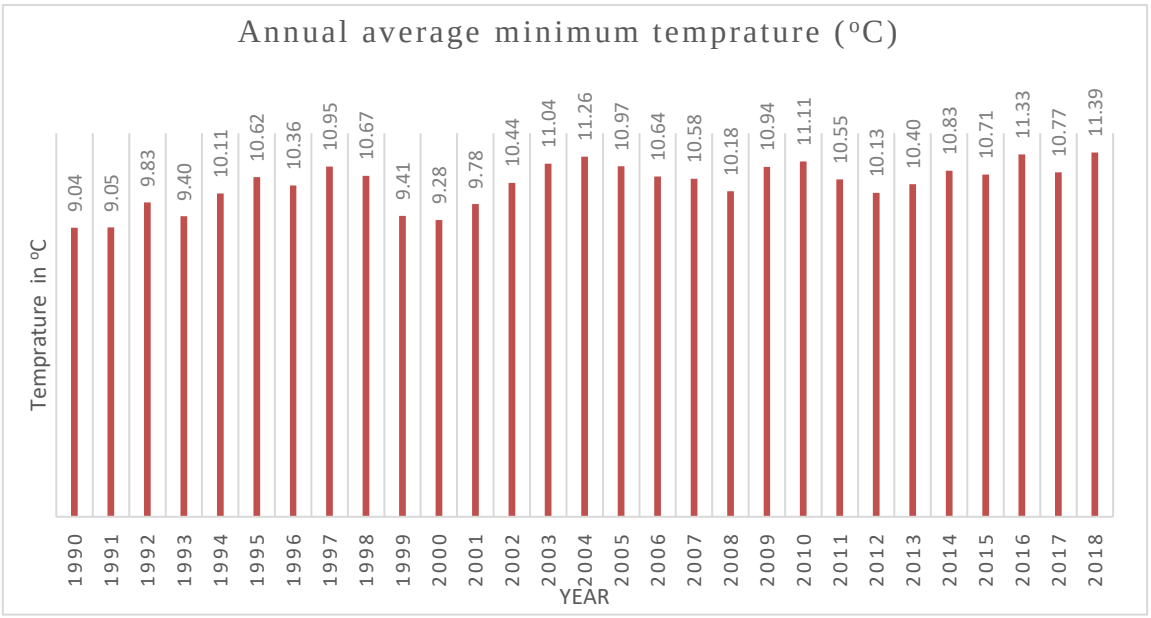


Figure 3-2: Annual average minimum temperature of the study Area

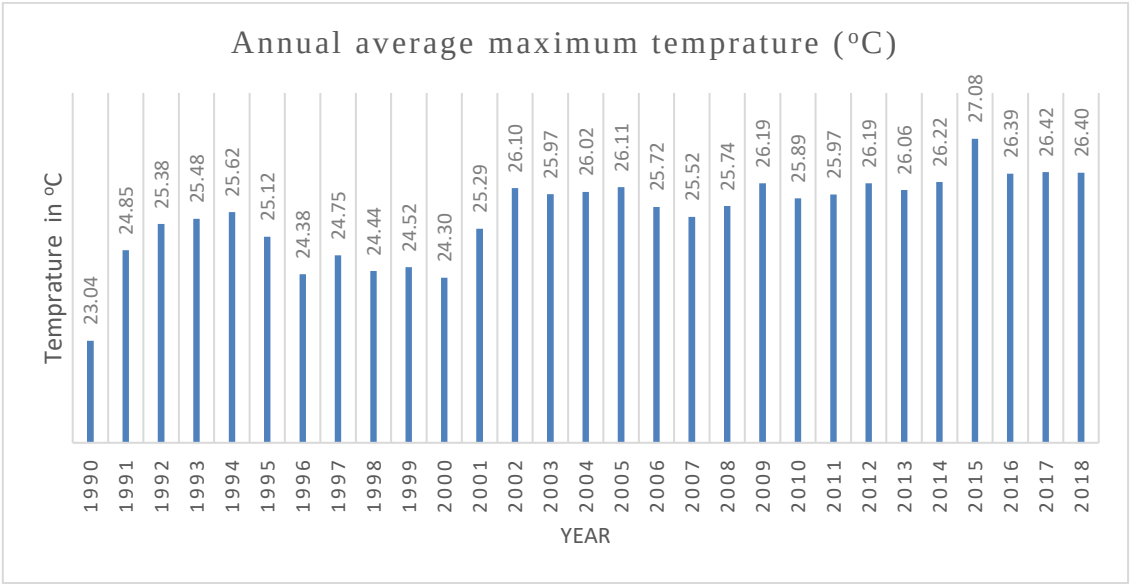


Figure 3-3: Annual average maximum temperature of the study area

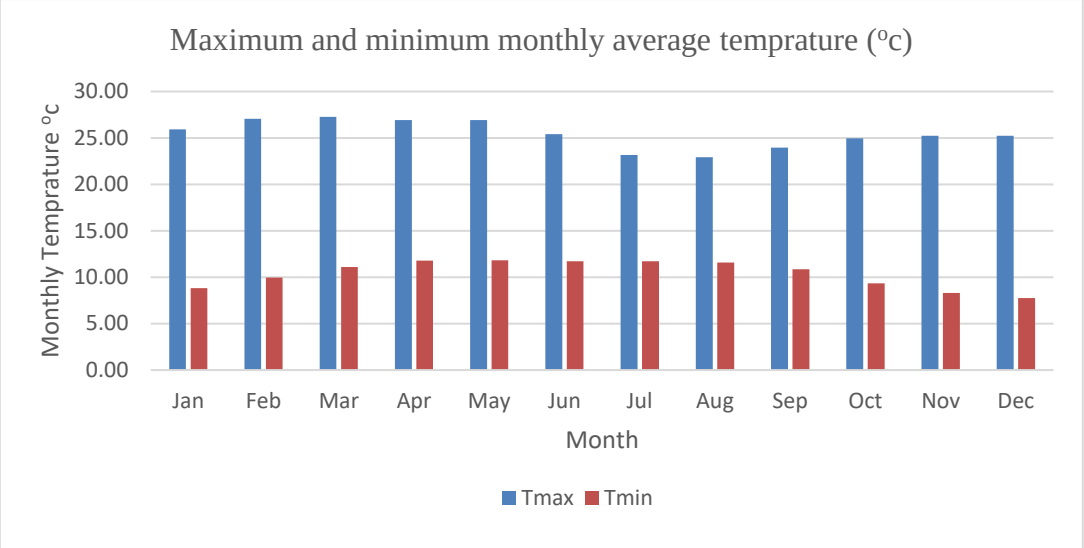


Figure 3-4: Average monthly maximum and minimum temperature of the study area.

### 3.1.6 River basin

The Ethiopia river basins are categorized based on topographical, hydrological, and administrative characteristics. There are twelve main river basins all of are composed of sub basin with river and stream network and other watercourses that flow into a single outlet. [48] The holeta to Ambo road is lay on the boundaries of Awash and Abay river basin.

As illustrated in the figure 3.5 below, the Holeta to Ambo Road watershed is suited in the Awash River Basin (62%), and in the Abay River Basin (38%). In order to properly identify the classification of the river basin for this road, it is necessary to refer official sources or reports, maps, or documentation from the Ethiopian Ministry of Water and Energy.

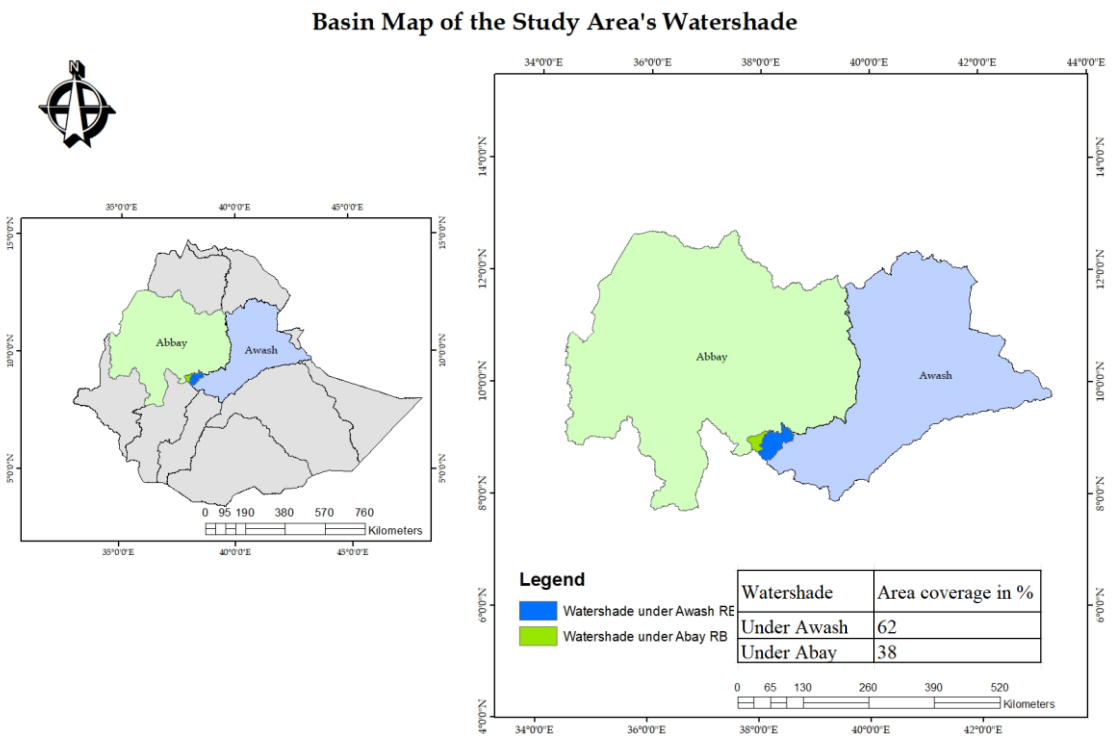


Figure 3-5: Map showing the river basin category of sub-basin watersheds in the study area

## 3.2 Research Design

To accomplish the objective of this research, a complete task was carried out. The steps followed to achieve the research objectives are depicted in the flow chart below figure 3.6. The procedures and methods to obtaining the key data for each phase or stage are described in the following sections.

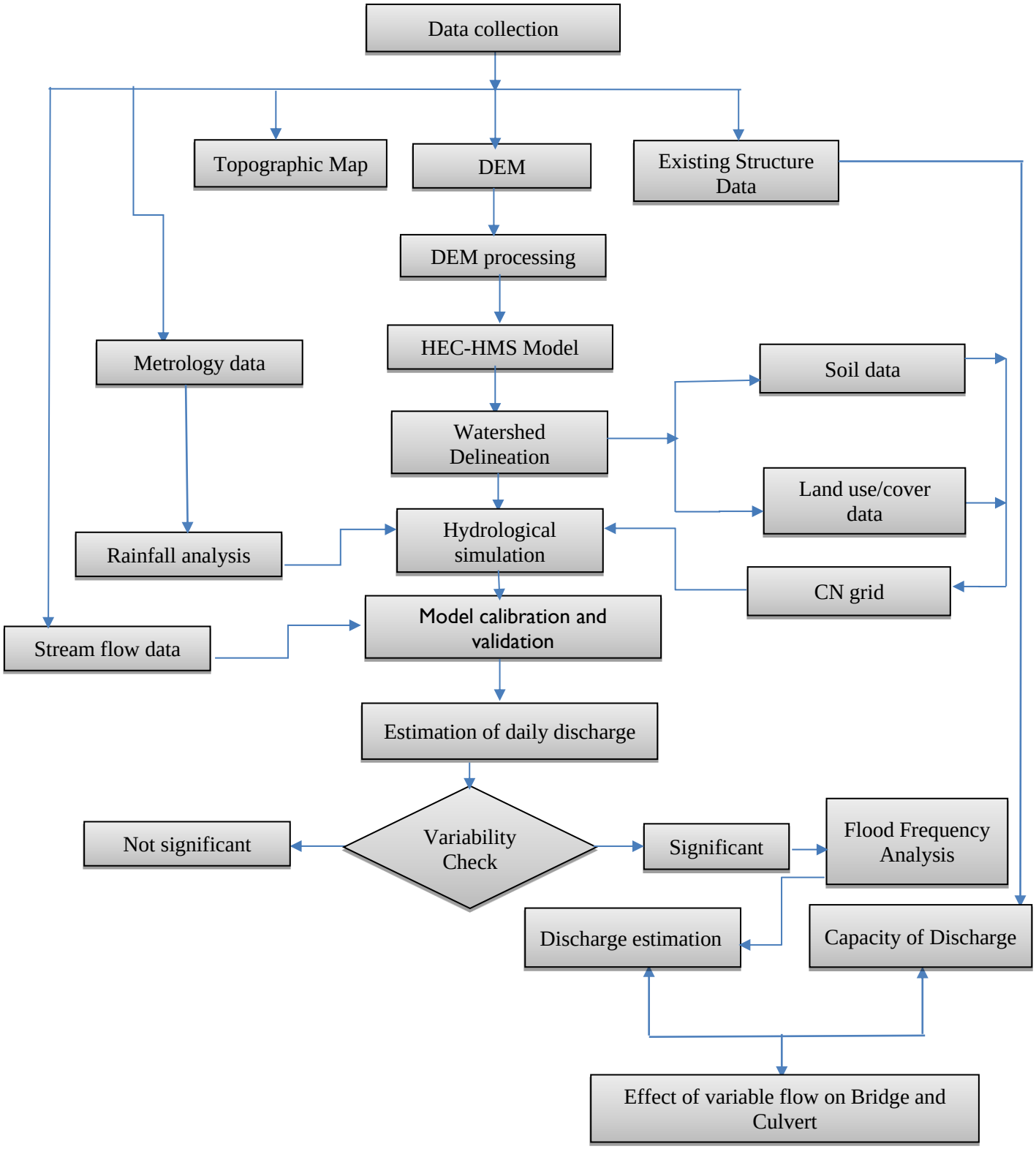


Figure 3-6: Flow chart of the research

## 3.3 Data required for the study

### 3.3.1 Roadway Alignment

The data related to roadway alignment and standards governing drainage structures including bridges and culverts for the study area were sourced from the Ethiopian Road Administration in Addis Ababa, Ethiopia.

### 3.3.2 Geographical data

The topographic conditions of the Holeta to Ambo road are characterized by a variety of geographical features, elevations, and terrain types. As the road traverses the region between Holeta and Ambo town in Ethiopia, it encounters diverse landscapes that influence its alignment and construction. As it is mentioned above the studying road is located in West Shewa zones, Oromia Region. It has a latitude and longitude of 9°3′N 38°30′E to 9°1' N 38°9' E and the road experiences fluctuations in elevation as it connects the towns of Holeta and Ambo. The elevation of the catchment area can vary significantly along the route due to the region's hilly and mountainous terrain an altitude of 3383-1786m above sea level.

The structure of the road is mostly affected by the natural flow of water due to the various type of landscape in the catchment area. To define the watershed region in the study area, a 12.5mx12.5m resolution DEM was employed. Constructing bridges, culverts, and drainage systems was essential wherever the road intersected with streams, rivers, and watercourses.

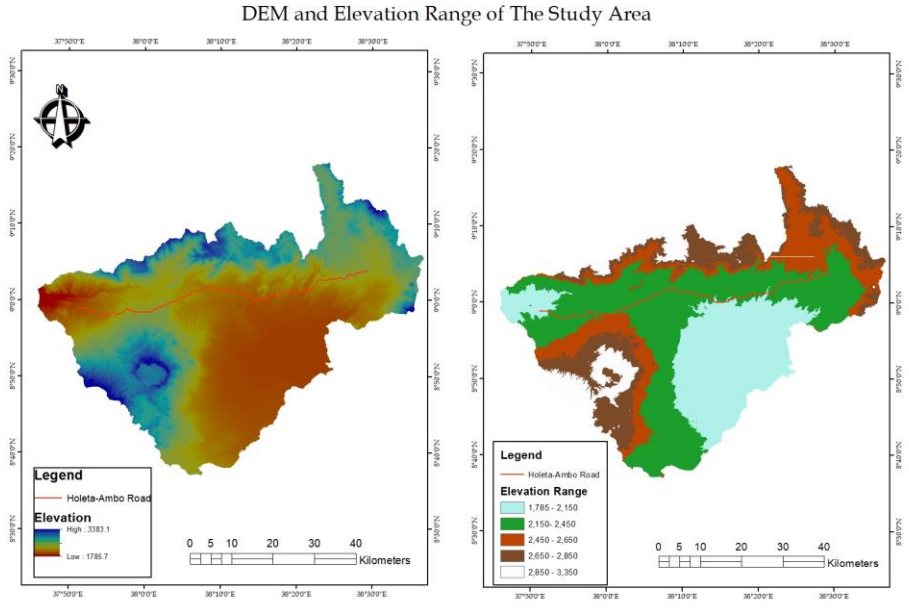


Figure 3-7: The DEM and Elevation range in the study area

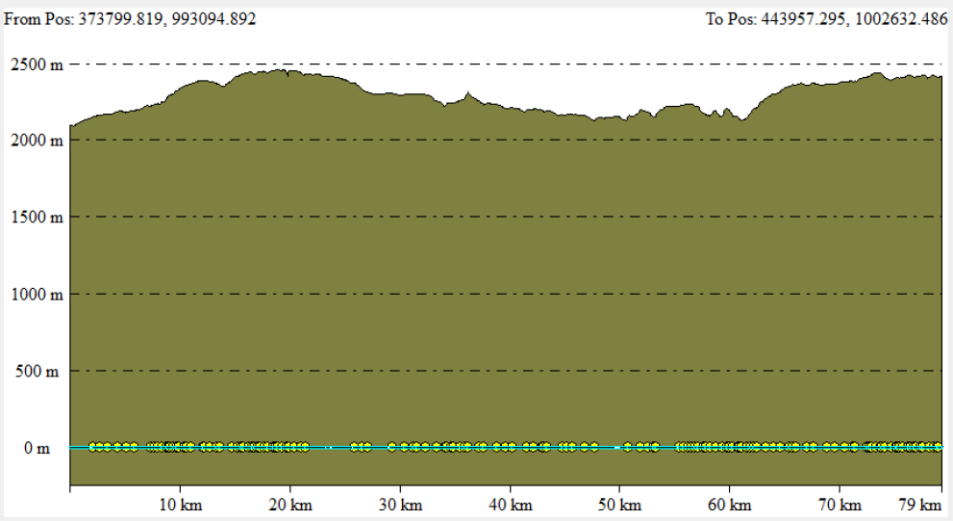


Figure 3-8: Project Road Route Profile

### 3.3.3 Meteorological Data

Metrology data is essential for every phase of road drainage structure management, including planning, design, construction, and maintenance. The daily rainfall and temperature data for the specified road that fall within the effect of the catchment areas for a period of 30 years (1991 to 2020) were accessed from the National Meteorological Agency of Ethiopia.

The locations, catchment areas, and weight of approximately seventeen meteorological gauge stations that comprise the watershed of the study area are listed table3.3 below.

Table 3-3: Location, area and weight of meteorological gauge stations

| No. | Station Name | Longitude | Latitude | Area(km2) | Weight |
|---|---|---|---|---|---|
| **1** | Abebe Keranso | 38.17 | 8.98 | 202.88 | 0.06 |
| **2** | Addis alem | 38.38 | 9.05 | 406.99 | 0.12 |
| **3** | Ambo Agriculture | 37.84 | 8.99 | 283.24 | 0.09 |
| **4** | Arb bila | 37.79 | 8.8 | 80.1 | 0.02 |
| **5** | Asgori | 38.34 | 8.8 | 143.14 | 0.04 |
| **6** | Busa | 38.14 | 8.77 | 415.82 | 0.12 |
| **7** | Dertuliben | 38.02 | 8.97 | 471.31 | 0.14 |
| **8** | Dilela | 38.05 | 8.64 | 146.29 | 0.04 |
| **9** | Enchini | 38.37 | 9.32 | 90.19 | 0.03 |
| **10** | Enselale (Hidosokoke) | 38.44 | 8.94 | 146.58 | 0.04 |
| **11** | Ginchi | 38.14 | 9.03 | 286.42 | 0.09 |
| **12** | Guranda Meta | 38.59 | 8.91 | 63.33 | 0.02 |
| **13** | Kimoye | 38.34 | 9.01 | 127.02 | 0.04 |
| **14** | Sebeta | 38.63 | 8.92 | 33.02 | 0.01 |
| **15** | Teji | 38.38 | 8.84 | 90.31 | 0.03 |
| **16** | Tulu Bolo | 38.21 | 8.66 | 110.86 | 0.03 |
| **17** | Welenkomi | 38.26 | 9 | 225.45 | 0.07 |

The Thiessen Polygon Map information from nearby gauge stations is used to calculate the annual rainfall in the catchment. The map developed in ArcGIS 10.4 is depicted in the figure 3.9 below.

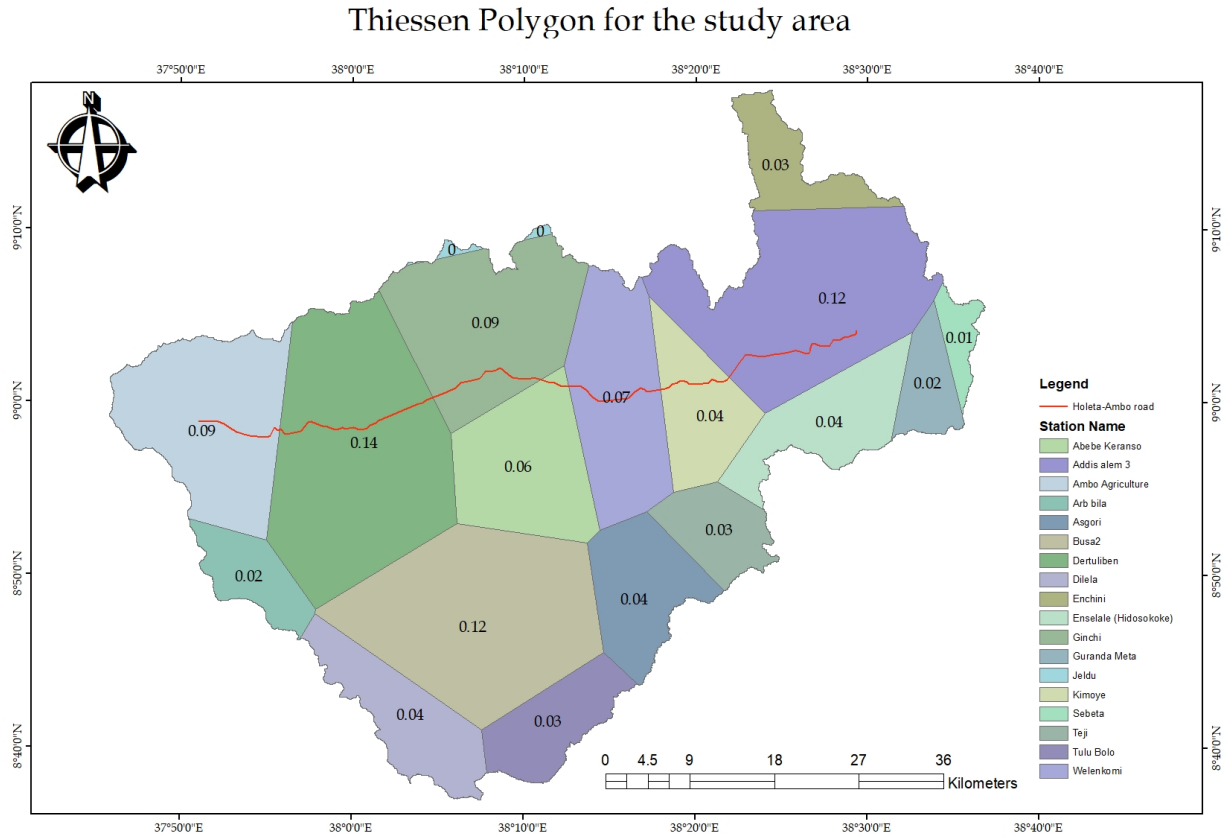


Figure 3-9: Thiessen Polygon Map of the study area

### 3.3.4 Observed discharge data

Observed discharge data is data including the volume and characteristics of water flowing through rivers, streams, and other comparable water bodies over a specific time period. Specifically, this data includes measurements of the volume, velocity, and, on rare occasions, quality if the water, which are essential for forecasting floods and distributes water for different purposes.(53)

In this particular study, this data is utilized to calibrate and validate the simulated data with observed data from three-gauge stations—Berga Nr. Addis Alem, Awash Bello (031020), and Debis Nr. Guder as shown in the figure 3.10.

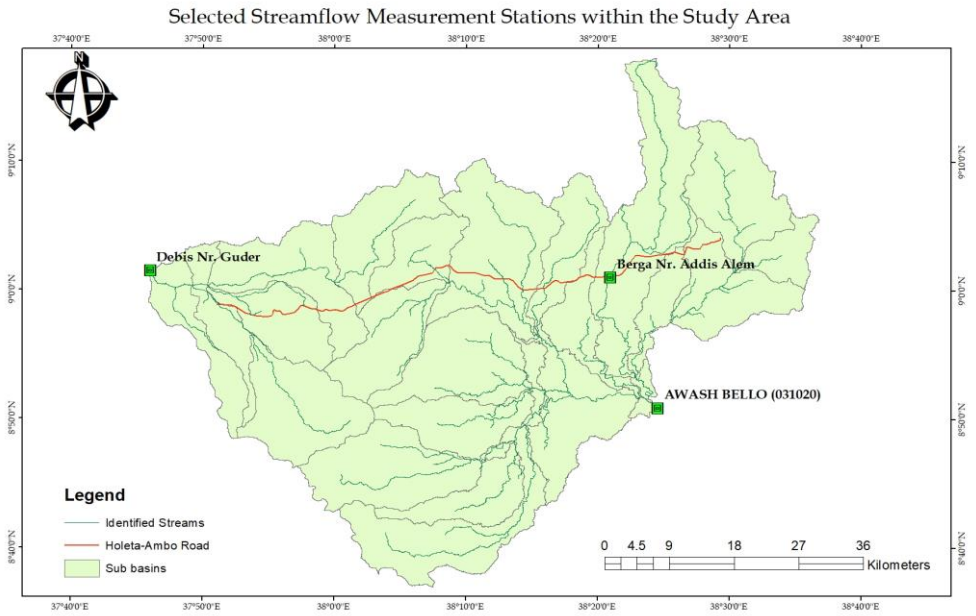


Figure 3-10: location of gauge station of observed stream flow

The annual and monthly observed discharge data are graphically presented in figure 3.11 and 3.12. The data were collected from Ministry of Water and Energy, Ethiopia, Addis Ababa.

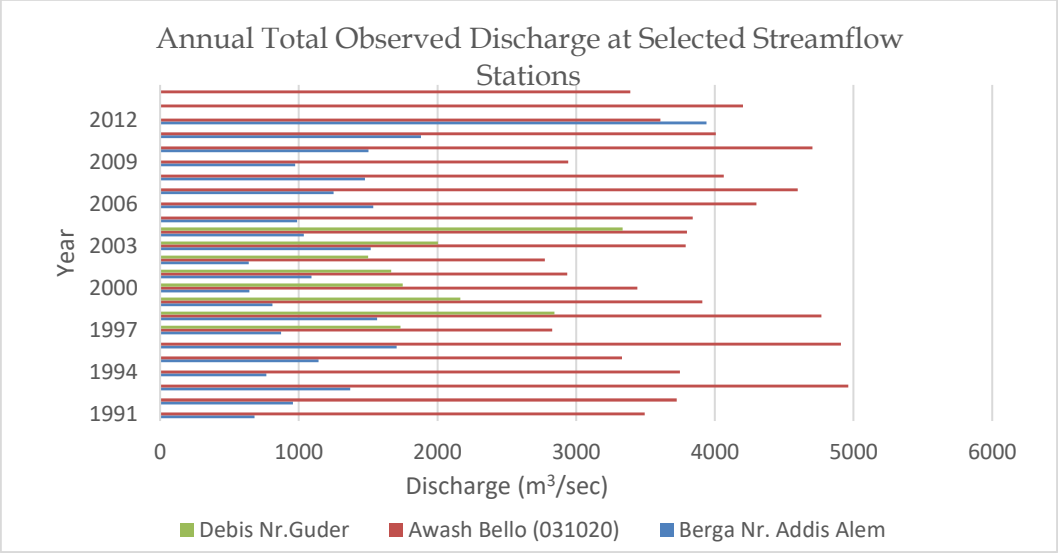


Figure 3-11: The annual total observed discharge ($m^3$/sec) the selected stream flow stations

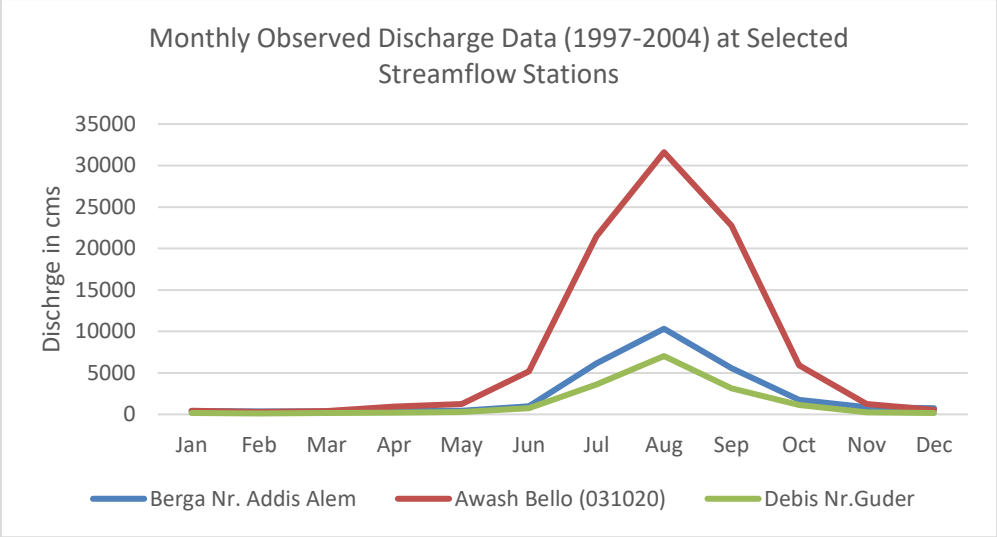


Figure 3-12: The monthly observed discharge data at selected stream flow stations

### 3.3.5 Land cover data

There was a variety of land cover in the Holeta to Ambo Road watershed, including forests, grasslands, and croplands, which benefited the nearby ecosystems and wildlife. There were several fields and orchards on agricultural property. The land cover data was gathered through site visits and cross-referenced with the LULC map of Ethiopia in 2016.The map is prepared by ArcGIS 10.4 using 1:1000000 scale map as shown in figure 3.13 of LULC map of Ethiopia sourced from Mapping Agency.

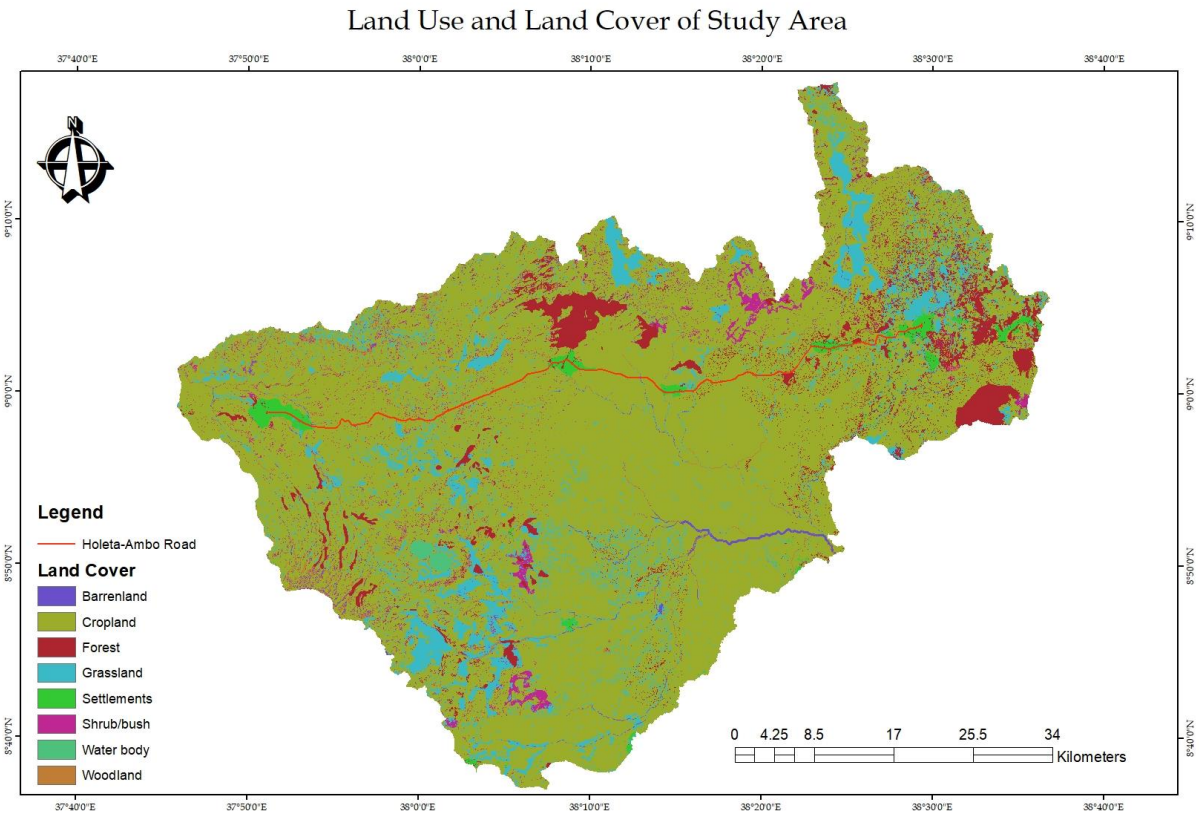


Figure 3-13: Land use and land cover type of the study area

Figure 3-14: Sample picture showing the land cover type of the study area

The area coverage of each LULC type of the watershed area in the catchment area is displayed in table 3.4 below.

**T**able 3-4: Area coverage of LULC type of the study area

| No. | LULC Type | Area (km2) | Area Coverage (%) |
|---|---|---|---|
| 1 | Forest | 105.96 | 3.61% |
| 2 | Woodland | 54.27 | 1.85% |
| 3 | Shrub/bush | 59.70 | 2.04% |
| 4 | Cropland | 2365.29 | 80.65% |
| 5 | Grassland | 280.81 | 9.57% |
| 6 | Barren land | 29.66 | 1.01% |
| 7 | Water body | 7.69 | 0.26% |
| 8 | Settlements | 29.53 | 1.01% |

### 3.3.6 Soil type data

The study area encompasses a mixture of soil types, influenced by terrain, parent material, and local climate. In figure 3.15 depicts the soil types of the catchments area based on the site visits and the 2016 soil map data, which is scaled 1:1000000 for Ethiopia in the project area. The soil map data is received from Mapping Agency, Addis Ababa, Ethiopia.

Based on infiltration rates, the soil conservation service (SCS) will be used to divide the soil type into four hydrologic soil groups according to ERA DDM therefore all the study area is covered with HSG-B and HSG-D in which soil having moderately low runoff potential due to moderate infiltration rates and a high runoff potential due to very slow infiltration rates respectively.(16) This is shown in the along with the soil type's area coverage table3.5.

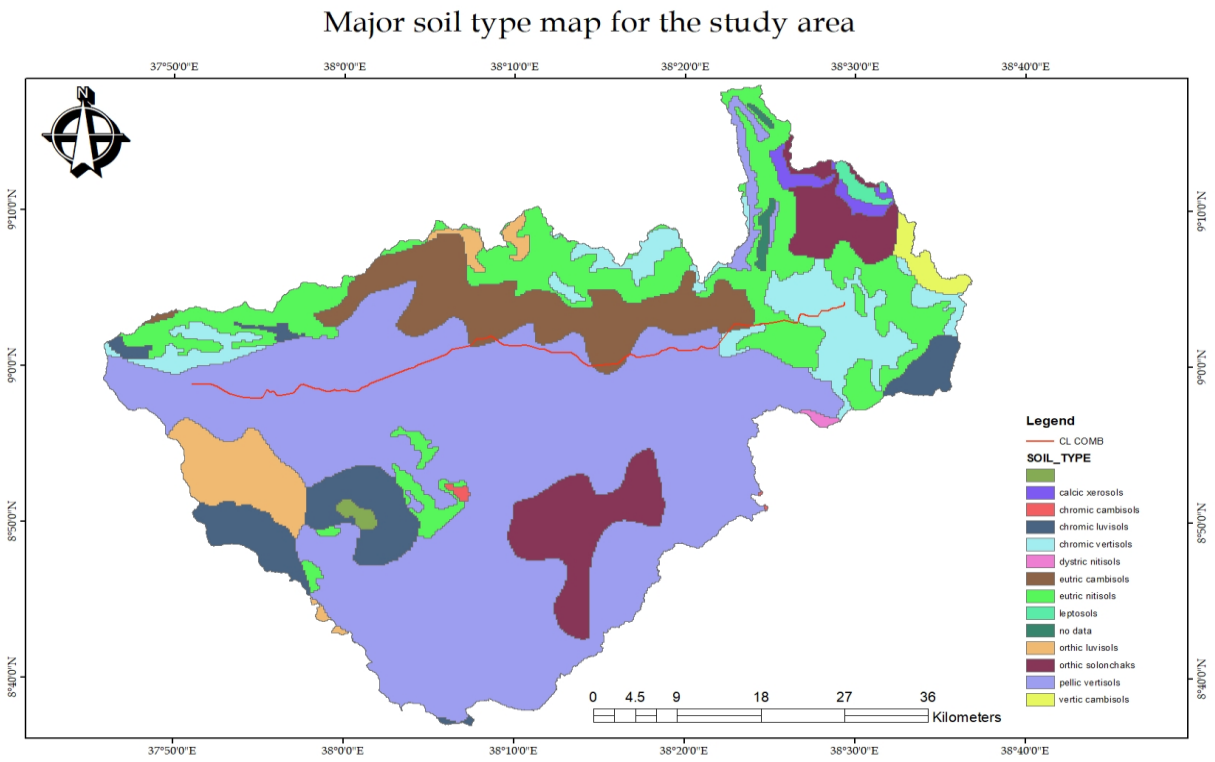


Figure 3-15: Major soil type of the study area

The area coverage of each soil type of the watershed area with its HSG displayed in the table below.

Table 3-5: The area coverage of each soil type of the watershed area with its HSG

| No. | Major Soil Type | Area(km2) | Area coverage (%) | HSG |
|---|---|---|---|---|
| 1 | Calcic Xerosols | 23.71558 | 0.71% | B |
| 2 | Chromic Cambisols | 3.407939 | 0.10% | |
| 3 | Chromic Luvisols | 188.1571 | 5.67% | |
| 4 | Dystric Nitisols | 4.038576 | 0.12% | |
| 5 | Eutric Cambisols | 272.8771 | 8.22% | |
| 6 | Eutric Nitisols | 472.4146 | 14.23% | |
| 7 | Leptosols | 11.75687 | 0.35% | |
| 8 | Orthic Luvisols | 131.296 | 3.95% | |
| 9 | 0rthic Solonchaks | 232.3084 | 7.00% | |
| 10 | Vertic Cambisols | 26.04976 | 0.78% | |
| 11 | Pellic Vertisols | 1737.276 | 52.32% | D |
| 12 | Chromic Vertisols | 217.1892 | 6.54% | |

## 3.4 Data Processing and Analysis

The data analysis involves several steps, which includes

- Data pre-processing
- Hydrological modelling and analysis
- Statistical analysis
- Assessing the relationships between flow variability and its effects on the structure.

### 3.4.1 Data Pre-processing

The meteorological data obtained by the NMAoE are all grid data, which functions similarly to a design for ensuring the proper operation of road drainage systems. The grid data is generated by merging gauged observable data with globally accessible products like satellite proxies and model reanalysis data which are more accurate for the data that have missing value.(54)

To verify the accuracy of the grid data, the double mass curve approach is applied. The cumulative rainfall comparison between selected samples such as Abebe Keranso and Addis alem rainfall stations and other stations were depicted in figure 3.16 and 3.17 respectively, and the result for the other station were included in the appendix 1 of this paper. The comparison analysis confirmed that the data maintains a high level of consistency, thus indicating its good accuracy.

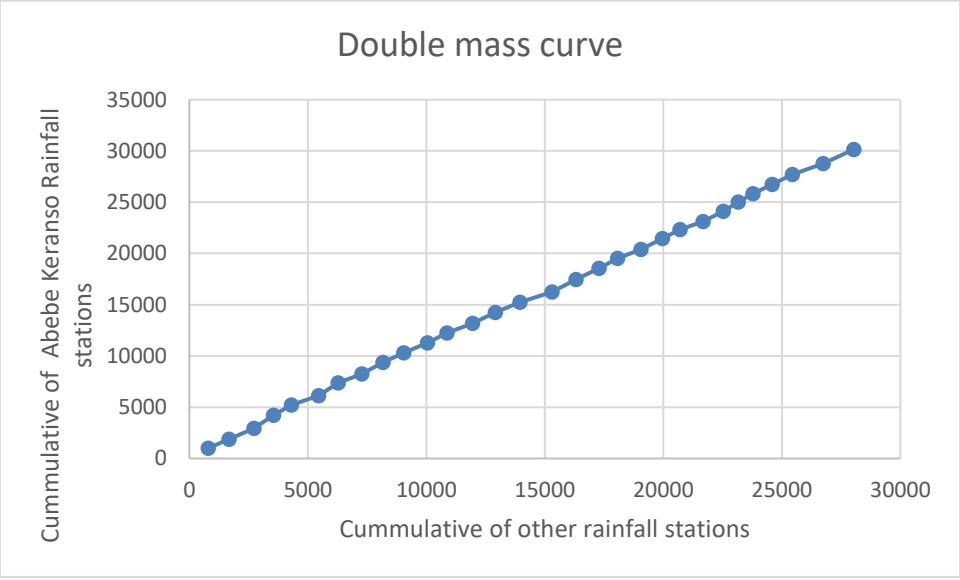

Figure 3-16: The cumulative rainfall comparison between Abebe Kerenso rainfall station and others using a double mass curve.

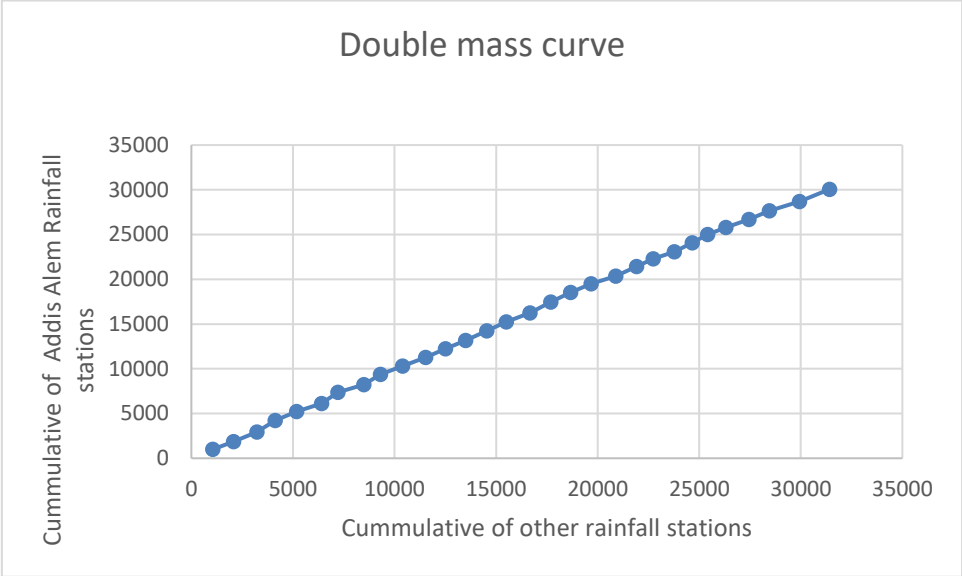


Figure 3-17: The cumulative rainfall comparison between Addis Alem rainfall station and others using a double mass curve.

### 3.4.2 Hydrological Modelling and Analysis

#### A. Assessment of hydrological model

The hydrological model selection assessment for this study involved assessment of various factors. This included analysis of the objectives, data availability and the intricacy of the subject area. In this study, due to their usability and capacity to handle data constraints, conceptual models like the Hydrological Simulation Program HEC-HMS were employed. HEC-HMS hydrological modelling is produced by the Hydrological Engineering center within the U.S Army Corps of Engineering. It is designed to simulate the complete hydrologic processes of watershed systems. In the model several data including rainfall, runoff, and stream flow routing were used to simulate the hydrologic processes within a watershed.

The selected model is sensitive to input parameters and spatial-temporal scales, eventually strikes a balance between accuracy and complexity, providing insights for drainage structure design and planning of emergency response in the Holeta to Ambo Road. Furthermore, the catchment delineation and preprocessing of drainage structures is performed using the Geographic Information System (GIS) tool integrated within the HEC-HMS 10.4 program.

### B. Model calibration and validation

Calibration and validation are critical steps in the hydrological modelling process that ensures the accuracy and reliability of the model's predictions when applied to real-world hydrological systems.(55)

In this study, the stream flow dataset was obtained from the Department of Hydrology, Ministry of Water and Energy in Ethiopia. The dataset was partitioned into two distinct sections. Section 1 comprises of time-series datasets 1991-2004 for Berga Nr. Addis Alem and Awash at Bello and 1997-2001 for Debris Nr. Guder that are used to calibrate the hydrologic model. Meanwhile, section B comprises of datasets from 2005-2011, 2005-2014 and 2002-2004 are used for Berga Nr. Addis Alem, Awash at Bello and Debris Nr.Guder respectively, and were used for model validation.

The dataset for the stream flow of each station was only complete for a specific period of time, and might not capture the latest stream flow data of the catchment. Hence, the Calibration and validation process exclusively focuses on hydro-gauge stations relevant to the case study area, and is based complete stream flow information in those stations.

The hydrological modelling is analysed using the HEC-HMS software. The efficiency and performance of HEC-HMS model is evaluated using different metrics, and some of the efficiency measure employed in the study were described below.[52]

#### i. Nash-Sutcliffe Efficiency

Nash-Sutcliffe Efficiency (NSE), also referred as the Nash-Sutcliffe model efficiency coefficient is a statistical measure used to assess the goodness of fit between observed and simulated hydrological data. It reflects the extent of the model in replicating the observed data.(56) NSE can be overly sensitive to extreme values or outliers in the dataset, which may skew the evaluation of model performance. It does not provide insights into other aspects of model behavior, such as pattern accuracy or timing accuracy.

The NSE formula is expressed as follows:

$$\boldsymbol{NSE = 1 - \frac{\sum_{i=1}^{n}(Q_o - Q_s)^2}{\sum_{i=1}^{n}(Q_o - \bar{Q}_o)^2}} \quad \text{----------Equation 3-1}$$

Where,

Σ: The summation symbol.

$Q_o$: The observed flow data.

Qs: The simulated flow data from the HEC-HMS model.
n: The number of observations
$\bar{Q}_o$: The mean of the observed flow data.

### ii. Root Mean Square Error

The Root Mean Square Error (RMSE) is another measure used to evaluate the accuracy of hydrological models. It indicates of the average magnitude of the errors between observed and simulated values. A lower value of RMSE is an indication of better fit of the model to the observed data. A value of zero indicates an accurate estimation. It is less sensitive compared to NSE but it is treats positive and negative errors equally, which may not be suitable if you want to distinguish between overestimations and underestimations. The RMSE formula is expressed as follows:

$$\boldsymbol{RMSE} = \sqrt{\frac{\mathbf{1}}{\boldsymbol{n}} \sum_{\boldsymbol{i=1}}^{\boldsymbol{n}} (\boldsymbol{Q_o} - \boldsymbol{Q_s})^{\mathbf{2}}} \quad \text{----------Equation 3-2}$$

Where,

$Q_o$: The observed flow data.
$Q_s$: Flow data from simulated HEC-HMS model.
n: The number of observations.

The value of RMSE is affected by outliers, where large errors have a greater effect on the result.

### iii. Coefficient of Determination ($R^2$):

The scatter plots of the computed discharge against the observed discharges are used to determine the coefficient of determination ($R^2$) for model calibration and validation at each hydrometric gauge station. The coefficient of determination, or $R^2$, is a metric that express the extent of the model explaining the variance in the observed data.it only focus on correction between the computed and observed one. A more satisfactory fit is indicated by higher values, which range from 0 to 1. However, it doesn't guarantee a good model fit if the errors are consistently biased in one direction.

$R^2$ is estimated using

$$\boldsymbol{R^2} = \left( \frac{\sum_{\boldsymbol{i=1}}^{\boldsymbol{n}} (\boldsymbol{Q_o} - \bar{\boldsymbol{Q}}_{\boldsymbol{o}})(\boldsymbol{Q_s} - \bar{\boldsymbol{Q}}_{\boldsymbol{s}})}{\sqrt{\sum_{\boldsymbol{i=1}}^{\boldsymbol{n}} (\boldsymbol{Q_o} - \bar{\boldsymbol{Q}}_{\boldsymbol{o}})^{\mathbf{2}} \sum_{\boldsymbol{i=1}}^{\boldsymbol{n}} (\boldsymbol{Q_s} - \bar{\boldsymbol{Q}}_{\boldsymbol{s}})^{\mathbf{2}}}} \right)^{\mathbf{2}} \quad \text{----------Equation 3-3}$$

Where,

$Q_o$: The observed flow data.
Qs: The simulated flow data from the HEC-HMS model.
n: The number of observations
$\bar{Q}_o$: The mean of the observed flow data.
$\bar{Q}_s$: The mean of the simulated runoff.

### iv. Percent Bias

The percent Bias (PBIAS) is a variation of bias that expresses the bias as a percentage of the mean observed flow. These measures show the direction and magnitude of the bias. But it does not provide insights into the pattern or directionality of errors.

The PBIAS is calculated as follows:

$$\boldsymbol{PBIAS = 100 * \frac{\sum_{i=1}^{n}(Q_s - Q_o)}{\sum_{i=1}^{n} Q_o}}$$ ----------Equation 3-4

Where,

$Q_o$: The observed flow data.
$Q_s$: Flow data from simulated HEC-HMS model.
n: The number of observations

In summary, the aforementioned four techniques (i-iv) are fundamental for assessing the performance of an HEC-HMS hydrological model. These measures offer insights on the extent of systematic bias, the extent of variance in the observed data and the extent of the model in reproducing the observed data. The use of this metrics together provides a comprehensive picture of the model efficiency and reliability. The performance rating of metric evaluation for daily flow presented in table below (57)

**Table 3-6** Summary statistic performance ratings ranges

| Performance Rating | NSE | RMSR | $R^2$ | PBIAS |
|---|---|---|---|---|
| Very Good | $0.65<NSE\leq1.00$ | $0.00<RMSR\leq0.60$ | $0.65< R^2\leq1.00$ | $PBIAS< \pm15$ |
| Good | $0.55<NSE\leq0.65$ | $0.60<RMSR\leq0.70$ | $0.55<R^2\leq0.65$ | $\pm15\leq PBIAS<\pm20$ |
| Satisfactory | $0.40<NSE\leq0.55$ | $0.70<RMSR\leq0.80$ | $0.40<R^2\leq0.55$ | $\pm20\leq PBIAS<\pm30$ |
| Unsatisfactory | $NSE\leq0.40$ | $RSMR>0.80$ | $R^2\leq0.40$ | $PBIAS\geq\pm30$ |

### C. Assessing Flow Variability

The coefficient of variation for the daily flows calculated for each drainage structure was computed in order to evaluate the flow variability. The study is predicated on a thorough dataset that includes thirty years' worth of rainfall data that has been gathered and examined to determine its variations over time. Through the examination of such a large time span, the study seeks to identify patterns and trends that may not be visible in analyses conducted over shorter time frames. A clear enhancement of variability occurs as the analytic scope increases, suggesting that rainfall patterns are dynamic in nature. Longer periods can give a clearer observation of how often variability occurred.

This coefficient of variance (CV) is estimated as follows

$$\mathbf{CV} = \frac{\boldsymbol{\sigma}}{\boldsymbol{X}} * 100 \quad \text{---------- Equation 3-5}$$

Where,

CV = Coefficient of Variance
$\sigma$ = Standard deviation of the daily flow
X = Mean of the daily flow

The higher the CV value, the more variable the flow time-series data. Typically, the CV value is classified as; low (CV<20%), moderate (20 %< CV<30%), high (CV<30%) and very high (CV>40%). (58, 59)

## 3.4.3 Statistical Analysis

The statistical analysis in hydrology helps in understanding the behavior of water resources, identifying trends, modelling of hydrological processes, and making informed decision-making in water resource management and environmental protection. It enables hydrologists to extract useful information from analysis and evaluate the impact human activity and natural variability on the water cycle.

### i. Frequency Analysis

A rainfall intensity-duration frequency curve is developed the design rainfall values at various return period and to estimate the peak flows at the outlet of the chosen drainage structures. The curve helps for estimating the intensity of rainfall events over various periods.

The process of estimating annual peak rainfall values involves the selection of the highest daily rainfall magnitude for each year, which represents the annual peak rainfall.(26) The table 3.6 shows the peak annual rainfall for the study period.

**Table 3-7: Estimated Annual peak Rainfall (mm)**

| Year | Annual Peak Rainfall (mm) | | Year | Annual Peak Rainfall (mm) |
|---|---|---|---|---|
| 1991 | 51.60 | | 2006 | 46.64 |
| 1992 | 59.13 | | 2007 | 46.41 |
| 1993 | 52.27 | | 2008 | 56.90 |
| 1994 | 65.47 | | 2009 | 55.90 |
| 1995 | 43.96 | | 2010 | 44.46 |
| 1996 | 75.75 | | 2011 | 43.30 |
| 1997 | 57.91 | | 2012 | 82.16 |
| 1998 | 56.13 | | 2013 | 59.23 |
| 1999 | 39.02 | | 2014 | 31.03 |
| 2000 | 58.00 | | 2015 | 36.23 |
| 2001 | 37.60 | | 2016 | 47.69 |
| 2002 | 41.61 | | 2017 | 66.54 |
| 2003 | 46.88 | | 2018 | 67.02 |
| 2004 | 43.36 | | 2019 | 48.13 |
| 2005 | 55.30 | | 2020 | 39.94 |

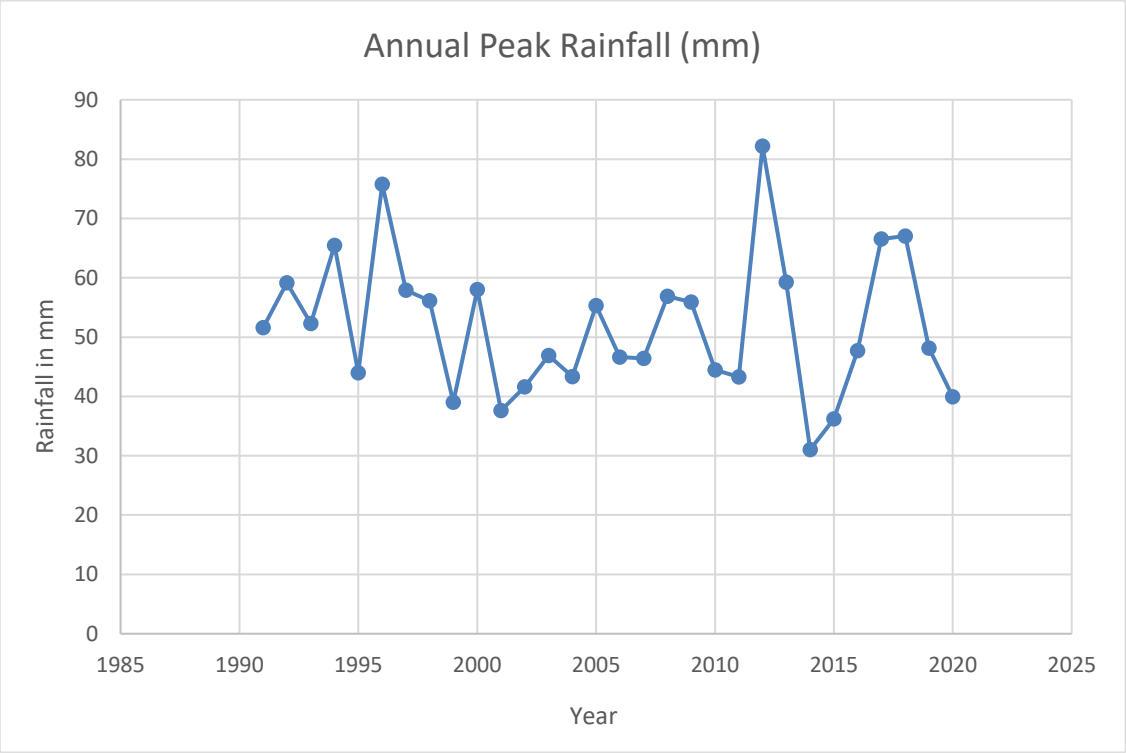


**Figure 3-18 Annual peak rainfall for the selected year**

### ii. Determination of Goodness-of-fit

In the development of the rainfall intensity-duration frequency curve, several probability distribution methods can be taken into account. Statistical analysis was performed on the peak yearly rainfall magnitudes to identify the probability distribution that best matches the patterns. Approximately twenty-three (23) distinct probability distributions, using the Easy Fit program, were selected for this study. The result of the three goodness-of-fit tests—the Anderson-Darling, Chi-Squared, and Kolmogorov tests were used to rank the distributions. The result is summarized in Table 3.7.

Therefore, the most widely used method the Gumbel Extreme Value Method (Gen. Extreme Value Method) was selected based on the ranking value of the goodness of fit summary. This Method assumes independence of extreme events, requires data to follow a Gumbel distribution, and may not be suitable for non-stationary conditions or situations with limited data. It might require a large amount of data to provide reliable estimates, which can be challenging to obtain, especially in cases where extreme events are rare.

Table 3-8: Goodness of Fit Summary Table used to rank distributions

**Goodness of Fit - Summary**

| # | Distribution | Kolmogorov Smirnov | | Anderson Darling | | Chi Squared | |
|---|---|---|---|---|---|---|---|
| | | Statistic | Rank | Statistic | Rank | Statistic | Rank |
| 1 | Beta | 0.08263 | 6 | 0.18566 | 4 | 6.8052 | 12 |
| 2 | Chi-Squared | 0.08831 | 8 | 0.40275 | 13 | 3.5969 | 2 |
| 3 | Chi-Squared (2P) | 0.10039 | 11 | 0.24227 | 10 | 4.9113 | 4 |
| 4 | Exponential | 0.43606 | 22 | 8.5141 | 22 | 20.618 | 20 |
| 5 | Exponential (2P) | 0.21187 | 19 | 3.5583 | 17 | 8.2576 | 19 |
| 6 | Gamma | 0.0974 | 10 | 0.21129 | 8 | 5.0835 | 6 |
| 7 | Gamma (3P) | 0.08078 | 3 | 0.17663 | 2 | 6.9612 | 13 |
| 8 | Gen. Extreme Value | 0.07762 | 1 | 0.17401 | 1 | 7.1621 | 16 |
| 9 | Gen. Pareto | 0.10858 | 12 | 4.0872 | 19 | N/A | |
| 10 | Gumbel Max | 0.07958 | 2 | 0.22479 | 9 | 7.0293 | 15 |
| 11 | Laplace | 0.17983 | 18 | 0.78757 | 16 | 4.9496 | 5 |
| 12 | Logistic | 0.13916 | 16 | 0.40717 | 14 | 4.0554 | 3 |
| 13 | Lognormal | 0.08979 | 9 | 0.1875 | 5 | 5.6317 | 10 |
| 14 | Lognormal (3P) | 0.08231 | 5 | 0.17975 | 3 | 7.0183 | 14 |
| 15 | Normal | 0.1237 | 14 | 0.37043 | 12 | 5.2802 | 8 |
| 16 | Pareto | 0.26067 | 21 | 5.8618 | 20 | 5.7824 | 11 |
| 17 | Rayleigh | 0.25174 | 20 | 3.8243 | 18 | 3.565 | 1 |
| 18 | Rayleigh (2P) | 0.08202 | 4 | 0.20241 | 7 | 7.5587 | 18 |
| 19 | Student's t | 0.96615 | 23 | 218.79 | 23 | 53437.0 | 21 |
| 20 | Triangular | 0.12492 | 15 | 0.30055 | 11 | 5.2655 | 7 |
| 21 | Uniform | 0.15293 | 17 | 7.905 | 21 | N/A | |
| 22 | Weibull | 0.11243 | 13 | 0.64725 | 15 | 5.347 | 9 |
| 23 | Weibull (3P) | 0.08385 | 7 | 0.19586 | 6 | 7.5279 | 17 |

The probability distribution curve is shown in Figure 3.19

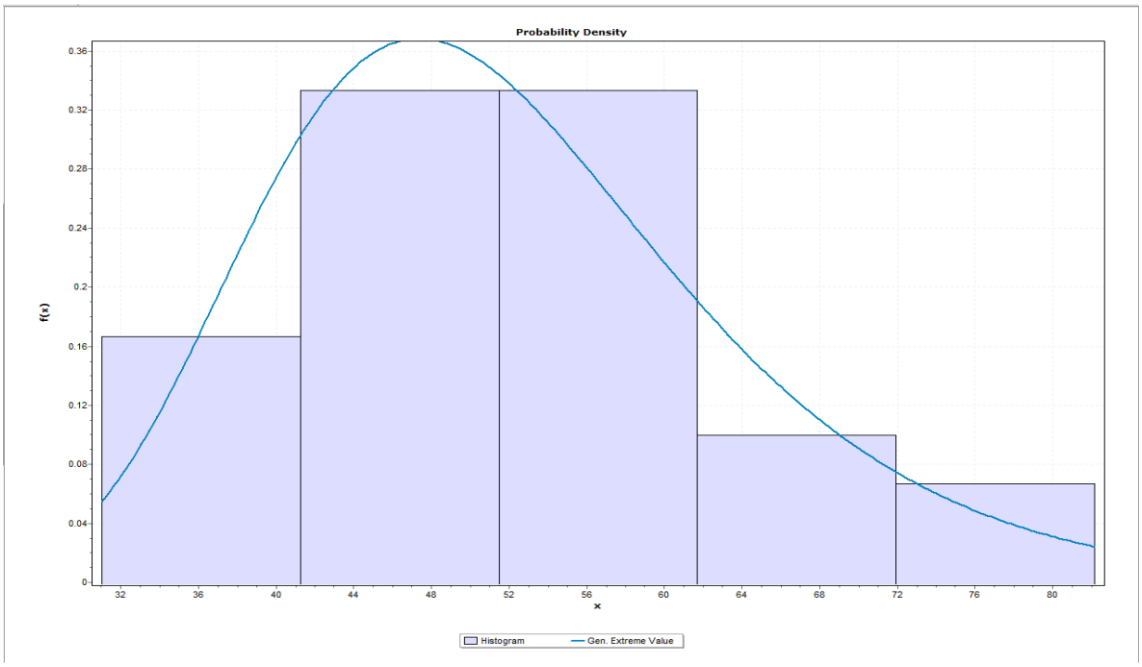


Figure 3-19: Probability Distribution Curve for Gen. Extreme Value

### iii. Flow estimation methods

There are several methods for predicting peak flow and estimating runoff. In this study, the SCS unit hydrograph lag time for transformation method, Muskingum routing method for routing method, and SCS Runoff Curve Number for loss method were used. The SCS Runoff Curve Number is a useful tool for estimating the quantity of rainfall that become runoff. These method uses the Curve Number (CN) concept and accounting for soil type, antecedent moisture conditions, and land use to predict runoff dynamics. It may not accurately represent complex hydrological processes in all situations, particularly in urban or heavily altered landscapes. The Muskingum Routing Method is used to simulate water flow through drainage. This method has limitations on its assumption of constant flow velocities and channel geometry, which may not reflect real-world conditions accurately. In addition, the SCS Unit Hydrograph Lag Time represents the delay between the peak of a rainfall event and the peak discharge but it does not account for distribution of travel times with in the watershed. The behaviour of watersheds, including flood response, flow routing, and runoff generation were simulated and forecasted using hydrological modelling.

By modelling the peak discharge that the structure is expected to accommodate for different return periods, the HEC-HMS can be used to perform a peak flow analysis for a drainage structure. The design rainfall data used as an input for the hydrological processes within the watershed. Estimation of the peak discharge regarding to different return period such as the 2-

year, 5-year, 10year, 25-year, or 100-year events, HEC-HMS uses complex hydrological algorithms and mathematical models.

### iv. Flood frequency

Flood frequencies are used to size different drainage projects in order to determine the best design that takes into account potential of damage as well as construction costs. The frequency of flooding should need to be considered during designing other structures along a road corridor. Using the size of the existing structure size, the frequency of the flood will be chosen for this particular project. Depending on the table 3.8 below sourced from ERADDM 2013.

Table 3-9: Design storm frequency (yrs) by geometric design criteria

| Structure Type | EW1/DC8/DC7 | | DC6/DC5 | | DC4/DC3 | | DC2/DC1/track | |
|---|---|---|---|---|---|---|---|---|
| | Design | Check | Design | Check | Design | Check | Design | Check |
| Gutters and Inlets* | 5/5/5 | 10/10/10 | 5/5 | 10/10 | 5/2 | 10/5 | --- | --- |
| Side Ditches | 10/10/10 | 25/25/25 | 5/5 | 10/10 | 5/2 | 10/5 | | |
| Ford/Low-Water Bridge | --- | --- | ---- | ---- | --- | --- | 5/5/5 | 10/10/10 |
| Culvert, pipe (see Note) Span<2m | 25/25/25 | 50/50/50 | 10/10 | 25/25 | 10/5 | 25/10 | 5/5/5 | 10/10/10 |
| Culvert, 2m< span<6m | 50/50/50 | 100/100/100 | 25/25 | 50/50 | 25/10 | 50/25 | 10/10/10 | 25/25/25 |
| Short Span Bridges 6m< span<15m | 50/50/50 | 100/100/100 | 25/25 | 50/50 | 25/10 | 50/25 | 10/10/10 | 25/25/25 |
| Medium Span Bridges 15m< span<50m | 100/100/100 | 200/200/200 | 50/50 | 100/100 | 50/25 | 100/50 | 50/25/25 | 100/50/50 |
| Long Span Bridges spans>50m | 100/100/100 | 200/200/200 | 50/50 | 100/100 | 50/25 | 100/50 | 50/25/25 | 100/50/50 |

## 3.4.4 Assessing the relationships between flow variability and its effects on the structure

## I. Assessing capacity of Existing Drainage Structures

To assess the capacity of drainage structures along the Holeta to Ambo road, the actual opening dimension of each drainage structure is measured on site. Once the span, vertical clearance

height, and pipe diameter are measured, the capacity of drainage structure to accommodate the incoming discharge is calculated using Manning's formula. This formula is widely used for open-channel flow calculations. The Manning formula is primarily suitable for steady, uniform flow conditions in natural or man-made channels with simple geometriesnd and also he formula depnd on accurate estimation of Manning's roughness coefficient (n value), which can vary significantly depending on factors such as channel geometry, surface roughness, and flow conditions. Small inaccuracies in the n value can lead to significant errors in calculated flow rates.Attached in appendix 3 of this research paper all the type and opening size of the structure,those are the flow variability observed over 30 years.

The Manning's formula isgiven by:

$$\boldsymbol{Q = \frac{1}{n} A R^{\frac{2}{3}} S^{\frac{1}{2}}}$$----------Equation 3-6

Where:

Q is the flow rate ($m^3$ /s)

A is the cross-sectional area of the flow ($m^2$)

S is the longitudinal gradient of the channel (m/m)

n is the Manning roughness coefficient

R is hydraulic radius expressed by R= $\frac{A}{P}$

P is wetted perimeter, m

The parameter used in manning's formula are either calculated or taken from ERA DDM 2013 for example roughness coefficient depending on the site visual observation the n value is obtained from the specified manual the others like area and perimeter are calculated the from the opening measured at site and slope is calculated the crossing profile of the stream channel.

## II. Flooding Risk

Assessing the discharge calculated for a design storm in relation to the capacity of drainage structures is important in hydraulic engineering. The design storm, which is created using historical rainfall data, is a benchmark for extreme but realistic precipitation within a defined return period.

Through hydrological models, computing the expected runoff for this scenario, representing the flow rate in the drainage system. Simultaneously, the capacity of drainage structures, determined by their specifications, is evaluated.

The ensuing comparison between the calculated discharge and the structural capacity of the drainage system serves as a crucial evaluation of its effectiveness. This comparison allows for insights into the adequacy of the system's design. Consistent underutilization of the structural capacity implies that the system may have been excessively designed, leading to inefficiencies and potentially unnecessary costs. On the other hand, if the calculated discharge consistently exceeds the structural capacity, it signals a significant concern for potential flooding risks. This scenario highlights the inadequacy of the drainage system to handle the expected water flow, posing a threat to infrastructure, property, and public safety. Therefore, in evaluating excess design and potential flood risk, the comparison between calculated discharge and structural capacity stands as a fundamental criterion.

## III. Sedimentation

Sedimentation mostly occur in culverts because culverts have relatively smaller opening this makes susceptible to blockage and hydraulic inefficiency compared to bridge. The accumulation of sediment,such as sand, silt, and gravel in culverts is reffered as sedimentation. Various factors can contribute to sedimentation, which includes erosion, flooding, heavy rainfall, poor drainage, and lack of maintenance. The culvert blockage caused by sedimentation may result in flooding and culvert damage.

Furthermore, factors such as the shape, size, and alignment of the culvert impact sediment behaviors. The effect of sedmentation on culverts were analysed by comparing the capacity of culverts before and after sedimented. Before sedimented using the opening size the culvert capacity is calculated and after sedimentation is the condition of culvert during site visit was measured and calculate the capacity remaing from sedimented section.

## IV. Scouring effect due to flow velocity

High speeds flow has the potential to scour and erode the river bed and bank. Permissible velocities are consequently the highest allowable speeds that can be used in an unlined channel without damaging the underlying material or producing scour.(59)

The flow velocity for each structure is calculated using the Manning's formula below, and the measurements of the opening size of the structures are taken on site measurement.

$$\boldsymbol{V = \frac{1}{n} R^{\frac{2}{3}} S^{\frac{1}{2}}}$$----------Equation 3-7

Where:

V is flow velocity in (m/s)
S is the longitudinal gradient of the channel (m/m)
n is the Manning roughness coefficient
R is hydraulic radius expressed as $R=\frac{A}{P}$, where, A is the cross-sectional area of the flow ($m^2$)
P is wetted perimeter, m

Table 3.9 contains a list of the commonly permissible maximum velocities for a few different types of soil and lining materials. (60)

Table 3-10: The permissible maximum velocities for soil types and lining materials

| **No.** | **Nature of boundary** | **Permissible maximum Velocity(m/s)** |
|---|---|---|
| 1 | Sandy soil | 0.30-0.60 |
| 2 | Black cotton soil | 0.60-0.90 |
| 3 | Muram and Hard soil | 0.90-1.10 |
| 4 | Firm clay and loam | 0.09-1.15 |
| 5 | Gravel | 1.2 |
| 6 | Disintegrated rock | 1.5 |
| 7 | Hard rock | 4 |
| 8 | Brick masonry with cement pointing | 2.5 |
| 9 | Brick masonry with cement plaster | 4 |
| 10 | Concrete | 6 |
| 11 | Steel lining | 10 |

*[source: K. Subramanya "Flow in open Channel "Third edition]*

# 4 RESULTS AND DISCUSSIONS

## 4.1 Hydrological Model Precision through Optimized Setup

The hydrological model setup for Berga Nr. Addis Alem, Awash Bello, and Debis Nr. Guder HG for catchment and river were delineated using the GIS tool of HEC-HMS. The hydrological model setup for the three gauge station is displayed in figure4.1-4.3

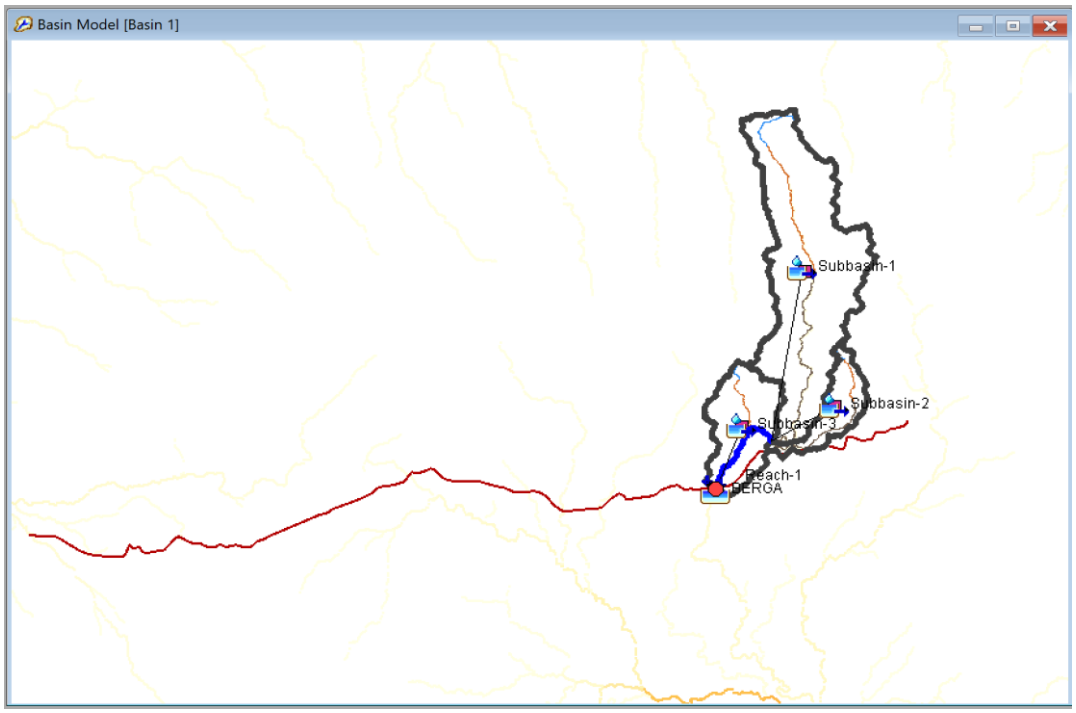


Figure 4-1: HEC-HMS Model Setup for Berga Nr. Addis Alem station

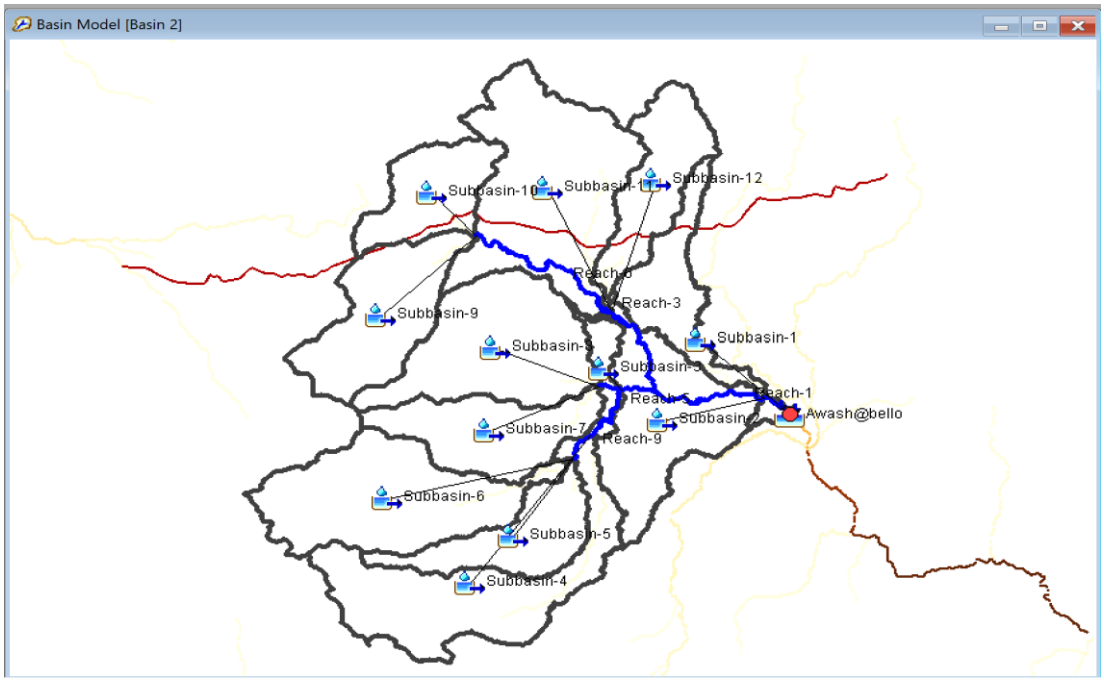


Figure 4-2: HEC-HMS Model Setup for Awash Bello station

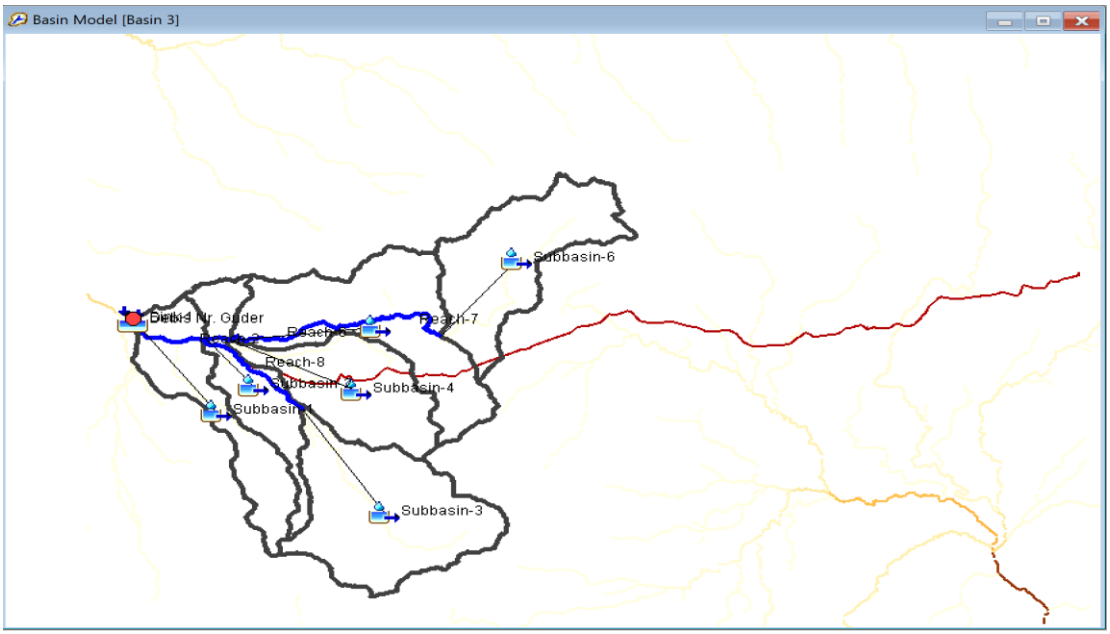


Figure 4-3: HEC-HMS Model Setup for Debis Nr. Guder station

## 4.2 Hydrological Model Calibration

The calibration and validation periods for each station, 1991-2004 and 2005-2011 for Berga Nr Addis Alem, 1991-2004 and 2005-2014 for Awash Bello and 1997-2001 and 2002-2004 for Debis Nr.Guder. Successful calibration yields a model accurately depicting watershed dynamics, establishing a reliable tool for precise hydrological predictions.

In this study, the hydrological process simulation is performed using loss method, specifically using the SCS Runoff Curve Number, which ranges from 70.05-79.63, the Muskingum routing method is used to simulate the movement of water through drainage overtime and the SCS unit hydrograph lag time is used to predict the hydrologic behaviour of watershed. The value of lag time ranges from 21.55-337.47.

The result of catchment area, CN value and lag time is presented in the accompanying table 4.1 for each selected drainage structures.

Table 4-1: The drainage structure catchment area, CN value and lag time

| ID | Area (sq.km) | CN | Lag Time(min) | | ID | Area (sq.km) | CN | Lag Time(min) |
|---|---|---|---|---|---|---|---|---|
| C1 | 1.46 | 72.46 | 75.71 | | C29 | 0.24 | 75 | 35.88 |
| C2 | 1.49 | 72.87 | 68.87 | | C30 | 2.30 | 77.69 | 33.59 |
| C3 | 0.39 | 72.02 | 36.82 | | C31 | 0.28 | 70.19 | 29.43 |
| C4 | 1.22 | 71.32 | 65.27 | | C32 | 0.25 | 70.19 | 24.55 |
| C5 | 7.59 | 79.63 | 82.81 | | C33 | 85.99 | 79.1 | 108.27 |
| C6 | 1.15 | 75.13 | 54.41 | | C34 | 0.20 | 70.9 | 23.88 |
| C7 | 1.05 | 75.89 | 50.91 | | C35 | 0.28 | 75.08 | 30.67 |
| C8 | 0.14 | 76.71 | 33.78 | | C36 | 0.25 | 75.78 | 28.53 |
| C9 | 215.06 | 73.29 | 337.47 | | C37 | 1.10 | 76.03 | 51.73 |
| C10 | 7.25 | 76.68 | 43.49 | | C38 | 0.39 | 74.5 | 34.66 |
| C11 | 12.43 | 72.4 | 50.46 | | C39 | 4.20 | 73.44 | 126.52 |
| C12 | 3.66 | 70.17 | 38.62 | | C40 | 3.84 | 78.58 | 70.03 |
| C13 | 4.50 | 75.63 | 32.38 | | C41 | 17.54 | 78.09 | 70.03 |
| C14 | 1.06 | 75.91 | 52.87 | | C42 | 8.39 | 77.34 | 45.13 |
| C15 | 8.03 | 77.57 | 75.91 | | C43 | 0.71 | 73.84 | 46.82 |
| C16 | 81.05 | 71.68 | 71.44 | | C44 | 3.81 | 78.98 | 79.69 |
| C17 | 0.41 | 70.06 | 39.56 | | C45 | 2.76 | 76.32 | 59.49 |
| C18 | 0.65 | 70.85 | 41.99 | | C46 | 30.70 | 77.43 | 62.46 |
| C19 | 136.22 | 74.35 | 202.84 | | C47 | 8.10 | 78.94 | 33.89 |
| C20 | 0.55 | 70.05 | 54.29 | | C48 | 15.66 | 75.06 | 53.98 |
| C21 | 0.53 | 70.6 | 48.87 | | C49 | 0.17 | 72.44 | 28.6 |
| C22 | 6.15 | 71.15 | 63.4 | | C50 | 2.92 | 71.77 | 58.01 |
| C23 | 25.79 | 76.4 | 141.05 | | C51 | 15.45 | 75.02 | 90.67 |
| C24 | 15.68 | 79.09 | 65.39 | | C52 | 0.12 | 74.89 | 21.55 |
| C25 | 25.61 | 76.79 | 56.15 | | C53 | 10.65 | 78.55 | 61.71 |
| C26 | 0.44 | 70.91 | 39.56 | | C54 | 1.87 | 77.55 | 72.47 |
| C27 | 0.23 | 70.64 | 31.64 | | C55 | 0.26 | 78.43 | 22.56 |
| C28 | 8.83 | 70.25 | 42.93 | | C56 | 245.76 | 79.34 | 158.68 |

In the summary result of calibrated model for the three station the peak Seems the model consistently underestimate as it is less than the observed flow this is because could be attributed to a combination of factors related to input data quality and uncertainties in observations

including measurement errors and spatial/temporal representativeness. The summary result of calibrated model for the three stations are depicted in Figure 4.4-4.6

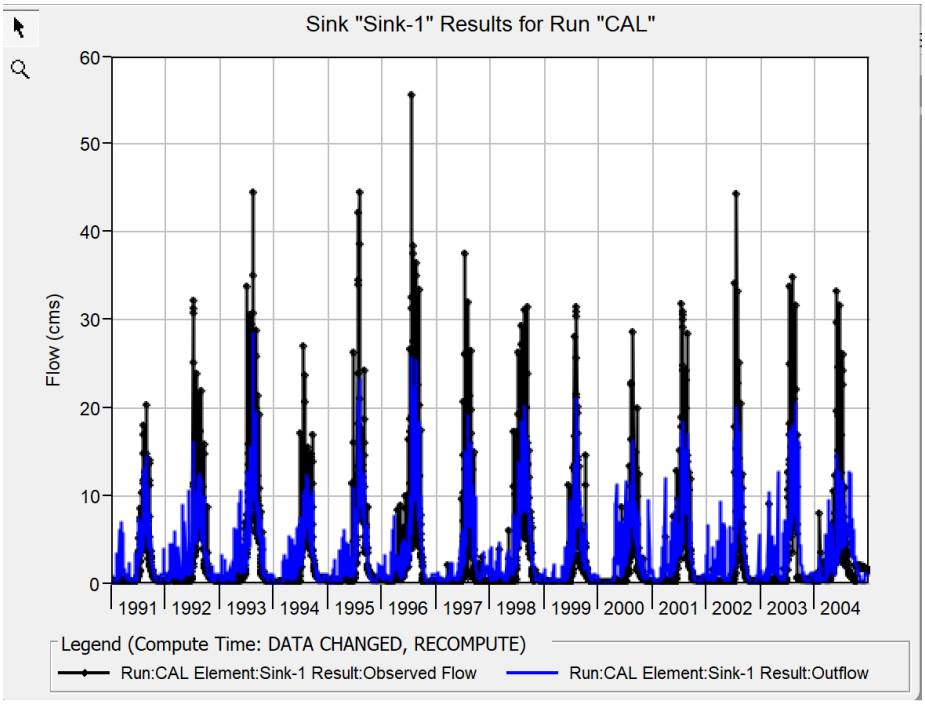


Figure 4-4: The model calibration result of Berga Nr. Addis alem Station

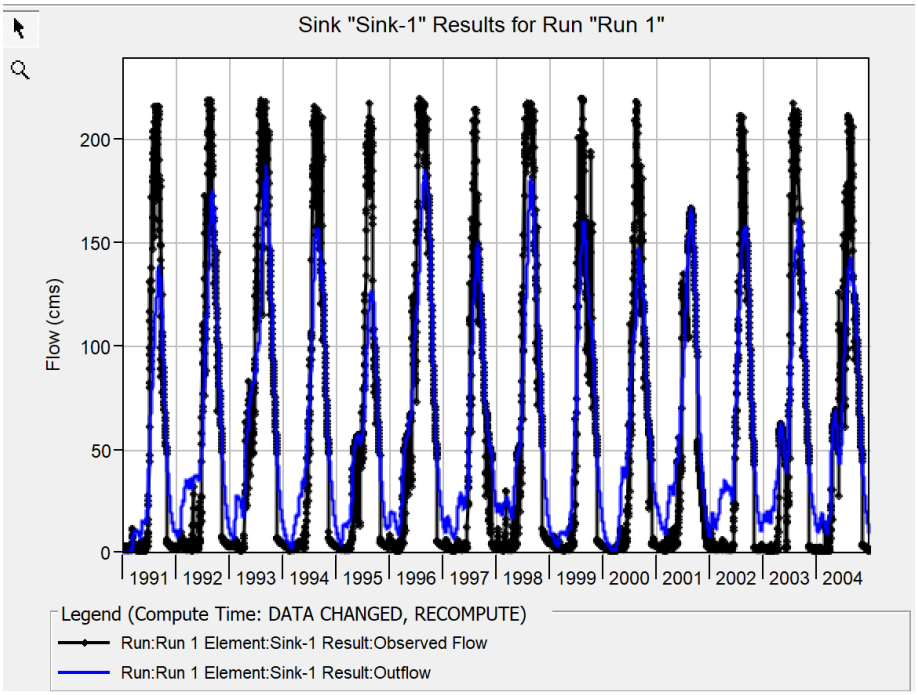


Figure 4-5: The model calibration results on Awash Bello Station

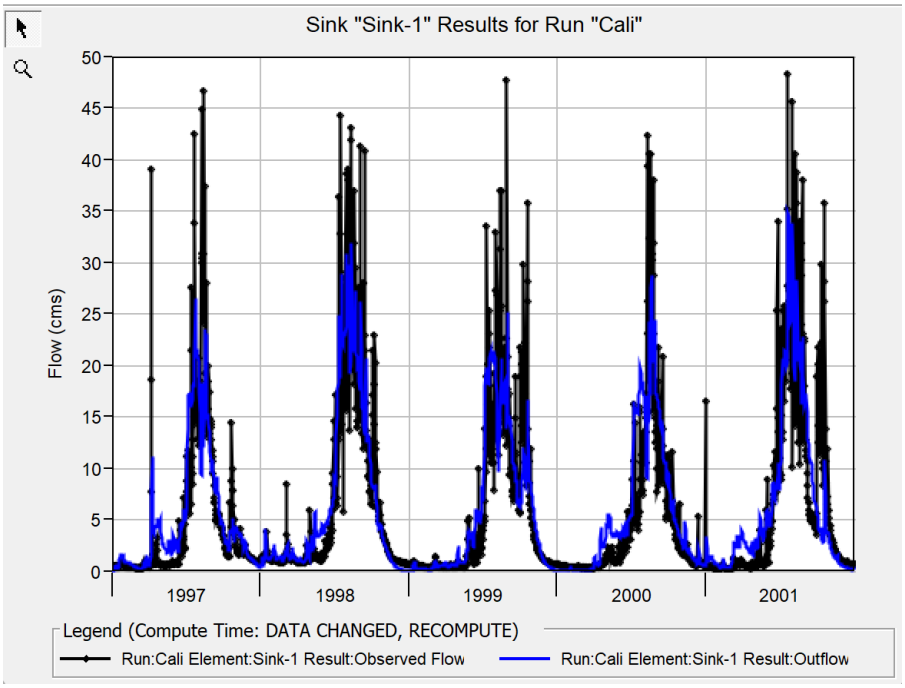


Figure 4-6: The model calibration result on Debis Nr. Guder Station

### 4.2.1 Model performance check result

**I. Nash and Sutcliffe Efficiency, root mean square error and percentage bias**

The model performance result using the Nash-Sutcliffe Efficiency (NSE) check is 0.684, 0.842, and 0.661 for the Berga Nr. Addis Alem, Awash Bello, and Debis Nr. Guder HG Stations, respectively. Similarly, the Root Mean Square Error of the three stations (i.e., Berga Nr. Addis Alem, Awash Bello, and Debis Nr. Guder HG Stations) is 0.6, 0.4, and 0.6, respectively. Furthermore, the percentage bias for the three stations is 4.79%, 3.91%, and 0.49%, respectively. The results are within the statistically acceptable range for surface runoff model calibration and validation. This value is greater than 0.65 for NSE, ranges from 0 to 0.6 for an RMSE, and less than 15% for PBIAS performance check measures. The finding of performance check assessments is shown in figure 4.7-4.9 below, which shows the model's calibration based on NSE, RMSE, and PBIAS metrics for the Berga Nr. Addis Alem, Awash Bello, and Debis Nr. Guder HG stations.

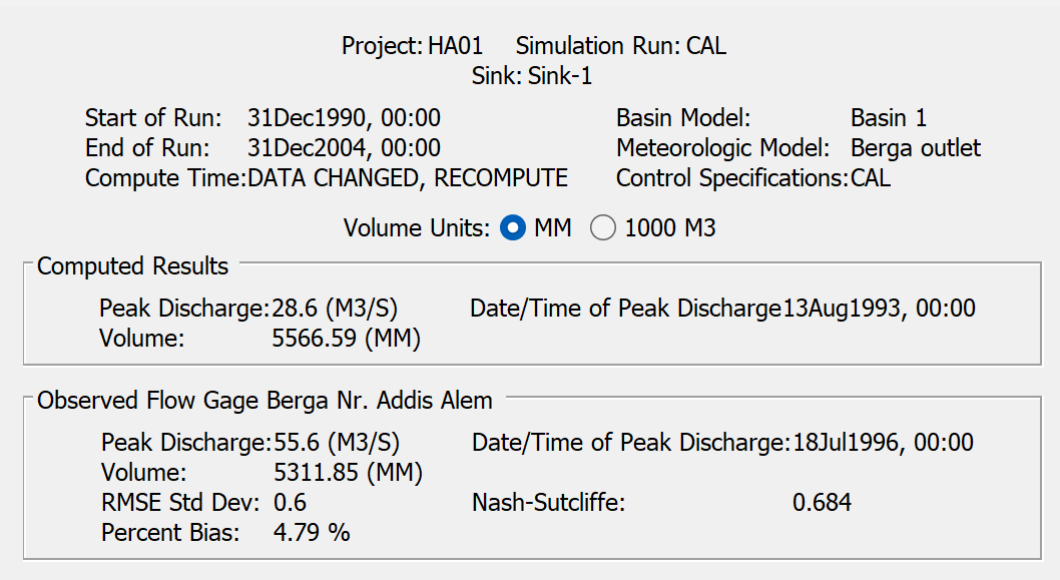


Figure 4-7: Summary table result of model calibration at Berga Nr. Addia alem station

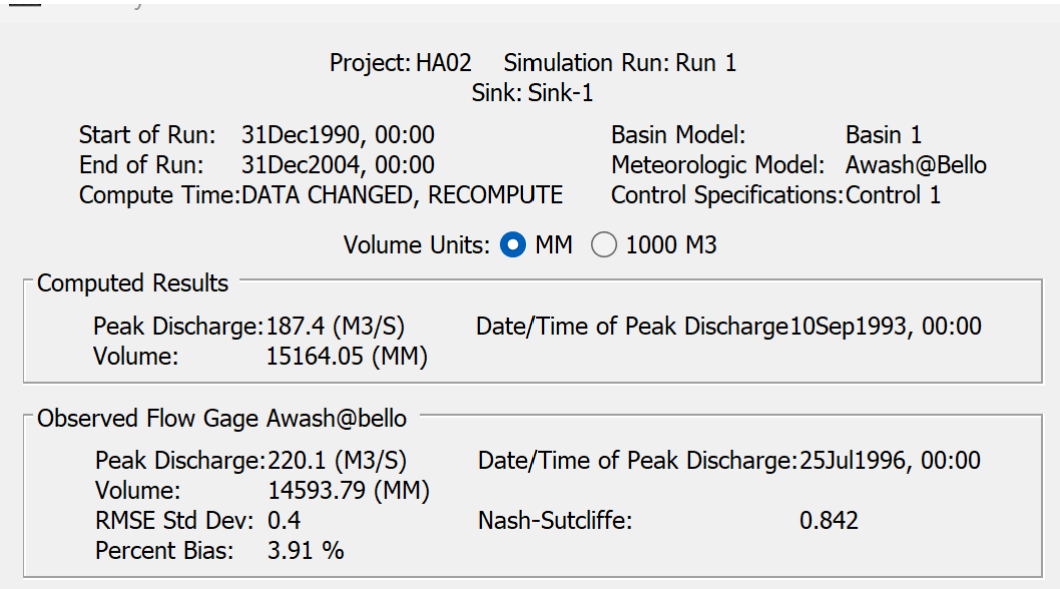


Figure 4-8: Summary table result of model calibration at Awash at Bello station

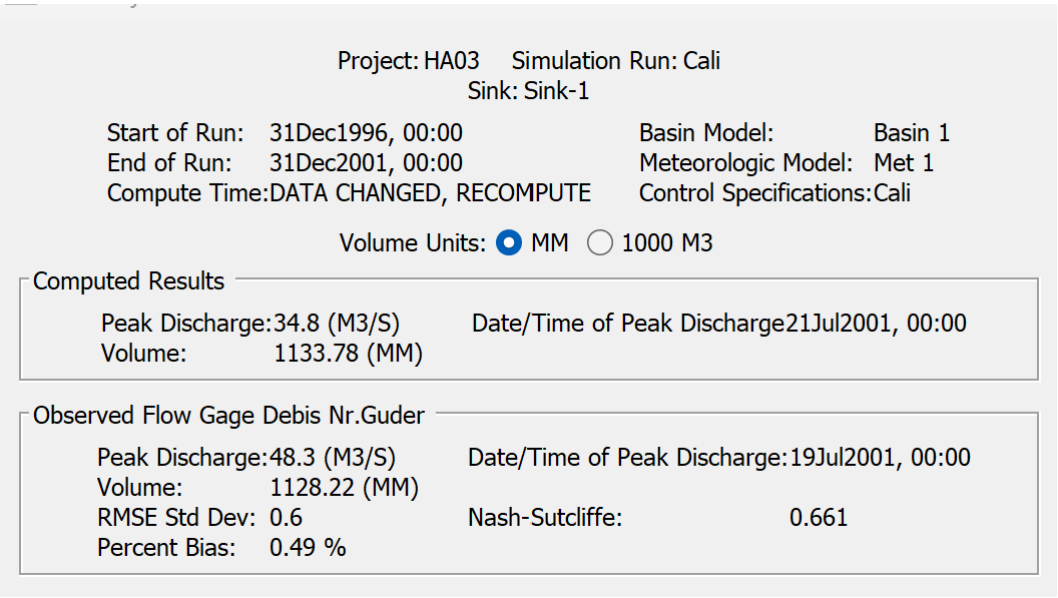


**Figure 4-9: Summary table result of model calibration at Debis Nr.Guder station**

## II. Coefficient of Determination, $R^2$

The scatter plots comparing the computed against the observed discharges showed a positive correlation for all the three stations: Berga Nr. Addis Alem, Awash Bello, and Debis Nr. Guder HG stations. This implies that the estimated discharge and the observed discharge increase simultaneously, and vice versa.

The R-squared values, the proportion of variance explained, Berga Nr. Addis Alem, Awash Bello, and Debis Nr. Guder HG stations are 0.71, 0.85, and 0.66, respectively. This implies that the model can efficiently predict future discharge events based on input data, enabling well-informed decisions on the management of water resources, and forecasting of flood. The plots of the computed against observed discharge values for each of the three stations are displayed in Figures 4.10- 4.12.

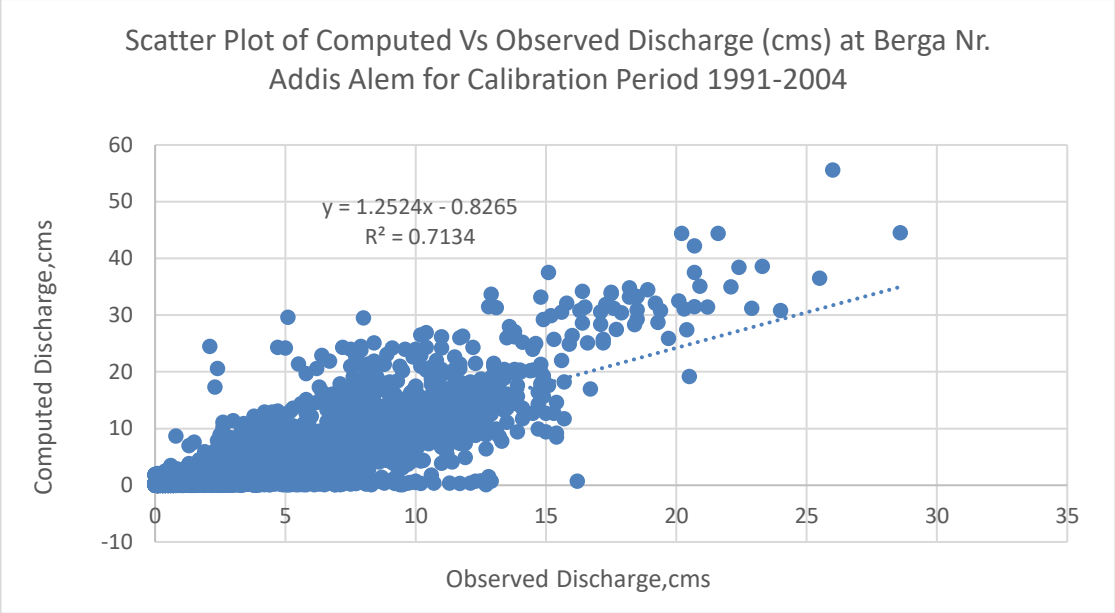


Figure 4-10: The coefficient of determination of model calibration at Berga Nr. Addis Alem Station (1991-2004)

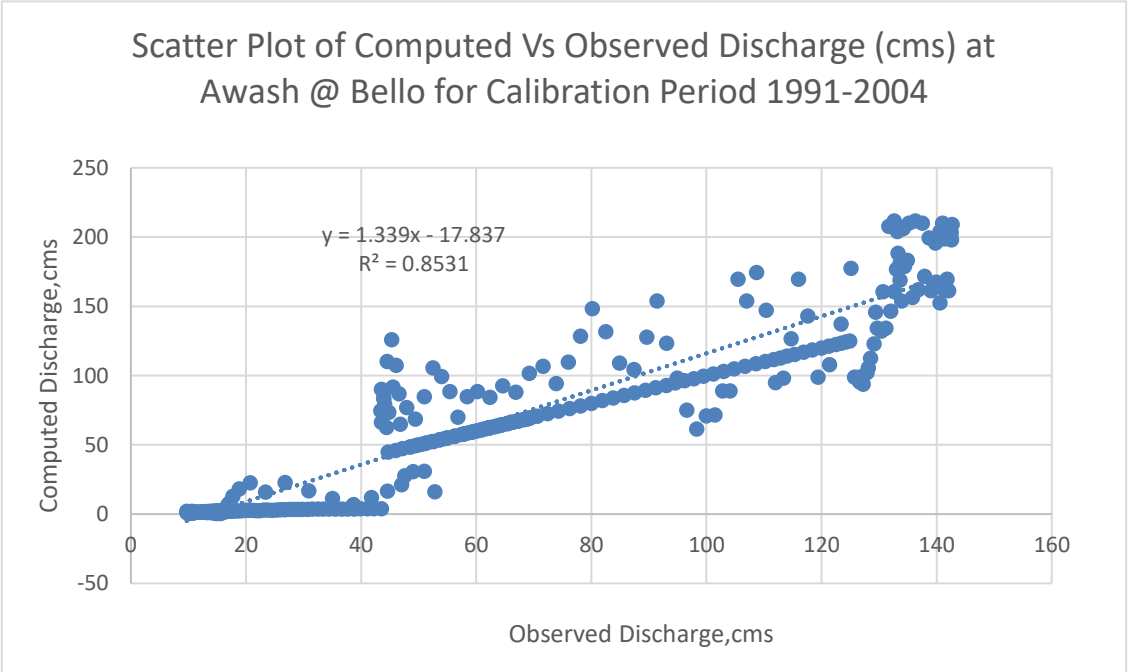


Figure 4-11: The coefficient of determination of model calibration at Awash at Bello Station (1991-2004)

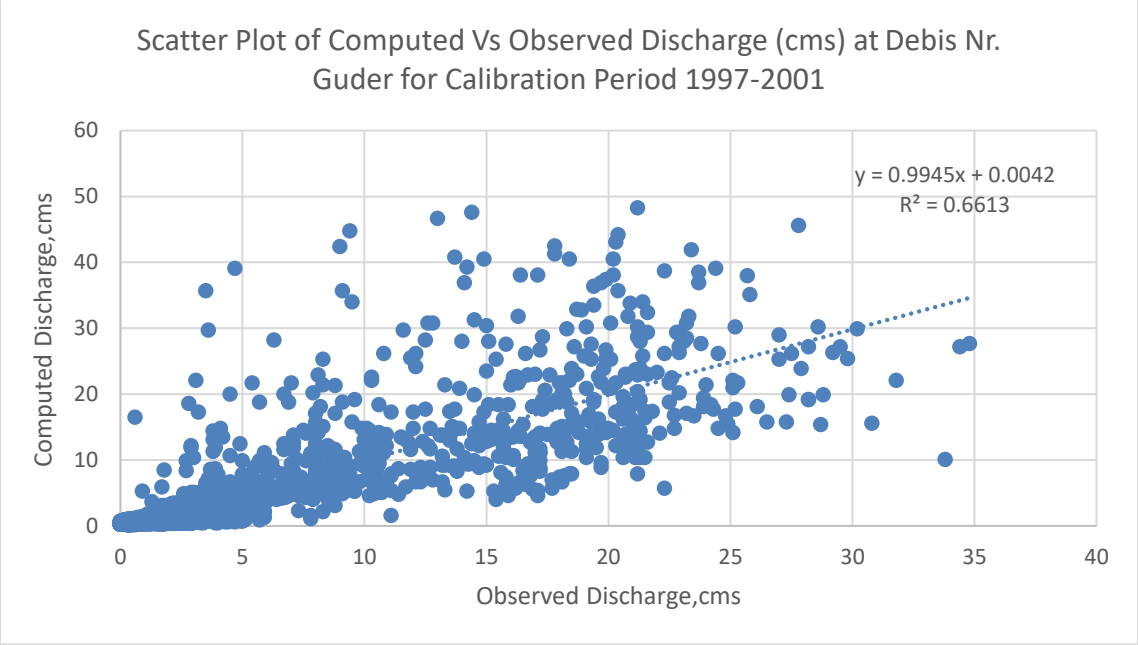


Figure 4-12: The coefficient of determination of model calibration at Debis Nr. Guder Station (1997-2001)

Table 4-2: Summary Table for the performance rating on Calibration and validation

| ***HG stations*** | ***Berga Nr. Addis Alem*** | ***Awash @ Bello*** | ***Debris Nr. Guder*** |
|---|---|---|---|
| ***Calibration Period*** | **1991-2004** | **1991-2004** | **1997-2001** |
| *NSE* | 0.684 | 0.842 | 0.661 |
| *RMSE* | 0.6 | 0.4 | 0.6 |
| *PBIAS* | 4.79 | 3.91 | 0.49 |
| $R^2$ | 0.7134 | 0.8485 | 0.6613 |
| *Performance Rating* | Very Good | Very Good | Very Good |
| ***Validation Period*** | **2005-2011** | **2005-2014** | **2002-2004** |
| *NSE* | 0.664 | 0.793 | 0.708 |
| *RMSE* | 0.6 | 0.5 | 0.5 |
| *PBIAS* | 16.58 | 13.4 | 14.56 |
| $R^2$ | 0.6959 | 0.8266 | 0.7165 |
| *Performance Rating* | Very Good | Very Good | Very Good |

## 4.3 Daily flow of each Drainage structures

This study examined 56 drainage structures, including bridges and culverts. For each of these, the daily flow was simulated using the calibrated HEC–HMS model for 30 years (1991–2020), as an example the result for C09 drainage structure is below. High coefficient of variation in daily flow variability for drainage structures can be attributed to a combination of natural hydrological processes and watershed characteristics.The plots for other drainage structure are included in the appendix 2.

The daily discharge flow graph of C09 spanning from 1991 to 2002 exemplifies the fluctuating nature of water flow. Notably, August consistently emerges as the peak flow period throughout these years. In 1991, the peak flow commenced at 23.9m3/s, steadily increasing over the subsequent years. By 1993, it surged to 27.1m3/s, signifying an upward trend. However, in 1994, a slight decline was observed, with the peak flow dropping to 22.2m3/s. Nevertheless, the trend swiftly reversed in 1995, recording a substantial peak flow of 28.6m3/s. This pattern persisted into 1996. Again from 1997 to 2020 it is decline from 21m3/s-23.9m3/s then it return back again increased to 25.5m3/s and 26.1m3/s in 2001 and 2002 respectively. Such fluctuations underscore the dynamic and variable nature of flow rates during this period.

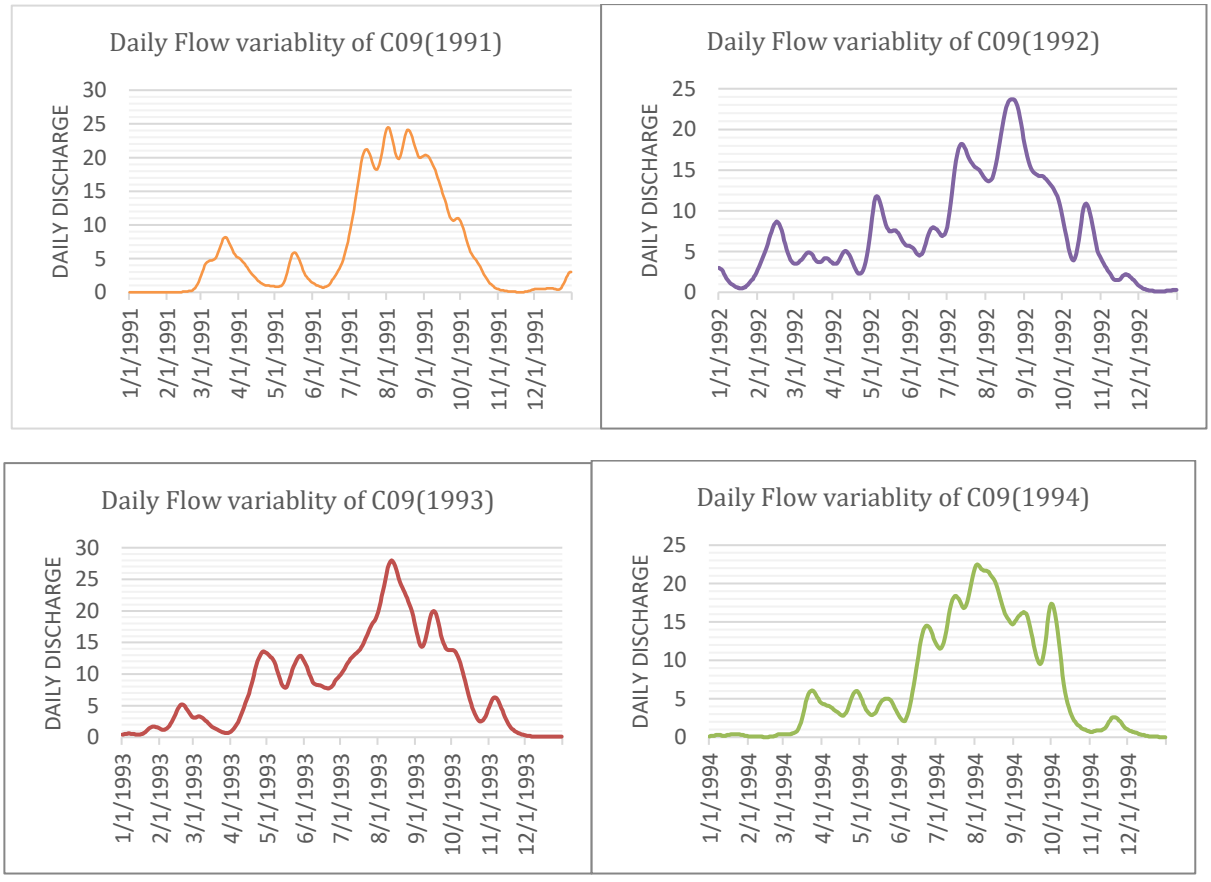

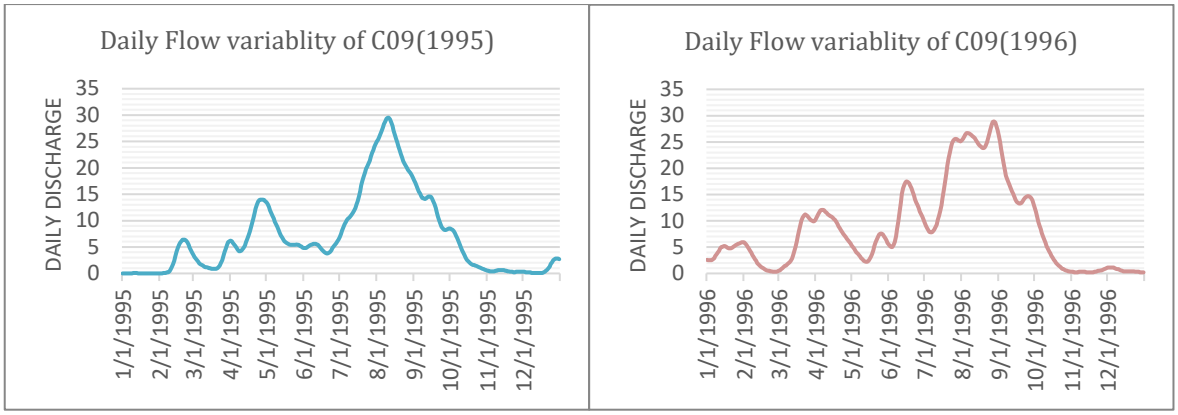


Figure 4-13: Daily flow discharge for C09 year (1991-1996)

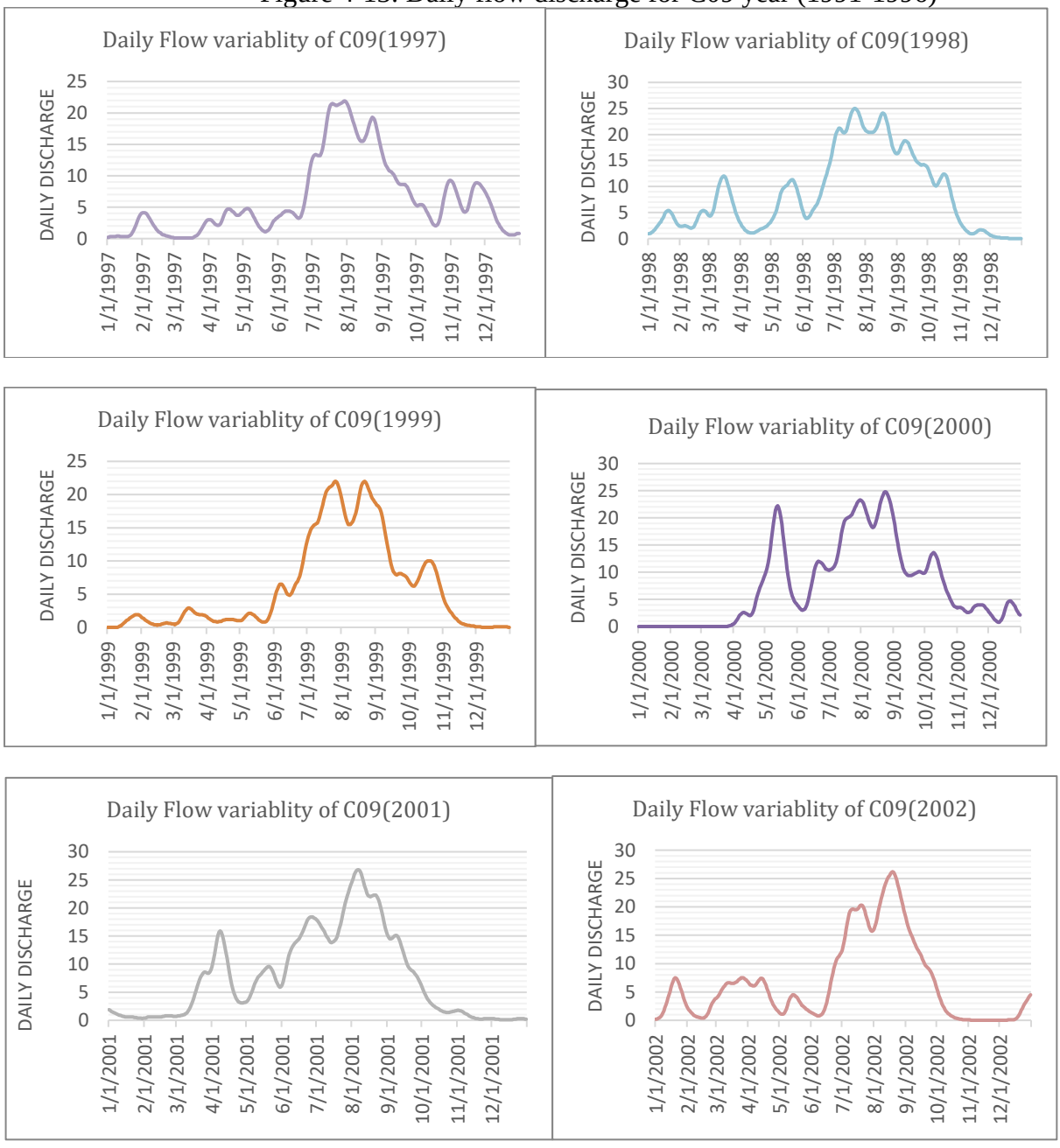


Figure 4-14: Daily flow discharge for C09 year (1997-2002)

### 4.3.1 Daily flow variability of each Drainage structure

The flow variability was investigated by calculating the coefficient of variance for each drainage structure daily flow estimates. The coefficient of variance (CV) for the drainage structure ranges from 5.7% (C08) to 99% (C09).

The wide range of coefficients of variance observed for drainage structures underscores the significant variability in their performance and characteristics. For culverts, where the coefficient spans from 5.7% to 95.6%, Similarly, the coefficient range of 2.5% to 99.2% for bridges implies an even broader spectrum of variability, indicating diverse structural designs, materials, and environmental influences.

The coefficient of variance of the drainage structures shows that 5% of the structures are showing low variability,11% of the structures showing moderate variability, 13% structures are showing high variability and the rest more than 71% of the structures have a coefficient of variance exceeding 40%. In this particular study the drainage structure which have high coefficient variance is selected in order to give priority for those structures. This indicates that approximately 40 structures are exposed to fluctuating flow. This implies that there is a considerable degree of flow variability present in these structures. The calculated CV for each structure is given in table 4.3.

**Table 4-3: Calculated coefficient of variance for the drainage structures**

| ID | MEAN | STD | CV (%) | | ID | MEAN | STD | CV (%) |
|---|---|---|---|---|---|---|---|---|
| C01 | 0.08 | 0.04 | 53.3% | | C29 | 0.07 | 0.02 | 31.9% |
| C02 | 0.05 | 0.04 | 77.6% | | C30 | 0.12 | 0.07 | 58.0% |
| C03 | 0.04 | 0.01 | 35.8% | | C31 | 0.07 | 0.02 | 26.6% |
| C04 | 0.05 | 0.03 | 68.0% | | C32 | 0.07 | 0.02 | 26.4% |
| C05 | 0.27 | 0.25 | 93.4% | | C33 | 3.44 | 3.10 | 89.9% |
| C06 | 0.09 | 0.07 | 83.6% | | C34 | 0.04 | 0.01 | 37.7% |
| C07 | 0.05 | 0.03 | 63.5% | | C35 | 0.04 | 0.01 | 39.2% |
| C08 | 0.01 | 0.00 | 5.7% | | C36 | 0.04 | 0.02 | 37.6% |
| C09 | 7.40 | 7.33 | 99.0% | | C37 | 0.07 | 0.04 | 52.8% |
| C10 | 0.24 | 0.22 | 93.7% | | C38 | 0.03 | 0.01 | 32.8% |
| C11 | 0.41 | 0.39 | 95.6% | | C39 | 0.24 | 0.14 | 60.4% |
| C12 | 0.14 | 0.13 | 95.6% | | C40 | 0.11 | 0.06 | 57.1% |
| C13 | 0.08 | 0.04 | 52.4% | | C41 | 0.06 | 0.04 | 74.9% |
| C14 | 0.06 | 0.03 | 48.7% | | C42 | 0.38 | 0.29 | 76.3% |
| C15 | 0.33 | 0.24 | 73.3% | | C43 | 0.04 | 0.02 | 47.8% |
| C16 | 3.64 | 2.55 | 70.0% | | C44 | 0.18 | 0.13 | 72.5% |
| C17 | 0.02 | 0.01 | 26.2% | | C45 | 0.11 | 0.08 | 75.9% |
| C18 | 0.12 | 0.04 | 33.2% | | C46 | 1.13 | 0.97 | 86.1% |
| C19 | 4.44 | 4.41 | 99.2% | | C47 | 0.04 | 0.02 | 44.1% |
| C20 | 0.02 | 0.01 | 48.0% | | C48 | 0.58 | 0.50 | 85.8% |
| C21 | 0.01 | 0.00 | 46.3% | | C49 | 0.00 | 0.00 | 2.5% |
| C22 | 0.20 | 0.18 | 92.2% | | C50 | 0.12 | 0.09 | 76.4% |
| C23 | 1.17 | 1.16 | 99.0% | | C51 | 0.57 | 0.49 | 85.8% |
| C24 | 0.89 | 0.88 | 98.4% | | C52 | 0.03 | 0.01 | 28.7% |
| C25 | 0.92 | 0.91 | 98.6% | | C53 | 0.39 | 0.34 | 86.7% |
| C26 | 0.30 | 0.09 | 28.9% | | C54 | 0.08 | 0.06 | 71.5% |
| C27 | 0.28 | 0.08 | 28.8% | | C55 | 0.02 | 0.00 | 19.9% |
| C28 | 0.25 | 0.24 | 95.9% | | C56 | 10.01 | 8.30 | 82.9% |

## 4.4 Design Rainfall Estimation

This study uses the Gen. Extreme Value (GEV) to estimate the design rainfall magnitudes at different return periods for different durations.

The depth of is the magnitude of rainfall per unit of time for a given return period (i.e., 2-500 years). For example, as shown in the table 4-4, over a 100-year period, a rainfall event with a magnitude of around 88.88 mm is expected to occur once per 100 years on average over 24-hour duration. This design rainfall used as un input for estimating the peak discharge in HEC-HMS under precipitation option frequency storm will be filled depending on its return period and duration. Estimating the depth of rainfall for given return periods is helpful in estimating

the potential impacts of extreme rainfall events, such as flooding or erosion and designing proper drainage systems.

The design rainfall table and rainfall intensity–duration frequency tables and curves were developed and the results were presented in Table 4.4, Table 4.5 and Figure 4.15 respectively

Table 4-4: Depth of rainfall for a given return periods (mm)

| **Duration (Minutes)** | **Depth of rainfall for a given Return periods (mm)** | | | | | | | |
|---|---|---|---|---|---|---|---|---|
| | **2 years** | **5 years** | **10 years** | **25 years** | **50 years** | **100 years** | **200years** | **500years** |
| 5 | 7.255 | 8.772 | 9.776 | 11.045 | 11.986 | 12.920 | 13.851 | 15.079 |
| 10 | 12.156 | 14.697 | 16.379 | 18.505 | 20.082 | 21.648 | 23.207 | 25.265 |
| 15 | 15.728 | 19.015 | 21.192 | 23.942 | 25.983 | 28.008 | 30.026 | 32.688 |
| 30 | 22.451 | 27.144 | 30.251 | 34.178 | 37.090 | 39.981 | 42.862 | 46.662 |
| 60 | 29.007 | 35.070 | 39.085 | 44.157 | 47.920 | 51.656 | 55.377 | 60.287 |
| 120 | 34.715 | 41.972 | 46.777 | 52.848 | 57.351 | 61.822 | 66.276 | 72.152 |
| 180 | 37.628 | 45.493 | 50.701 | 57.281 | 62.162 | 67.008 | 71.836 | 78.205 |
| 360 | 42.053 | 50.843 | 56.663 | 64.017 | 69.473 | 74.888 | 80.283 | 87.402 |
| 720 | 46.059 | 55.687 | 62.062 | 70.116 | 76.091 | 82.023 | 87.932 | 95.728 |
| 1440 | 49.913 | 60.347 | 67.255 | 75.983 | 82.458 | 88.886 | 95.290 | 103.739 |

The rate of rainfall per unit time for a given return period (i.e., 2-500 years) is represented by intensity of rainfall. The result of rainfall intensity for a given return periods (mm) were given in table below.

Table 4-5: Intensity of rainfall for given return periods (mm/hr)

| Duration (Minutes) | Intensity for given return periods (mm/hr) | | | | | | | |
|---|---|---|---|---|---|---|---|---|
| | 2 years | 5 years | 10 years | 25 years | 50 years | 100 years | 200years | 500years |
| 5 | 87.062 | 105.261 | 117.311 | 132.536 | 143.830 | 155.041 | 166.212 | 180.949 |
| 10 | 72.936 | 88.182 | 98.277 | 111.031 | 120.493 | 129.885 | 139.243 | 151.589 |
| 20 | 62.910 | 76.061 | 84.768 | 95.769 | 103.930 | 112.032 | 120.103 | 130.752 |
| 30 | 44.902 | 54.288 | 60.503 | 68.355 | 74.180 | 79.962 | 85.723 | 93.324 |
| 60 | 29.007 | 35.070 | 39.085 | 44.157 | 47.920 | 51.656 | 55.377 | 60.287 |
| 90 | 17.358 | 20.986 | 23.389 | 26.424 | 28.676 | 30.911 | 33.138 | 36.076 |
| 180 | 12.543 | 15.164 | 16.900 | 19.094 | 20.721 | 22.336 | 23.945 | 26.068 |
| 360 | 7.009 | 8.474 | 9.444 | 10.670 | 11.579 | 12.481 | 13.381 | 14.567 |
| 720 | 3.838 | 4.641 | 5.172 | 5.843 | 6.341 | 6.835 | 7.328 | 7.977 |
| 1440 | 2.080 | 2.514 | 2.802 | 3.166 | 3.436 | 3.704 | 3.970 | 4.322 |

The intensity of rainfall for a given return period (mm/hr, 2-500 years) tends to decrease as the rainfall duration in minutes increases Figure 4 -15 and 4-16 Intensity-Duration-Frequency

(IDF) curve of the Study area Rainfall and rainfall region A2 as shown in the graph below almost both of them are the same magnitude of intensity with return period.

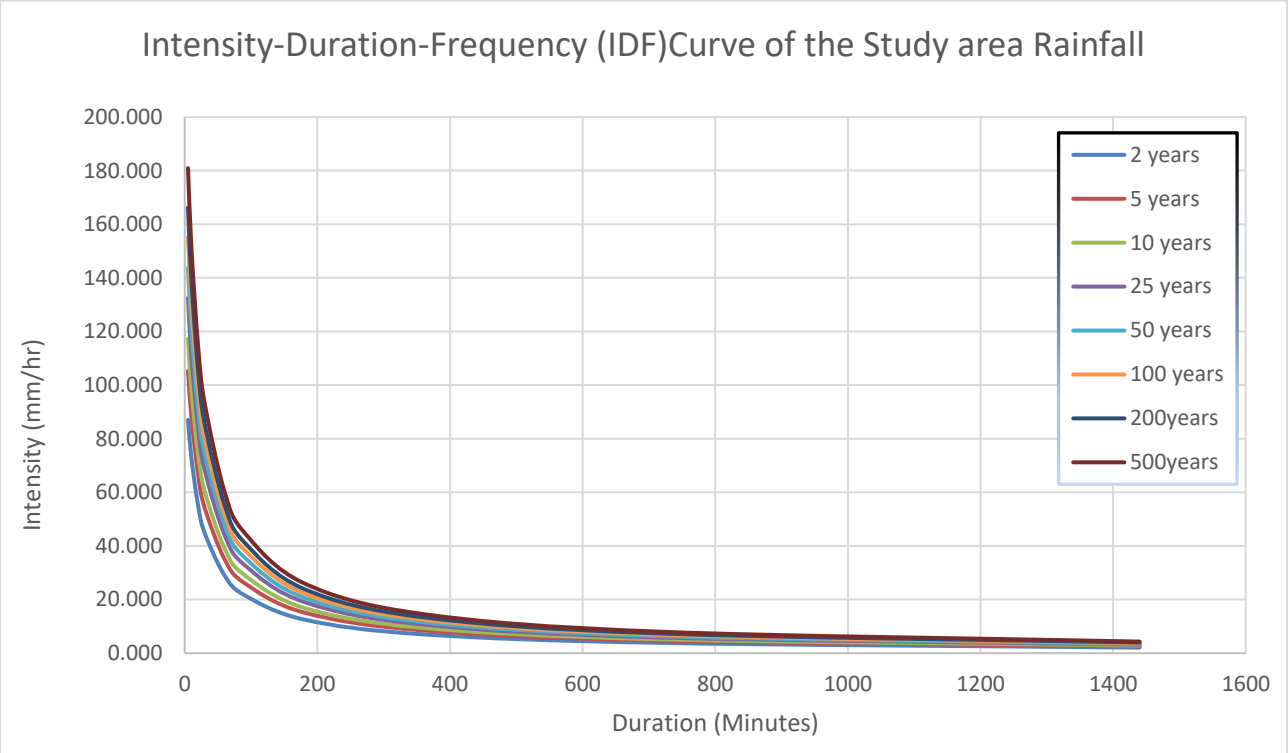


Figure 4-15: Intensity-Duration-Frequency (IDF) curve of the Study area Rainfall

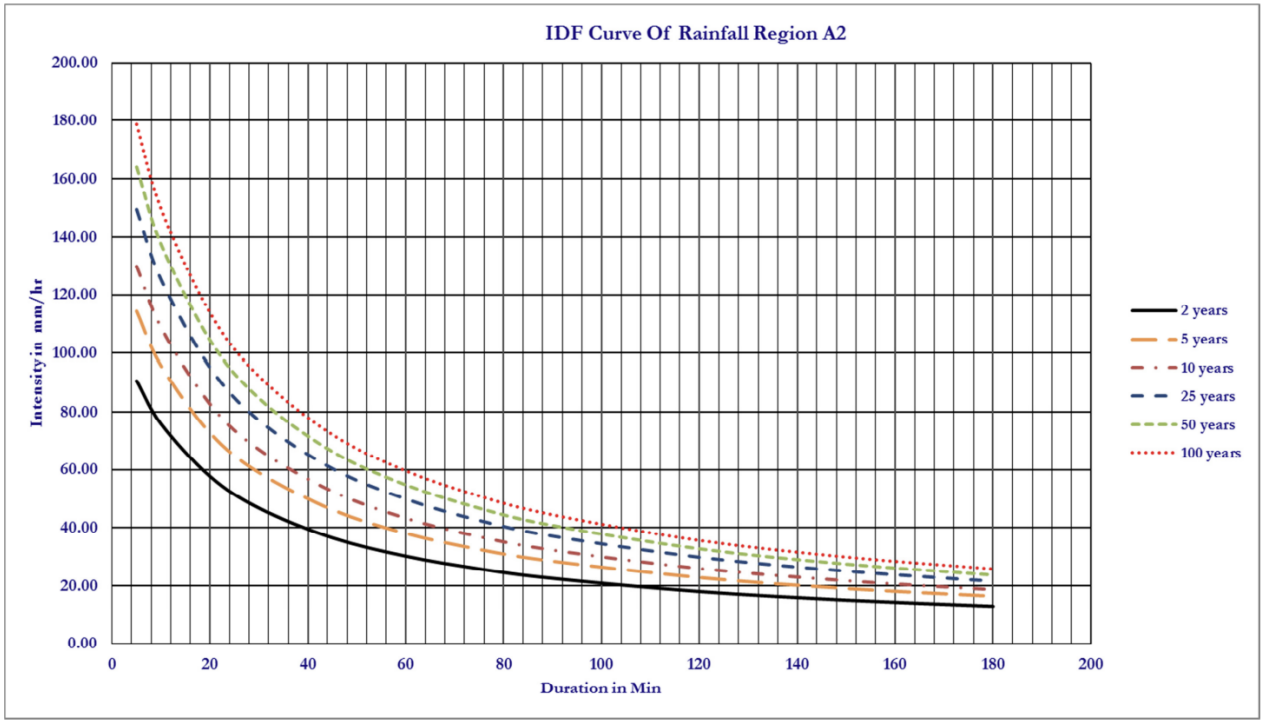


Figure 4-16: Intensity-Duration-Frequency (IDF) curve of the rainfall region A2

## 4.5 Flood Frequency Analysis

Using HEC-HMS, the peak flow estimation for each drainage structures is computed. These structures were chosen based on their flow variability. According to the ERA DDM 2013, this employs the use of design rainfall input data and rainfall intensity-duration-frequency curves for different return periods. The output for structure C01 is displayed below as an illustration Figure 4-17 the estimated discharge for C01 respected to its return period is 2.3m3/s,3.2m3/s,3.8m3/s,4.7m3/s,5.3m3/s and 6m3/s for 2year, 5 year, 10year, 25year, 50year and 100year return period respectively. The discharge estimates for different return periods provide essential guidance for designing resilient infrastructure, assessing flood risk, and making informed decisions to enhance community safety and resilience in the face of changing environmental conditions.

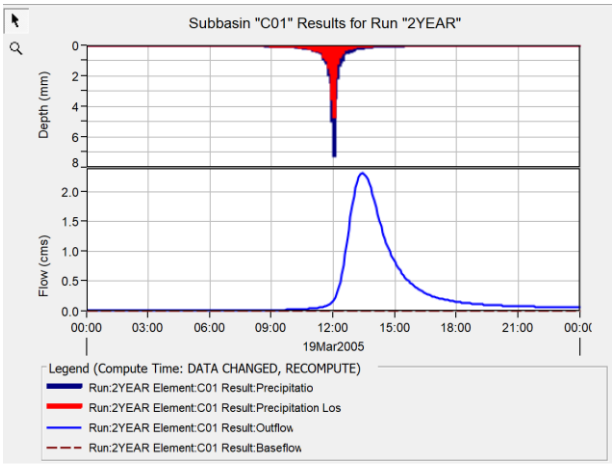


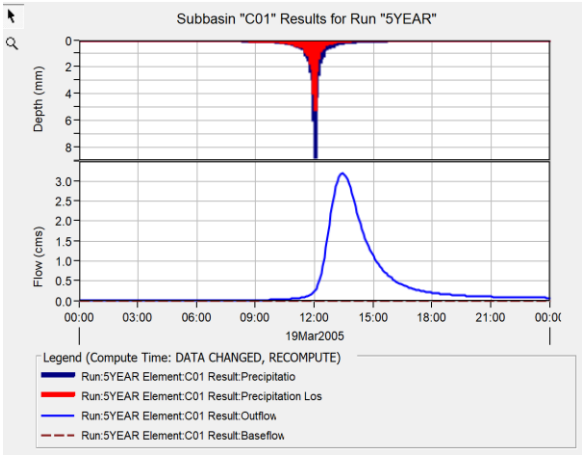


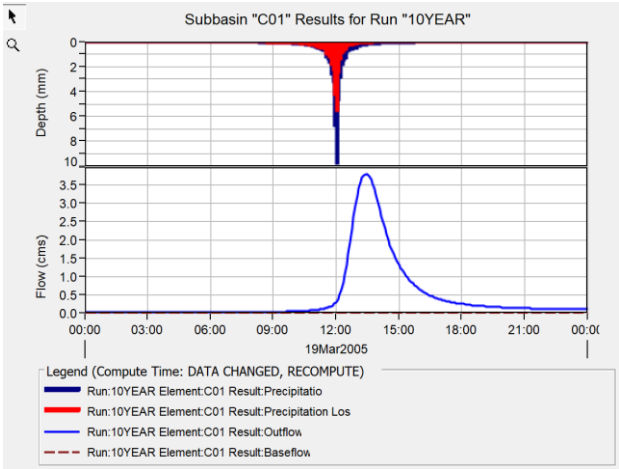


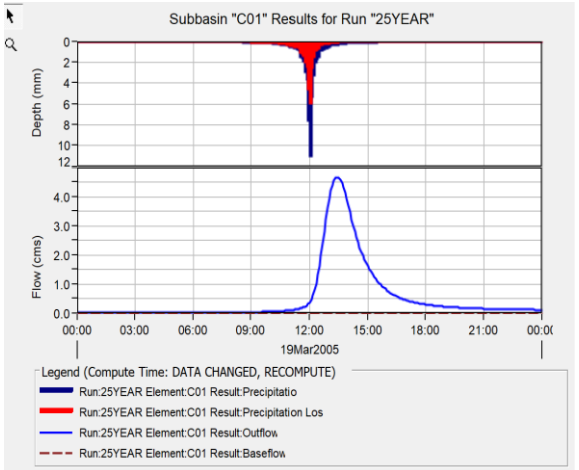

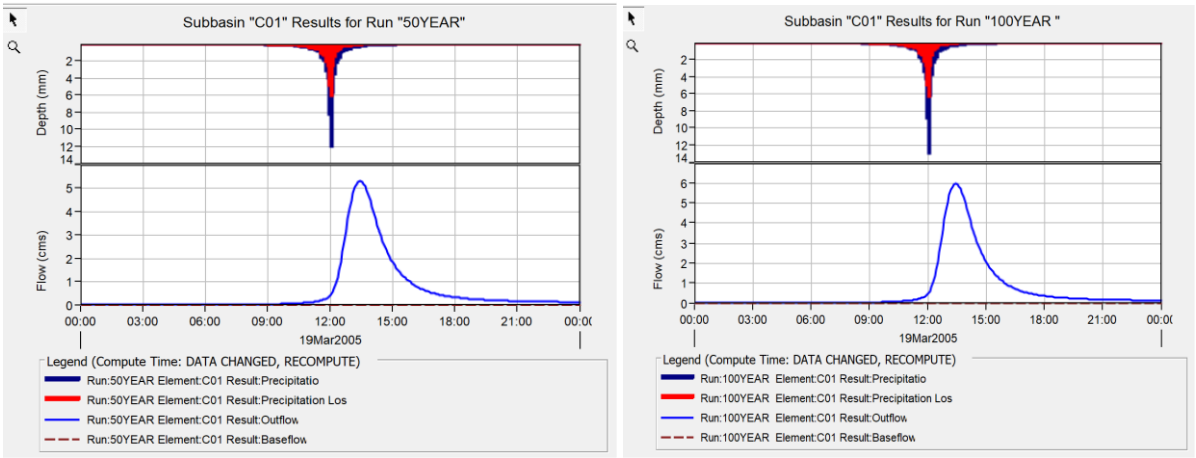


Figure 4-17: Simulation run results output of estimated peak flow for C01 from 2 -100year return period

The results of the simulation run for estimated peak flow for each drainage structures with different return periods (2 –100 years) were display below in Table 4.6.

Table 4-6: Estimated peak flow of each drainage structures with 2-100 year return period

| ID | Area ($km^2$) | Peak Discharge | | | | | |
|---|---|---|---|---|---|---|---|
| | | 2 year | 5 year | 10 year | 25 year | 50 year | 100 year |
| **C1** | 1.46 | 2.30 | 3.20 | 3.80 | 4.70 | 5.30 | 6.00 |
| **C2** | 1.49 | 2.60 | 3.50 | 4.20 | 5.20 | 5.90 | 6.60 |
| **C4** | 1.22 | 2.20 | 3.10 | 3.70 | 4.50 | 5.10 | 5.70 |
| **C5** | 7.59 | 11.60 | 16.00 | 19.10 | 23.30 | 26.60 | 30.00 |
| **C6** | 1.15 | 2.40 | 3.30 | 3.90 | 4.80 | 5.40 | 6.10 |
| **C7** | 1.05 | 2.30 | 3.10 | 3.70 | 4.50 | 5.20 | 5.80 |
| **C9** | 215.06 | 108.40 | 149.10 | 178.20 | 217.10 | 247.40 | 278.50 |
| **C10** | 7.25 | 17.30 | 23.80 | 28.60 | 34.90 | 39.80 | 44.80 |
| **C11** | 12.43 | 26.90 | 37.10 | 44.40 | 54.20 | 61.80 | 69.70 |
| **C12** | 3.66 | 9.40 | 13.00 | 15.60 | 19.00 | 21.70 | 24.50 |
| **C13** | 4.50 | 12.90 | 17.80 | 21.30 | 26.00 | 29.60 | 33.40 |
| **C14** | 1.06 | 1.50 | 2.10 | 2.50 | 3.10 | 3.50 | 4.00 |
| **C15** | 8.03 | 10.30 | 14.40 | 17.30 | 21.30 | 24.50 | 27.70 |
| **C16** | 81.05 | 107.00 | 149.40 | 180.20 | 221.90 | 254.60 | 288.50 |
| **C19** | 136.22 | 86.70 | 120.30 | 144.50 | 177.10 | 202.60 | 229.00 |
| **C20** | 0.55 | 1.00 | 1.40 | 1.60 | 2.00 | 2.30 | 2.60 |
| **C21** | 0.53 | 0.80 | 1.10 | 1.30 | 1.60 | 1.80 | 2.10 |
| **C22** | 6.15 | 9.90 | 13.70 | 16.50 | 20.30 | 23.20 | 26.30 |
| **C23** | 25.79 | 25.80 | 35.80 | 43.00 | 52.80 | 60.40 | 68.30 |
| **C24** | 15.68 | 24.70 | 34.30 | 41.30 | 50.70 | 58.00 | 65.60 |
| **C25** | 25.61 | 44.90 | 62.40 | 75.00 | 92.10 | 105.40 | 119.20 |
| **C28** | 8.83 | 16.90 | 23.50 | 28.30 | 34.70 | 39.80 | 45.00 |
| **C30** | 2.30 | 5.90 | 8.20 | 9.80 | 16.10 | 13.70 | 10.70 |
| **C33** | 85.99 | 97.70 | 135.30 | 162.50 | 198.90 | 227.40 | 256.70 |
| **C37** | 1.10 | 2.60 | 3.60 | 4.30 | 5.20 | 5.90 | 6.60 |
| **C39** | 4.20 | 5.30 | 7.30 | 8.70 | 10.50 | 12.00 | 13.40 |
| **C40** | 3.84 | 5.70 | 7.90 | 9.50 | 11.60 | 13.30 | 15.00 |
| **C41** | 17.54 | 37.50 | 51.70 | 61.90 | 75.60 | 86.20 | 97.10 |

| ID | Area ($km^2$) | Peak Discharge | | | | | |
|---|---|---|---|---|---|---|---|
| | | 2 year | 5 year | 10 year | 25 year | 50 year | 100 year |
| **C42** | 8.39 | 24.20 | 32.90 | 39.10 | 47.30 | 53.60 | 60.10 |
| **C43** | 0.71 | 1.60 | 2.20 | 2.70 | 3.30 | 3.70 | 4.20 |
| **C44** | 3.81 | 6.00 | 8.30 | 9.90 | 12.10 | 13.80 | 15.60 |
| **C45** | 2.76 | 6.40 | 8.70 | 10.40 | 12.50 | 14.20 | 16.00 |
| **C46** | 30.70 | 67.40 | 91.90 | 109.30 | 132.30 | 150.10 | 168.30 |
| **C47** | 8.10 | 27.10 | 37.00 | 44.00 | 53.30 | 60.40 | 67.80 |
| **C48** | 15.66 | 40.10 | 54.40 | 64.80 | 78.30 | 88.80 | 99.40 |
| **C50** | 2.92 | 7.40 | 10.00 | 11.90 | 14.30 | 16.20 | 18.20 |
| **C51** | 15.45 | 22.00 | 30.30 | 36.30 | 44.20 | 50.40 | 56.80 |
| **C53** | 10.65 | 23.10 | 31.30 | 37.70 | 45.70 | 51.90 | 58.20 |
| **C54** | 1.87 | 4.00 | 5.50 | 6.50 | 7.80 | 8.90 | 9.90 |
| **C56** | 245.76 | 271.10 | 366.30 | 433.20 | 521.40 | 589.10 | 657.90 |

## 4.6 Variable flow effects on drainage structures

### 4.6.1 Over flooding check

The drainage structure's opening dimensions are measured, and based on this measurement the Manning formula is used to calculate the discharge capacity of each structure. Using this gathered data, the calculated discharge capacity is compared to the estimated discharge values.

Figure 4-18: Sample drainage structure from the study area

An estimated 38% of drainage structures are vulnerable to flooding, this might be due possible consequences of changes in land use. The watershed area mostly changed from forest to agricultural land and urbanization this will increase runoff and decrease infiltration. Understanding the impacts of land cover changes on flow variability is essential for informed land use planning and effective management of drainage systems to mitigate flood risks.

Table 4-7: Comparison between the estimated discharge with discharge capacity of the structure

| ID | Q Capacity (m3/s) | Q Estimated (m3/s) | Remark | | ID | Q Capacity (m3/s) | Q Estimated (m3/s) | Remark |
|---|---|---|---|---|---|---|---|---|
| C1 | 3.25 | 4.70 | π | | C25 | 92.16 | 105.40 | π |
| C2 | 3.25 | 5.20 | π | | C28 | 58.41 | 39.80 | π π |
| C4 | 0.81 | 3.70 | π | | C30 | 631.44 | 13.70 | π π |
| C5 | 36.00 | 23.30 | π π | | C33 | 286.67 | 227.40 | π π |
| C6 | 2.12 | 3.90 | π | | C37 | 8.07 | 5.2 | π π |
| C7 | 2.12 | 3.70 | π | | C39 | 9.57 | 12.00 | π |
| C9 | 673.84 | 247.40 | π π | | C40 | 19.79 | 13.30 | π π |
| C10 | 62.83 | 34.90 | π π | | C41 | 768.04 | 86.20 | π π |
| C11 | 101.02 | 61.80 | π π | | C42 | 1634.74 | 53.60 | π π |
| C12 | 64.00 | 19.00 | π π | | C43 | 32.09 | 3.70 | π π |
| C13 | 71.54 | 29.60 | π π | | C44 | 73.26 | 13.80 | π π |
| C14 | 0.81 | 2.50 | π | | C45 | 85.94 | 14.20 | π π |
| C15 | 37.93 | 21.30 | π π | | C46 | 223.48 | 150.10 | π π |
| C16 | 252.61 | 254.60 | π | | C47 | 61.29 | 60.40 | π π |
| C19 | 205.80 | 202.60 | π π | | C48 | 247.50 | 88.80 | π π |
| C20 | 1.63 | 1.60 | π π | | C50 | 54.20 | 16.20 | π π |
| C21 | 4.74 | 1.60 | π π | | C51 | 27.71 | 44.20 | π |
| C22 | 21.30 | 23.20 | π | | C53 | 45.31 | 51.90 | π |
| C23 | 48.39 | 60.40 | π | | C54 | 11.87 | 7.80 | π π |
| C24 | 41.70 | 58.00 | π | | C56 | 1735.49 | 589.10 | π π |

π:-disposed to Flood Risk; π π :- Not disposed to Flood Risk.

In particular, some drainage structures have variability in flow, as shown in the result, however, because of the river morphology crating create a gorge, this variable is not as noticeable. For instance, on Bridge C42, the flow is very small at the structure's crossing, but the structures are beyond the flow this is due to the extensive gorge carved out by the river over time.

### 4.6.2 Sedimentation Effect

In order to evaluate the flow variability in fifteen (15) culverts, a number of factors such as structural characteristics, on-site inspections, and catchment data obtained from DEM resolution were considered and examined carefully. These road segment culverts are positioned strategically and come in many structural types, such as slab/box culverts, corrugated steel pipes, and concrete pipe culverts.

However, sediment accumulation affects a large percentage of these culverts. As shown above around 47% of culverts experience the effects of initial floods. When sedimentation is considered, however, this number increases by 13%, indicating that 60% of culverts are

affected by fluctuating flow conditions in table 4.8 displays. The capacity of culverts to handle water flow will decrease overtime as sedimentation of the structure increase. The result of how sedimented culverts affect their capacity to accommodate estimated discharge.

Table 4-8: Comparative Analysis: Discharge Capacity, Sedimented Discharge Capacity, and Estimated Discharge

| ID | Q Capacity (m3/s) | Q Capacity (m3/s) (sedimented) | Q Estimated (m3/s) |
|---|---|---|---|
| C1 | 3.25 | 2.44 | 4.7 |
| C2 | 3.25 | 0.00 | 5.2 |
| C4 | 0.81 | 0.73 | 3.7 |
| C5 | 36.00 | 36.00 | 23.3 |
| C6 | 2.12 | 1.91 | 3.9 |
| C7 | 2.12 | 1.59 | 3.7 |
| C10 | 62.83 | 42.10 | 34.9 |
| C12 | 64.00 | 38.40 | 19 |
| C14 | 0.81 | 0.00 | 2.5 |
| C15 | 37.93 | 34.14 | 21.3 |
| C20 | 1.63 | 1.22 | 1.6 |
| C21 | 4.74 | 2.37 | 1.6 |
| C37 | 8.07 | 8.07 | 5.2 |
| C51 | 27.71 | 24.94 | 44.2 |
| C54 | 11.87 | 2.37 | 7.8 |

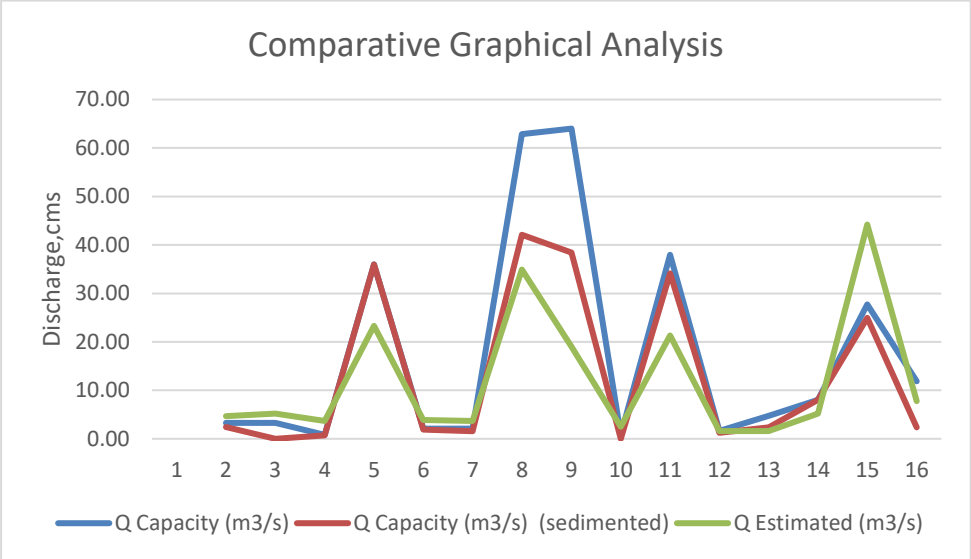


Figure 4-19: Comparative Graphical Analysis: Discharge Capacity, Sedimented Discharge Capacity, and Estimated Discharge

### 4.6.3 Scouring effect due to velocity

The scouring effect analysed by comparing permissible velocity, which varies depending on the type of structure constructed with the calculated velocity. The velocity is calculated using

Manning's formula and opening dimensions that are measured on the site. Depend on this result 25% of the drainage structures are vulnerable to the effect of scouring as shown in Table 4-9

Table 4-9: Comparison between calculated velocities of each structure with permissible velocity

| ID | A (m2) | P (m) | R(m) | n | s | Flow Velocity (m/s) | Permissible Velocity (m/s) | Remark |
|---|---|---|---|---|---|---|---|---|
| C1 | 1.76 | 6.6568 | 0.27 | 0.05 | 0.05 | 1.85 | 6 | ** |
| C2 | 1.76 | 6.6568 | 0.27 | 0.05 | 0.05 | 1.85 | 6 | ** |
| C4 | 0.64 | 2.826 | 0.23 | 0.05 | 0.03 | 1.28 | 6 | ** |
| C5 | 9.00 | 9 | 1.00 | 0.05 | 0.04 | 4.00 | 2.5 | * |
| C6 | 1.17 | 3.8308 | 0.31 | 0.05 | 0.04 | 1.81 | 10 | ** |
| C7 | 1.17 | 3.8308 | 0.31 | 0.05 | 0.04 | 1.81 | 10 | ** |
| C9 | 112.00 | 30 | 3.73 | 0.08 | 0.04 | 6.02 | 4 | * |
| C10 | 32.40 | 28.2 | 1.15 | 0.08 | 0.02 | 1.94 | 6 | ** |
| C11 | 36.00 | 18 | 2.00 | 0.08 | 0.02 | 2.81 | 4 | ** |
| C12 | 16.00 | 16 | 1.00 | 0.05 | 0.04 | 4.00 | 6 | ** |
| C13 | 21.00 | 13 | 1.62 | 0.07 | 0.03 | 3.41 | 4 | ** |
| C14 | 0.64 | 2.826 | 0.23 | 0.05 | 0.03 | 1.28 | 6 | ** |
| C15 | 20.00 | 18 | 1.11 | 0.08 | 0.02 | 1.90 | 6 | ** |
| C16 | 70.00 | 24 | 2.92 | 0.08 | 0.02 | 3.61 | 4 | ** |
| C19 | 96.00 | 28 | 3.43 | 0.15 | 0.02 | 2.14 | 2.5 | ** |
| C20 | 0.88 | 3.3284 | 0.27 | 0.05 | 0.05 | 1.85 | 6 | ** |
| C21 | 2.34 | 7.6616 | 0.31 | 0.05 | 0.05 | 2.03 | 10 | ** |
| C22 | 15.00 | 11 | 1.36 | 0.15 | 0.03 | 1.42 | 2.5 | ** |
| C23 | 18.00 | 12.5 | 1.44 | 0.15 | 0.10 | 2.69 | 2.5 | * |
| C24 | 18.00 | 12 | 1.50 | 0.08 | 0.02 | 2.32 | 2.5 | ** |
| C25 | 30.00 | 16 | 1.88 | 0.07 | 0.02 | 3.07 | 4 | ** |
| C28 | 21.00 | 13 | 1.62 | 0.07 | 0.02 | 2.78 | 4 | ** |
| C30 | 98.00 | 28 | 3.50 | 0.08 | 0.05 | 6.44 | 4 | * |
| C33 | 54.00 | 21 | 2.57 | 0.05 | 0.02 | 5.31 | 4 | * |
| C37 | 3.00 | 5 | 0.60 | 0.07 | 0.07 | 2.69 | 6 | ** |
| C39 | 6.00 | 7 | 0.86 | 0.08 | 0.02 | 1.60 | 2.5 | ** |
| C40 | 8.00 | 8 | 1.00 | 0.07 | 0.03 | 2.47 | 2.5 | ** |
| C41 | 112.50 | 30 | 3.75 | 0.1 | 0.08 | 6.83 | 10 | ** |
| C42 | 160.00 | 36 | 4.44 | 0.07 | 0.07 | 10.22 | 6 | * |
| C43 | 8.80 | 8.4 | 1.05 | 0.08 | 0.08 | 3.65 | 4 | ** |
| C44 | 16.00 | 12 | 1.33 | 0.07 | 0.07 | 4.58 | 4 | * |
| C45 | 24.00 | 14 | 1.71 | 0.08 | 0.04 | 3.58 | 4 | ** |
| C46 | 45.00 | 19 | 2.37 | 0.08 | 0.05 | 4.97 | 4 | * |
| C47 | 16.00 | 12 | 1.33 | 0.1 | 0.1 | 3.83 | 4 | ** |
| C48 | 70.00 | 24 | 2.92 | 0.1 | 0.03 | 3.54 | 4 | ** |
| C50 | 12.00 | 10 | 1.20 | 0.05 | 0.04 | 4.52 | 4 | * |
| C51 | 8.00 | 8 | 1.00 | 0.05 | 0.03 | 3.46 | 4 | ** |
| C53 | 13.60 | 10.8 | 1.26 | 0.07 | 0.04 | 3.33 | 4 | ** |
| C54 | 5.00 | 6.5 | 0.77 | 0.05 | 0.02 | 2.37 | 2.5 | ** |
| C56 | 162.00 | 39 | 4.15 | 0.08 | 0.11 | 10.71 | 6 | * |

* disposed to scouring effect, ** Not disposed to Scouring effect

# 5 CONCLUSION AND RECOMMENDATION

## 5.1 Conclusion

The findings of this study provide valuable insights into the complex dynamics of flow variability and its effect on drainage structures along the Holeta to Ambo Road in Ethiopia. The conclusions drawn from the study highlights several key aspects of hydrological analysis, including flood risk, sedimentation, scouring effect and structural vulnerabilities.

The hydrological analysis of the study area exhibited satisfactory simulation and forecasting of future scenarios, with the model performance rating in range of $0.66 < R^2 \leq 0.848$, $0.66 < NSE \leq 0.842$, and PBIAS is between 0.49-4.79.

Hence, the daily flow estimated for each drainage structure is calculated using a well-validated and calibrated model. The greater the coefficient of variance, the larger the flow variability. As a result, over 71% of the structures have a coefficient of variance greater than 40% and revealing a large flow variability. This variability poses difficulties in designing structures that can efficiently handle a broad range of fluctuating flow conditions.

Furthermore, the study revealed that more than one-third of the drainage structure are prone to flooding risk, based on the discharge calculated for a design storm or the estimated peak discharge in relation to the capacity of drainage structures. This highlights the importance of managing alterations in land cover to mitigate the flood risks.

In addition, sedimentation emerged as a major factor affecting culverts. Of the 15 culverts examined, around 47% the structures were affected by flooding prior to sedimentation; with a substantial increase from 47% to 60% of structures impacted after sedimentation. Last but not the least, the scouring effect by comparing the permissible velocity with the calculated velocity showed that 25% of the structures are vulnerable to the scouring effect.

## 5.2 Recommendation

The following recommendation are made based on the results and conclusions of the study;

- Improving the infrastructure capable of managing variable flow through replacing the existing structures with the new structure. Furthermore, to reduce the risk of damage due to flooding along Holeta-Ambo Road implementing natural based solutions are required such as creating green spaces and using natural vegetation to absorb and slow down flood water this can help reduce the impact of flooding by increasing infiltration and reducing runoff.
- Structure like C1, C2, C10, C12, C20, C21 and C54 are need urgent replacing due to sedimentation. In order to improve the durability and functionality of culvert overtime beyond cleaning and maintaining other alternative approach such as sediment management technique like sediment traps and sediment pond and implement erosion resistance measure such as vegetative buffer erosion resistance material to stabilize banks and prevent sediment to entering waterway.
- Most of the older structures along the route such as C23, C30, C33 and C46 need to be replaced they are showing of scouring, require ongoing maintenance, and exceeded their design lifespan. Hence, investing in new infrastructure will improve performance, durability and safety, while lowering maintenance cost of the road system.
- Furthermore, the data collected on the drainage structure type and opening sizes of drainage structures on the study area can be valuable for future research and planning purpose.

The implementation of the recommended measures improves the durability of drainage structures, and ensure the long-term functionality and safety of the road network. As a result, stakeholders can work towards putting the recommended measures into practice along the Holeta to Ambo Road in order to ensure the functionality and safety of the road system.

# REFERENCES


1. Ali M, Meaza H. Geographical analysis of road transportation of Ethiopia. Ethiopian Journal of Environmental Studies and Management. 2015;8:846.
2. Ng CP, Law TH, Mohd Jakarni F, Subramaniam K. Road infrastructure development and economic growth. IOP Conference Series: Materials Science and Engineering. 2019;512:012045.
3. Barinov AK. Transport Infrastructure in Ethiopia. Outlines of global transformations: politics, economics, law. 2018;11(5).
4. Luthuli M, Qwatekana Z, Zondi N, Ndlovu T. Interconnectedness of road infrastructure and tourism development: Perspectives from residents and enterprises. Turkish Online Journal of Qualitative Inquiry. 2021;12:2719-39.
5. Global Cement. Available from: https://globalcement.com./ [Accessed 15.06.2023].
6. EARI list of research centres Archived 2009-04-23 at the Way back Machine (Accessed 30 April 2009).
7. Wikipedia the free encyclopedia (2014), Addis Ababa.
8. "Important Bird Area factsheet: Chilimo forest, Ethiopia", BirdLife International website (accessed 1 September 2009).
9. Ogato GS, Boon E, Subramani J. Gender Roles in Crop Production and Management Practices: A Case Study of Three Rural Communities in Ambo District, Ethiopia. J Hum Ecol. 2009;27:1-20.
10. Briggs P. Ethiopia: The Bradt Travel Guide: Bradt Travel Guides; 2005.
11. FAO Conservation Guide 13/5. Watershed management field manual; Road design and construction in sensitive watersheds. Food and agriculture organization of the United Nations Rome 1998.
12. Pojani D, Stead D. Sustainable Urban Transport in the Developing World: Beyond Megacities. Sustainability. 2015;2015:7784-805.
13. Singh, R. R., Navpreet, K. and Er.Nitin, G. (2014). Drainage on roads. International Journal of Progresses in Civil Engineering. Vol. 1(1). Pp. 2394 – 4684. Available from: https://www.troindia.in/journal/IJPCE/IJPCE/19-21.pdf.
14. Vitalis I. THE EFFECTS OF POOR DRAINAGE SYSTEM ON ROAD PAVEMENT: A REVIEW. INTERNATIONAL JOURNAL FOR INNOVATIVE RESEARCH IN MULTIDISCIPLINARY FIELD. 2016;2:218-25.
15. Cullom Walker., Drainage Structures & Their Role in Modern Roadway Infrastructure. 2021. Available from: Drainage Structures & Their Role in Modern Roadway Infrastructure - InfraSteel® [Accessed 25.2.2023].
16. Ethiopia Road Authority. Drainage design manual. 2013.
17. Tung, Y.-K., & Bao, Y. (1990). Optimal design of highway drainage structures. In H. H. Chang, & J. C. Hill (Eds.), Hydraulic Engineering - Proceedings of the 1990 National Conference (pp. 210-215). (Hydraulic Engineering - Proceedings of the 1990 National Conference). Publ by ASCE. .
18. Kang Ms, Koo J, Chun JA, Her Y, Park S, Yoo K. Research Paper: SWdSoil and Water Design of drainage culverts considering critical storm duration. Biosystems Engineering. 2009;104:425-34.
19. Propika J, Laila Lestari L, Muti J. The Use of Box Culvert Precast as a Main Bridge Structure in Arterial Highway Road: An Analysis Study. IPTEK Journal of Proceedings Series. 2018.
20. Highway Engineering Handbook: Building and Rehabilitating the Infrastructure. 3rd Edition ed. New York: McGraw-Hill Education; 2009.

21. Glenn E. Moglen. Fundamentals of Open Channel Flow. Second. CRC Press is an imprint of Taylor & Francis Group LLC; 2023.
22. Chanson H. The hydraulics of open channel flow : an introduction ; basic principles, sediment motion, hydraulic modelling, design of hydraulic structures. Amsterdam: Elsevier Butterworth Heinemann; 2004. Available from: http://site.ebrary.com/id/10169733.
23. Zhang G, Liu Y, Liu J, Lan S, Yang J. Causes and statistical characteristics of bridge failures: A review. Journal of Traffic and Transportation Engineering (English Edition). 2022;9(3):388-406.
24. Legese B, Gumi B, editors. Flooding in Ethiopia ; Causes , Impact , and Coping Mechanism . A Review2020.
25. Weldegebriel ZB, Amphune BE. Livelihood resilience in the face of recurring floods: an empirical evidence from Northwest Ethiopia. Geoenvironmental Disasters. 2017;4(1):10.
26. Solihu, Habeeb & Kidanewold, Belete & Abdulkadir, Abdulwasiu. (2022). Flood Risk and Flow Variability Assessment at the Railway Drainage Structures: A Case of the Ethio - Djibouti Railway Line, Ethiopia. 14. 175-208. 10.4314/gjg.v14i3.7.
27. Woldegebrael SM, Kidanewold B, Melesse A. Historical Flood Events and hydrological extremes in Ethiopia. 2019. p. 379-84.
28. Jemberie MA, Melesse AM, Abate B. Urban Drainage: The Challenges and Failure Assessment Using AHP, Addis Ababa, Ethiopia. 2023;15(5):957.
29. Beshir AA, Song J. Urbanization and its impact on flood hazard: the case of Addis Ababa, Ethiopia. Natural Hazards. 2021;109(1):1167-90.
30. Bibi TS, Reddythta D, Kebebew AS. Assessment of the drainage systems performance in response to future scenarios and flood mitigation measures using stormwater management model. City and Environment Interactions. 2023;19:100111.
31. Weday MA, Tabor KW, Gemeda DO. Flood hazards and risk mapping using geospatial technologies in Jimma City, southwestern Ethiopia. Heliyon. 2023;9(4):e14617.
32. Herslund L, Backhaus A, Fryd O, Jørgensen G, Jensen MB, Limbumba TM, et al. Conditions and opportunities for green infrastructure – Aiming for green, water-resilient cities in Addis Ababa and Dar es Salaam. Landscape and Urban Planning. 2018;180:319-27.
33. Federal Democratic Republic of Ethiopia, Minister of Planning and Development. Ethiopia's long-term low emission and climate resilient development strategy (2020-2050). Addis Ababa, Ethiopia.
34. Kondolf GM, Gao Y, Annandale GW, Morris GL, Jiang E, Zhang J, et al. Sustainable sediment management in reservoirs and regulated rivers: Experiences from five continents. 2014;2(5):256-80.
35. Motuma D. The Effect of Discharge Amount on Drainage Structure Failure A case Study on Ambo Town. 2016. Jimma, Ethiopia. Available from: https://repository.ju.edu.et/bitstream/handle/123456789/5418/Motii.pdf?sequence=1&isAllowed=y Accessed [3.5.2023].
36. C N X Quang et al 2022. Effects of sediment deposit on the hydraulic performance of the urban stormwater drainage system IOP Conf. Ser.: Earth Environ. Sci. 964 012020.
37. Mamo A, Kabite G. Responses of soil erosion and sediment yield to land use/land cover changes: in the case of Fincha'a Watershed, upper Blue Nile Basin, Ethiopia. Environmental Challenges. 2023;13:100789.
38. Woldearegay K. Review of the occurrences and influencing factors of landslides in the highlands of Ethiopia: With implications for infrastructural development. Momona Ethiopian Journal of Science. 2013;5:3.
39. Nicholls R, Zanuttigh B, Vanderlinden Jean P, Weisse R, Silva R, Hanson S, et al. Chapter 2 - Developing a Holistic Approach to Assessing and Managing Coastal Flood Risk. In:

Zanuttigh B, Nicholls R, Vanderlinden JP, Burcharth HF, Thompson RC, editors. Coastal Risk Management in a Changing Climate. Boston: Butterworth-Heinemann; 2015. p. 9-53.
40. Hurni H, Wa B, P C, D D, Zeleke G, M G, et al. Soil and Water Conservation in Ethiopia (Guidelines for Development Agents). Ministry of Agriculture (MoA). Ethiopia 20162018.
41. Mitiku, Haile; Herweg, Karl; Stillhardt, Brigitta (2006). Sustainable land management: A new approach to soil and water conservation in Ethiopia. Bern, Switzerland: Centre for Development and Environment (CDE) and NCCR North-South
42. Brandimarte L, Paron P, Di Baldassarre G. Bridge pier scour: A review of processes, measurements and estimates. Environmental engineering and management journal. 2012;11.
43. Shahriar AR, Ortiz AC, Montoya BM, Gabr MA. Bridge Pier Scour: An overview of factors affecting the phenomenon and comparative evaluation of selected models. Transportation Geotechnics. 2021;28:100549.
44. Prendergast LJ, Gavin K. A review of bridge scour monitoring techniques. Journal of Rock Mechanics and Geotechnical Engineering. 2014;6(2):138-49.
45. Pizarro A, Manfreda S, Tubaldi E. The Science behind Scour at Bridge Foundations: A Review. 2020;12(2):374.
46. Khan K, Waseem M, Alam M, Khan M, Leta MK. Experimental investigation of pier scour depth and its scour hole pattern for different shapes. Journal of Infrastructure, Policy and Development. 2024;8.
47. Kidanie Y, Grum B, Yemane S. Hydrologic and hydraulic assessment of scour problems at bridge sites in Tigray region, northern Ethiopia. Journal of Applied Water Engineering and Research. 2022;10(2):144-56.
48. Khan W. Flood Mitigation of Goro Catchment in DireDawa. 2023.
49. Mehari B, G/mariam B, Ayele G, Demissie S, Jemberie M. Investigating Highway Drainage Problems in the Sile River Bridge, South, Ethiopia. Journal of Multidisciplinary Engineering Science and Technology (JMEST). 2015;Vol. 2.
50. Uge BUJC, research e. Performance, Problems and Remedial Measures for Roads Constructed on Expansive Soil in Ethiopia – A Review. 2017;9:28-37.
51. Ministry of Transport, Ethiopia. Ethiopia's Climate Resilient Transport Sector Strategy. Addis Ababa, Ethiopia.
52. Addisu, Solomon. Assessment of the Impact of Road Construction on Physical Land Degradation in Central Highlands of Ethiopia: The Case of Two Selected Projects. 2009. Addis Ababa University, Addis Ababa, Ethiopia.
53. Gravelle R. Discharge Estimation: Techniques and Equipment. 2015.
54. Dinku, Tufa & Hailemariam, Kinfe & Grimes, David & Asefa, Kidane & Connor, Stephen. Improving Availability, Access and Use of Climate Information. 2011. WMO Bulletin. 60. 80-86.
55. Daggupati P, Pai N, Ale S, Mankin K, Zeckoski R, Jeong J, et al. A Recommended Calibration and Validation Strategy for Hydrologic and Water Quality Models. Transactions of the ASABE (American Society of Agricultural and Biological Engineers). 2015;58:1705-19.
56. Worqlul A. Hydrological Balance of Lake Tana Upper Blue Nile Basin, Ethiopia. Physics and Chemistry of The Earth - PHYS CHEM EARTH. 2008.
57. HEC-HMS Tutorial and Guides. Available from: Calculate Performance Metrics for Daily Flows (army.mil) accessed 4.8.24
58. Hayelom B, Chen Y, Marsie Z, Negash M. Temperature and Precipitation Trend Analysis over the Last 30 Years in Southern Tigray Regional State, Ethiopia2017.

59. Asfaw A, Simane B, Hassen A, Bantider A. Variability and time series trend analysis of rainfall and temperature in northcentral Ethiopia: A case study in Woleka sub-basin. Weather and Climate Extremes. 2018;19:29-41.
60. SUBRAMANYA K. Flow in Open Channels, 3e: Tata McGraw-Hill; 1982.

# APPENDICES

## **Appendix 1:** Double mass curve all rainfall stations

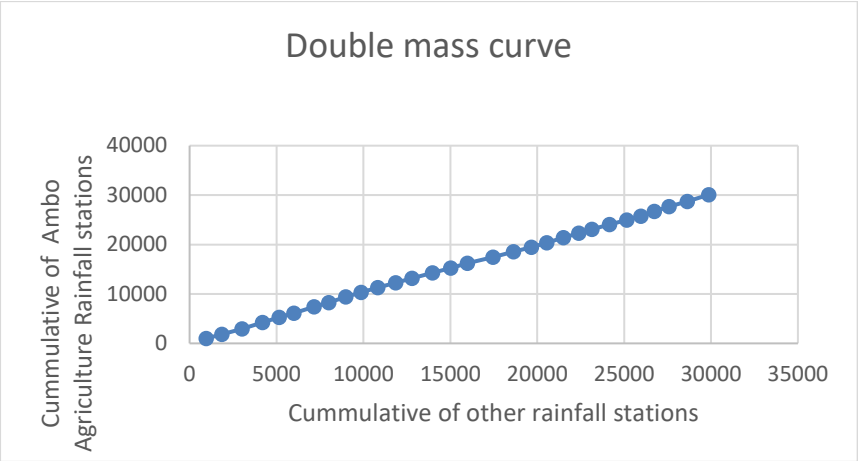


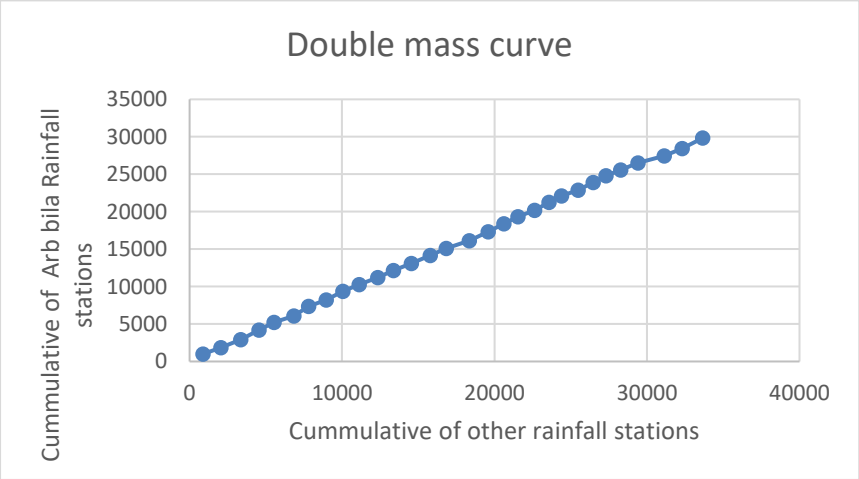


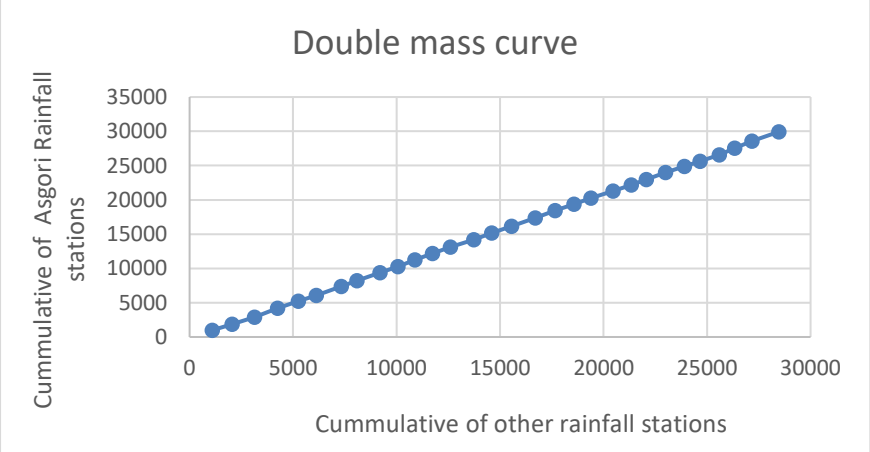

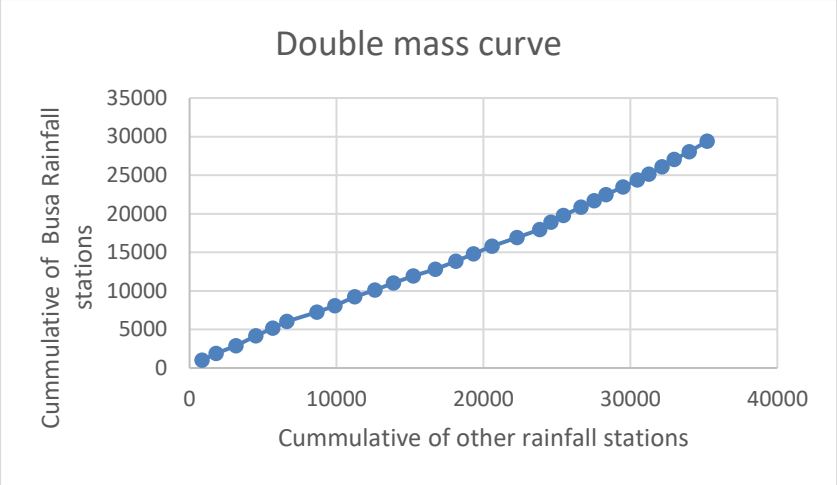
Double mass curve
Cummulative of Busa Rainfall stations
35000
30000
25000
20000
15000
10000
5000
0
0
10000
20000
30000
40000
Cummulative of other rainfall stations

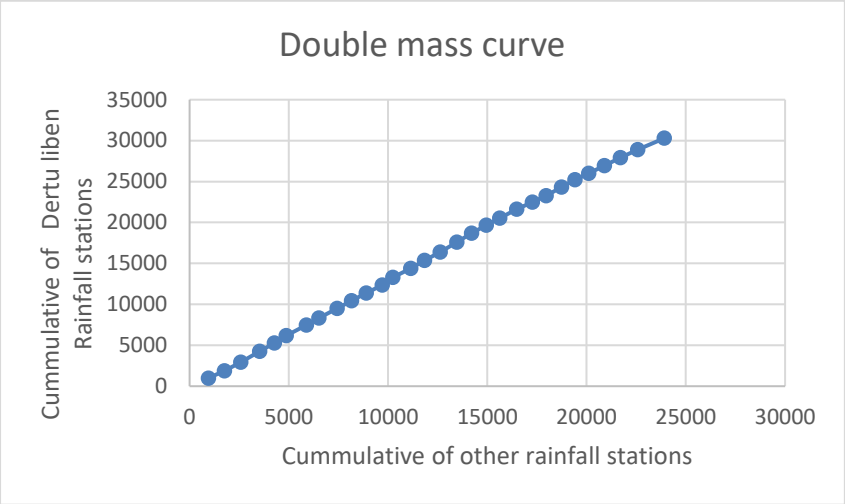
Double mass curve
Cummulative of Dertu liben Rainfall stations
35000
30000
25000
20000
15000
10000
5000
0
0
5000
10000
15000
20000
25000
30000
Cummulative of other rainfall stations

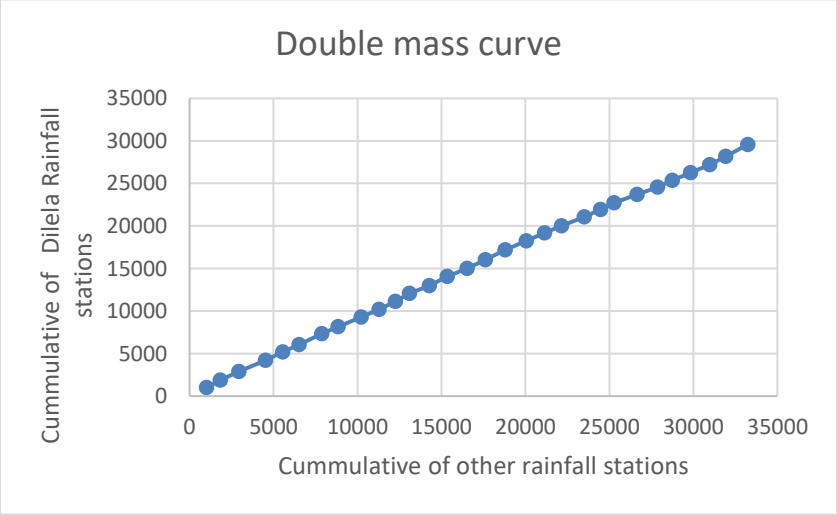
Double mass curve
Cummulative of Dilela Rainfall stations
35000
30000
25000
20000
15000
10000
5000
0
0
5000
10000
15000
20000
25000
30000
35000
Cummulative of other rainfall stations

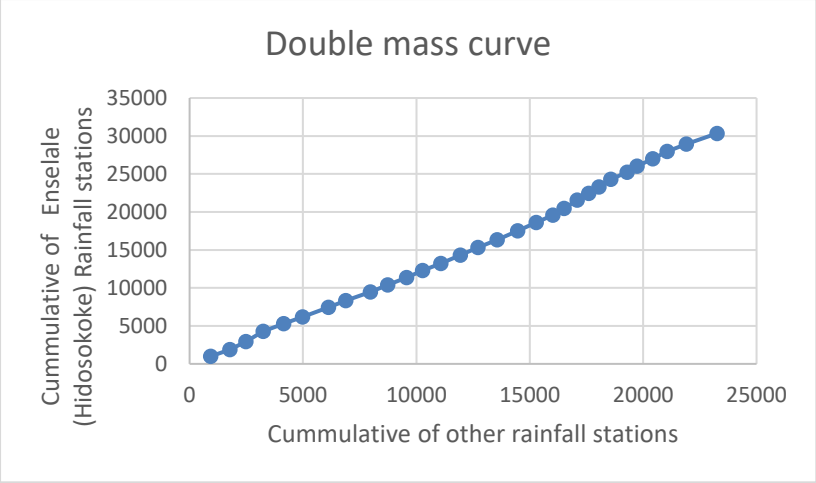
Double mass curve
Cummulative of Enselale (Hidosokoke) Rainfall stations
35000
30000
25000
20000
15000
10000
5000
0
0
5000
10000
15000
20000
25000
Cummulative of other rainfall stations

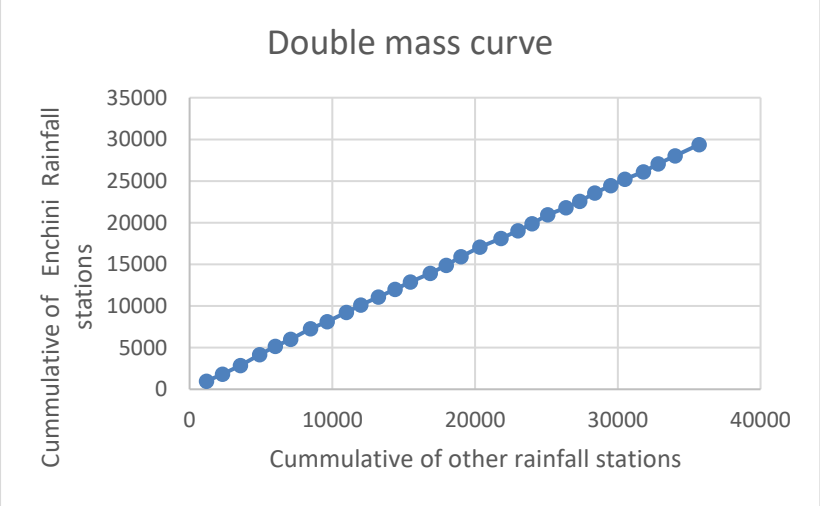
Double mass curve
Cummulative of Enchini Rainfall stations
35000
30000
25000
20000
15000
10000
5000
0
0
10000
20000
30000
40000
Cummulative of other rainfall stations

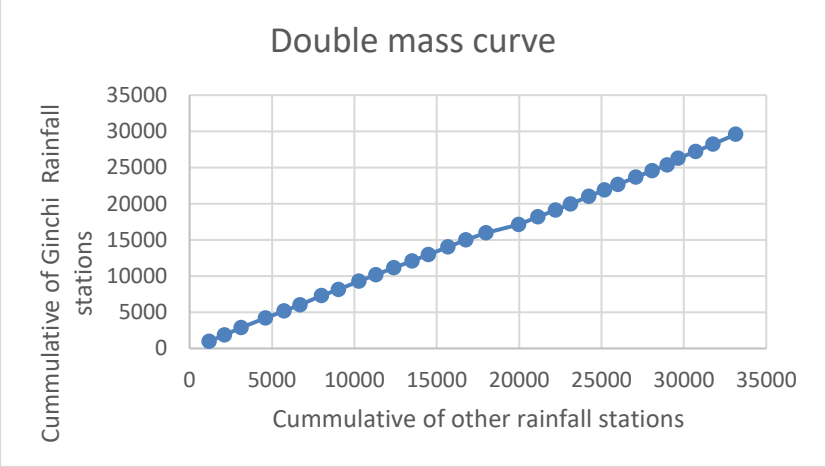
Double mass curve
Cummulative of Ginchi Rainfall stations
35000
30000
25000
20000
15000
10000
5000
0
0
5000
10000
15000
20000
25000
30000
35000
Cummulative of other rainfall stations

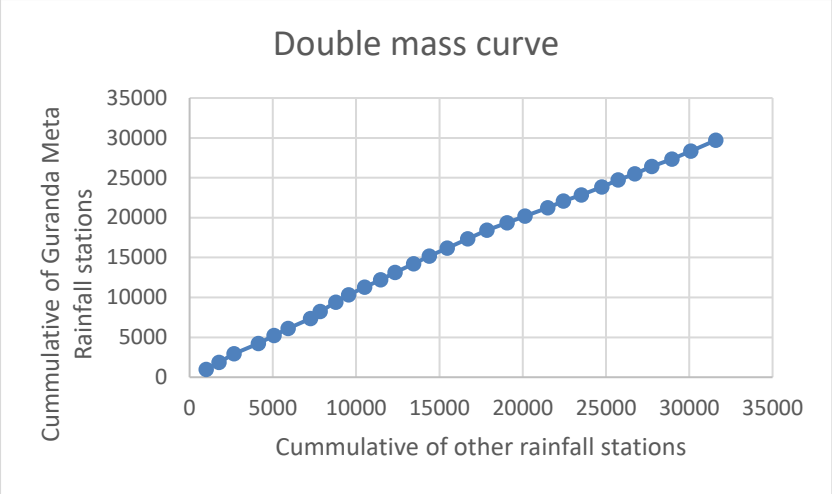
Double mass curve
Cummulative of Guranda Meta Rainfall stations
35000
30000
25000
20000
15000
10000
5000
0
0
5000
10000
15000
20000
25000
30000
35000
Cummulative of other rainfall stations

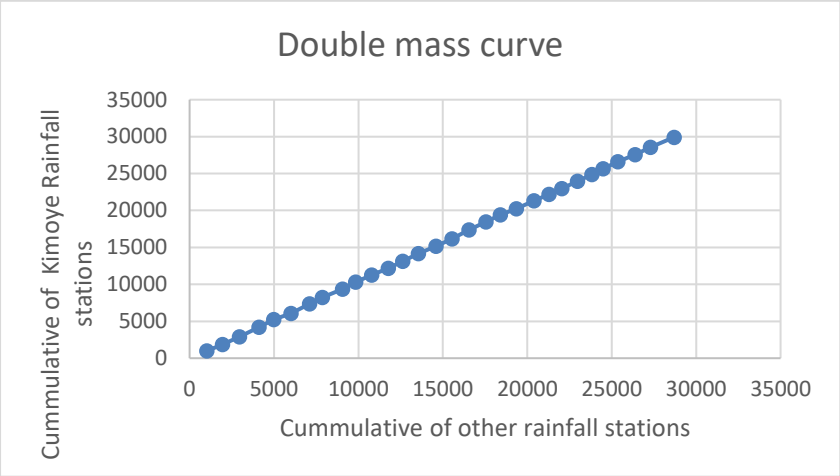
Double mass curve
Cummulative of Kimoye Rainfall stations
35000
30000
25000
20000
15000
10000
5000
0
0
5000
10000
15000
20000
25000
30000
35000
Cummulative of other rainfall stations

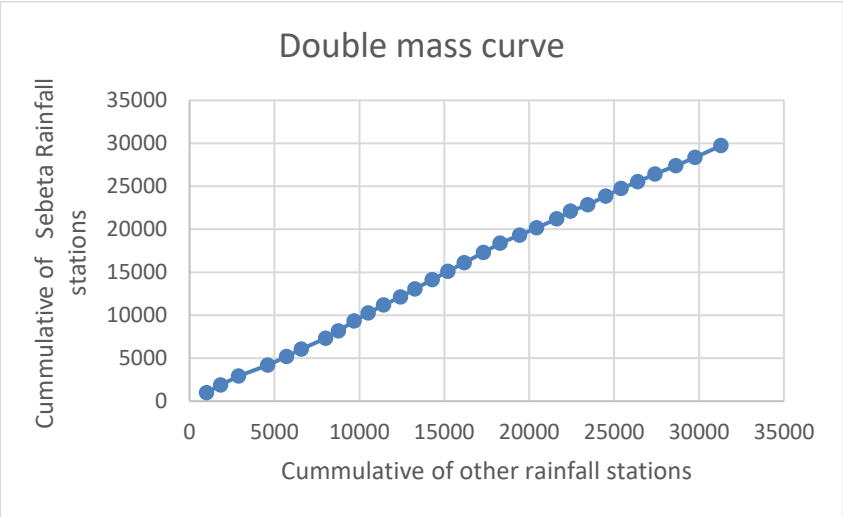
Double mass curve
Cummulative of Sebeta Rainfall stations
35000
30000
25000
20000
15000
10000
5000
0
0
5000
10000
15000
20000
25000
30000
35000
Cummulative of other rainfall stations

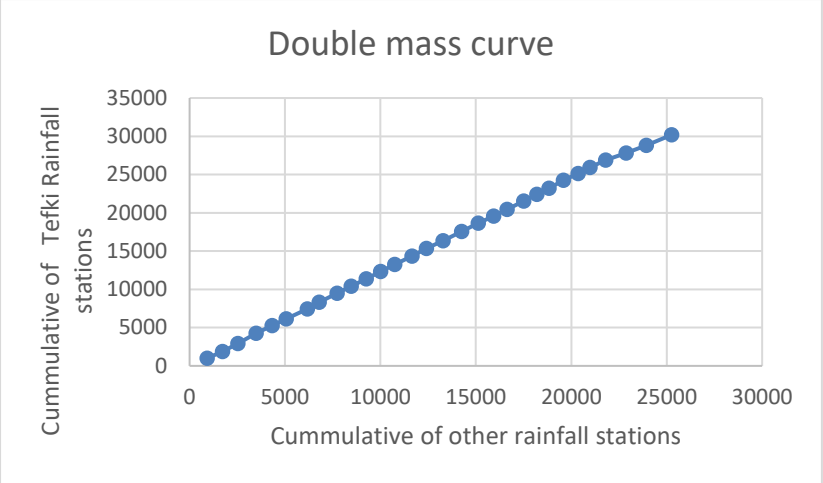
Double mass curve
Cummulative of Tefki Rainfall stations
35000
30000
25000
20000
15000
10000
5000
0
0
5000
10000
15000
20000
25000
30000
Cummulative of other rainfall stations

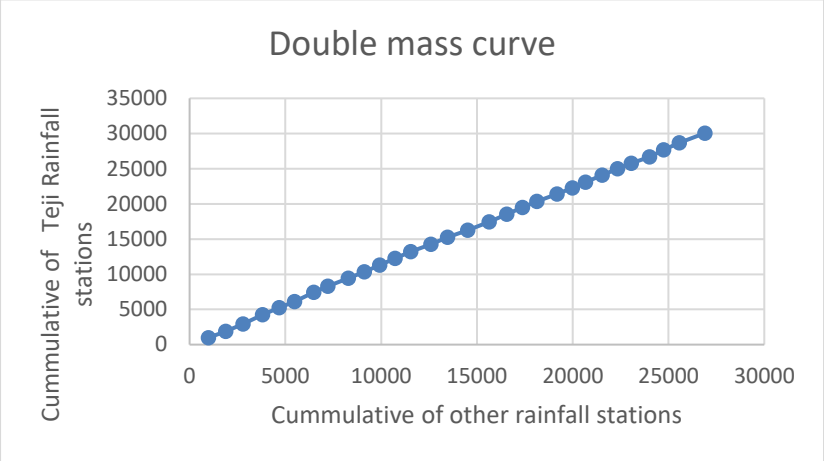
Double mass curve
Cummulative of Teji Rainfall stations
35000
30000
25000
20000
15000
10000
5000
0
0
5000
10000
15000
20000
25000
30000
Cummulative of other rainfall stations

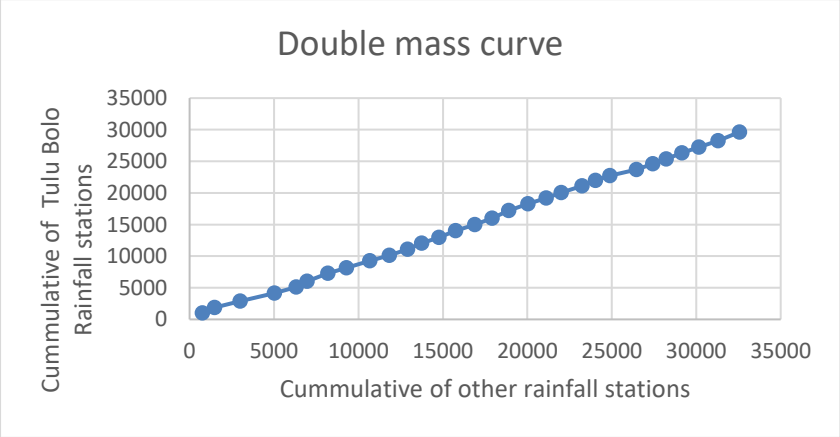
Double mass curve
Cummulative of Tulu Bolo Rainfall stations
35000
30000
25000
20000
15000
10000
5000
0
0
5000
10000
15000
20000
25000
30000
35000
Cummulative of other rainfall stations

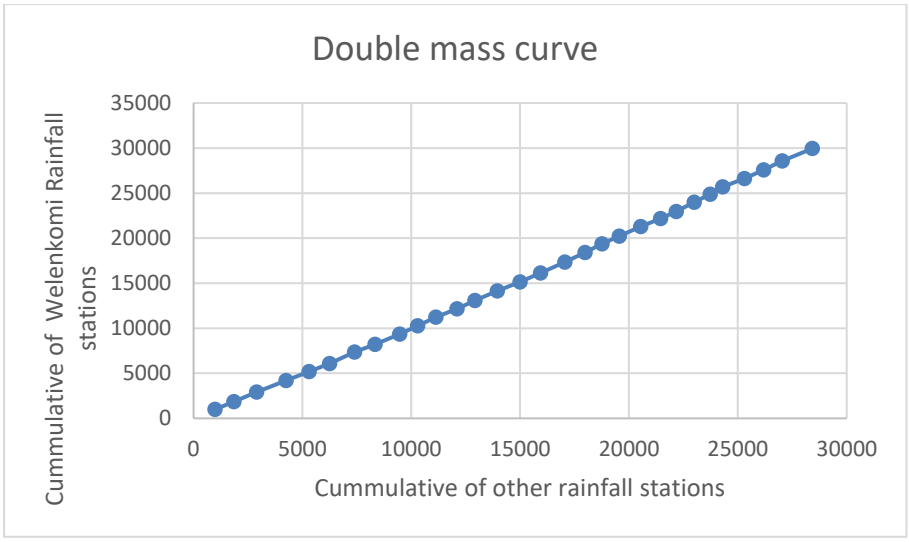
Double mass curve
Cummulative of Welenkomi Rainfall stations
35000
30000
25000
20000
15000
10000
5000
0
0
5000
10000
15000
20000
25000
30000
Cummulative of other rainfall stations

**Appendix 2:** Graphical Representations of the simulated daily flows from 1991 to 2020 for selected drainage structures

- C05 (Slab culvert with 3m span by 3m height)

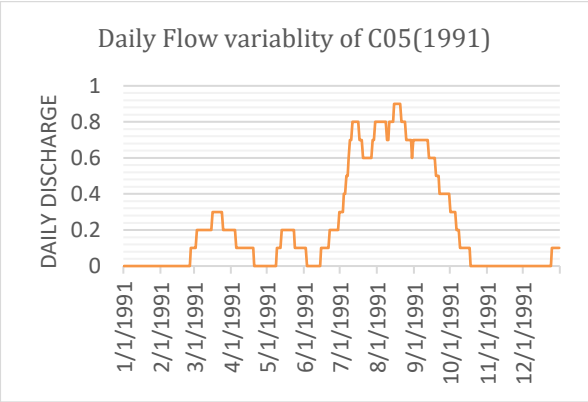


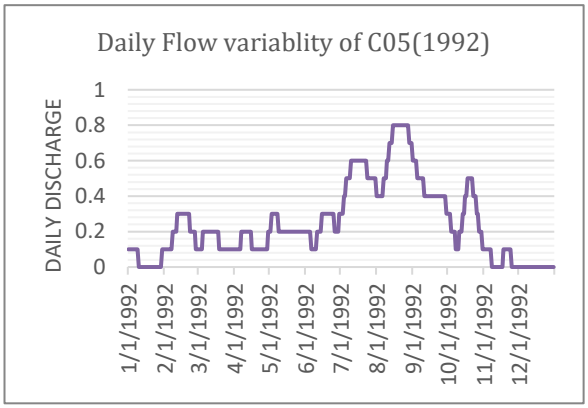


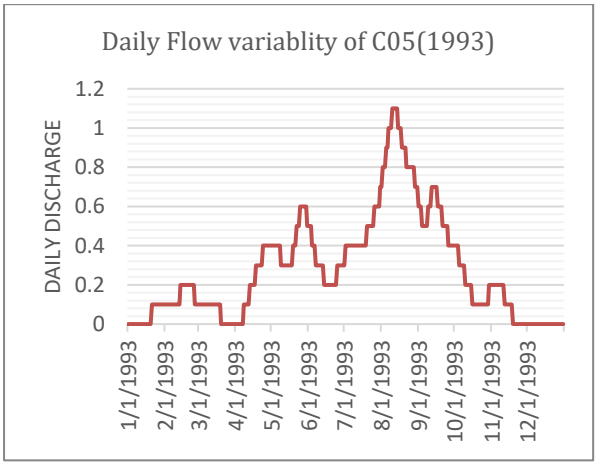


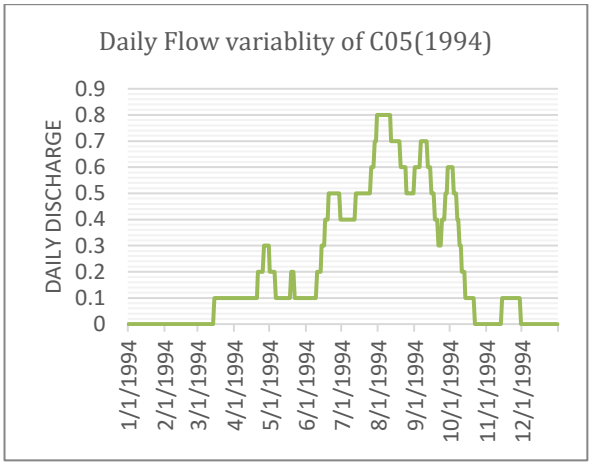


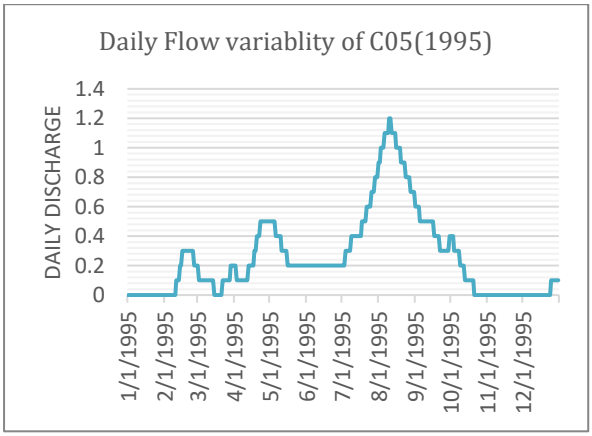


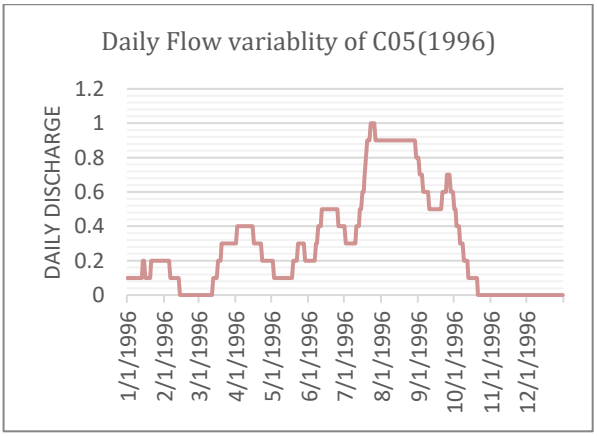

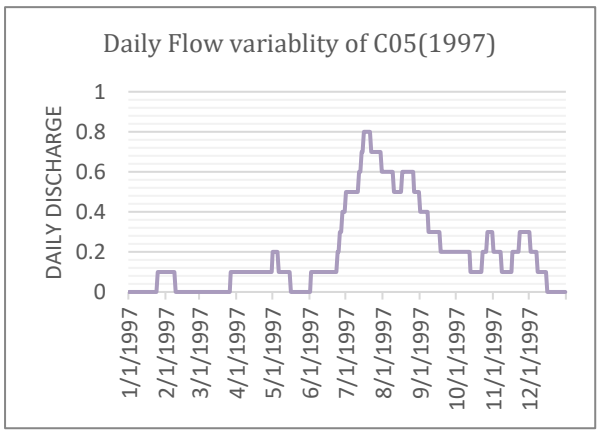
Daily Flow variablity of C05(1997)
DAILY DISCHARGE
1
0.8
0.6
0.4
0.2
0
1/1/1997
2/1/1997
3/1/1997
4/1/1997
5/1/1997
6/1/1997
7/1/1997
8/1/1997
9/1/1997
10/1/1997
11/1/1997
12/1/1997

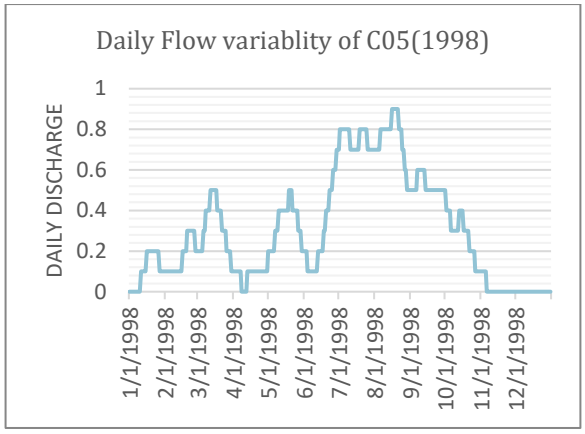
Daily Flow variablity of C05(1998)
DAILY DISCHARGE
1
0.8
0.6
0.4
0.2
0
1/1/1998
2/1/1998
3/1/1998
4/1/1998
5/1/1998
6/1/1998
7/1/1998
8/1/1998
9/1/1998
10/1/1998
11/1/1998
12/1/1998

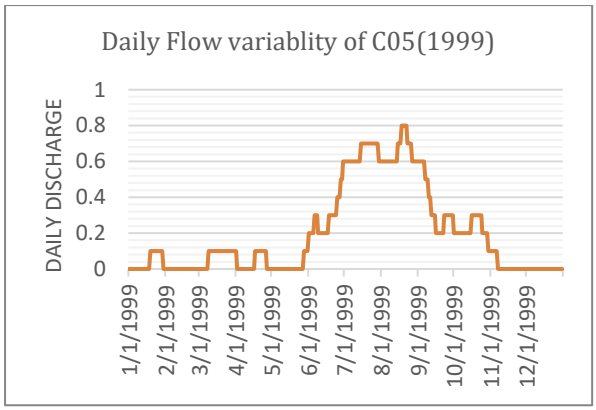
Daily Flow variablity of C05(1999)
DAILY DISCHARGE
1
0.8
0.6
0.4
0.2
0
1/1/1999
2/1/1999
3/1/1999
4/1/1999
5/1/1999
6/1/1999
7/1/1999
8/1/1999
9/1/1999
10/1/1999
11/1/1999
12/1/1999

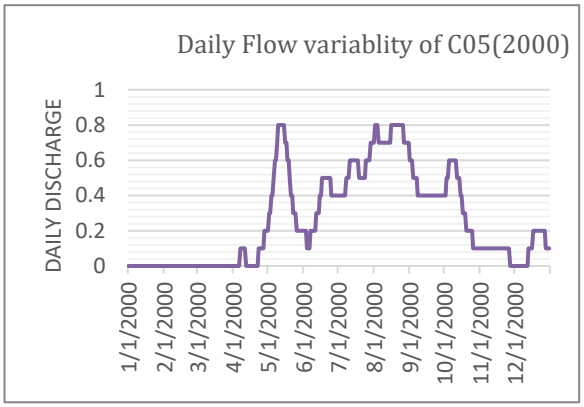
Daily Flow variablity of C05(2000)
DAILY DISCHARGE
1
0.8
0.6
0.4
0.2
0
1/1/2000
2/1/2000
3/1/2000
4/1/2000
5/1/2000
6/1/2000
7/1/2000
8/1/2000
9/1/2000
10/1/2000
11/1/2000
12/1/2000

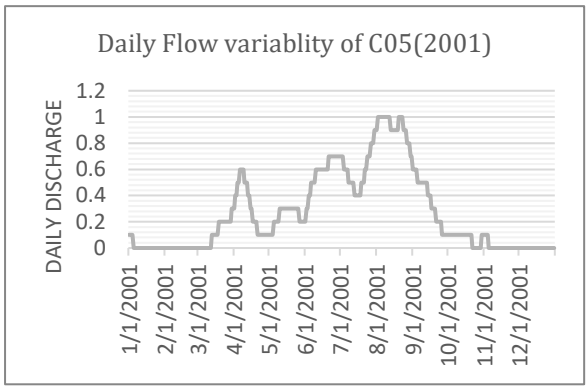
Daily Flow variablity of C05(2001)
DAILY DISCHARGE
1.2
1
0.8
0.6
0.4
0.2
0
1/1/2001
2/1/2001
3/1/2001
4/1/2001
5/1/2001
6/1/2001
7/1/2001
8/1/2001
9/1/2001
10/1/2001
11/1/2001
12/1/2001

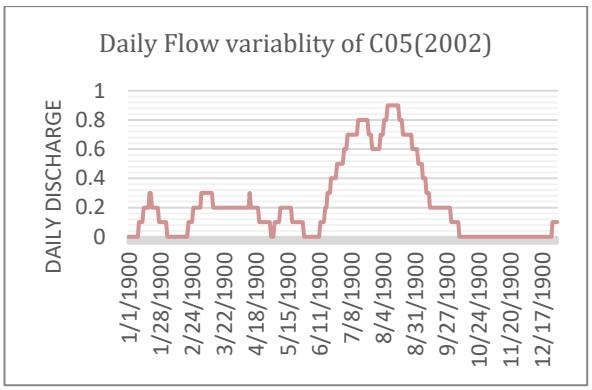
Daily Flow variablity of C05(2002)
DAILY DISCHARGE
1
0.8
0.6
0.4
0.2
0
1/1/1900
1/28/1900
2/24/1900
3/22/1900
4/18/1900
5/15/1900
6/11/1900
7/8/1900
8/4/1900
8/31/1900
9/27/1900
10/24/1900
11/20/1900
12/17/1900

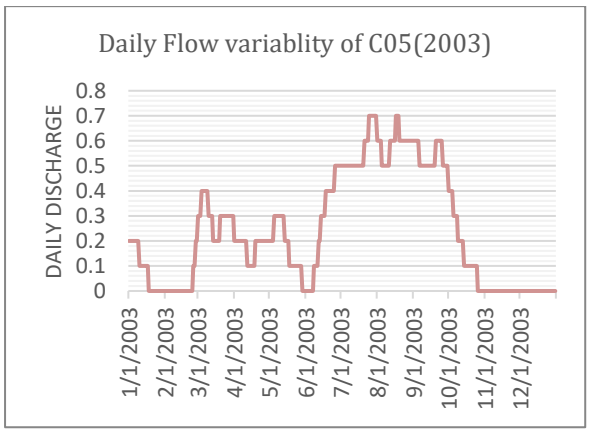
Daily Flow variablity of C05(2003)
DAILY DISCHARGE
0.8
0.7
0.6
0.5
0.4
0.3
0.2
0.1
0
1/1/2003
2/1/2003
3/1/2003
4/1/2003
5/1/2003
6/1/2003
7/1/2003
8/1/2003
9/1/2003
10/1/2003
11/1/2003
12/1/2003

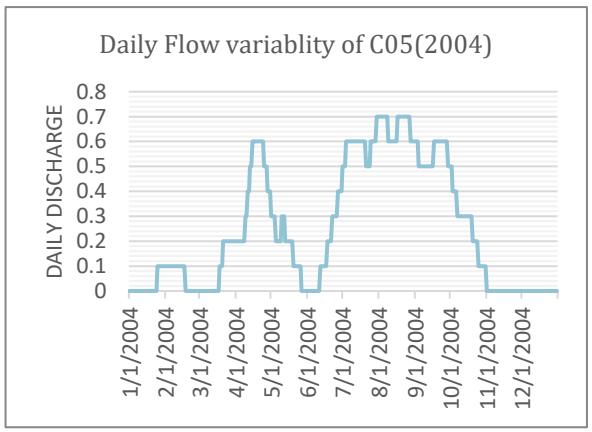
Daily Flow variablity of C05(2004)
DAILY DISCHARGE
0.8
0.7
0.6
0.5
0.4
0.3
0.2
0.1
0
1/1/2004
2/1/2004
3/1/2004
4/1/2004
5/1/2004
6/1/2004
7/1/2004
8/1/2004
9/1/2004
10/1/2004
11/1/2004
12/1/2004

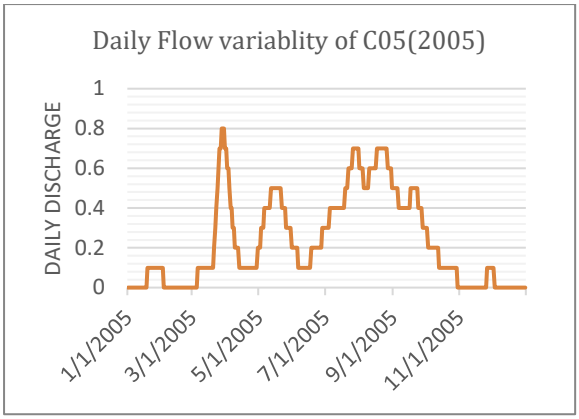
Daily Flow variablity of C05(2005)
DAILY DISCHARGE
1
0.8
0.6
0.4
0.2
0
1/1/2005
3/1/2005
5/1/2005
7/1/2005
9/1/2005
11/1/2005

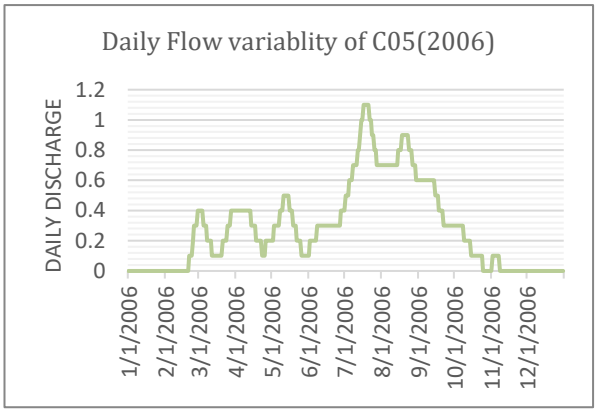
Daily Flow variablity of C05(2006)
DAILY DISCHARGE
1.2
1
0.8
0.6
0.4
0.2
0
1/1/2006
2/1/2006
3/1/2006
4/1/2006
5/1/2006
6/1/2006
7/1/2006
8/1/2006
9/1/2006
10/1/2006
11/1/2006
12/1/2006

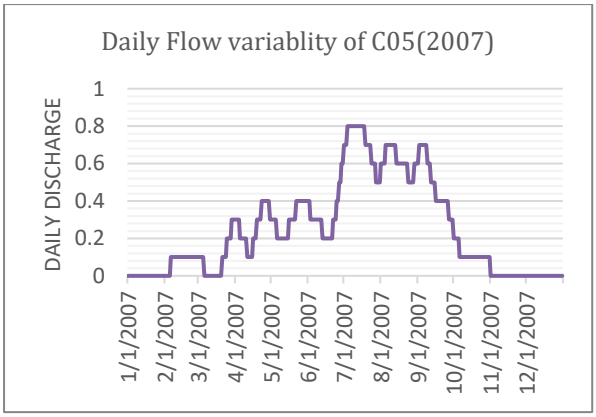
Daily Flow variablity of C05(2007)
DAILY DISCHARGE
1
0.8
0.6
0.4
0.2
0
1/1/2007
2/1/2007
3/1/2007
4/1/2007
5/1/2007
6/1/2007
7/1/2007
8/1/2007
9/1/2007
10/1/2007
11/1/2007
12/1/2007

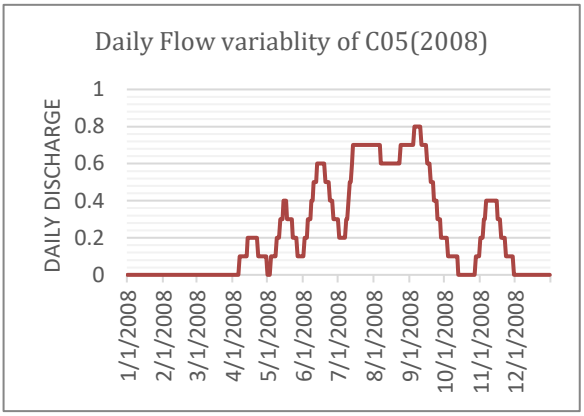
Daily Flow variablity of C05(2008)
DAILY DISCHARGE
1
0.8
0.6
0.4
0.2
0
1/1/2008
2/1/2008
3/1/2008
4/1/2008
5/1/2008
6/1/2008
7/1/2008
8/1/2008
9/1/2008
10/1/2008
11/1/2008
12/1/2008

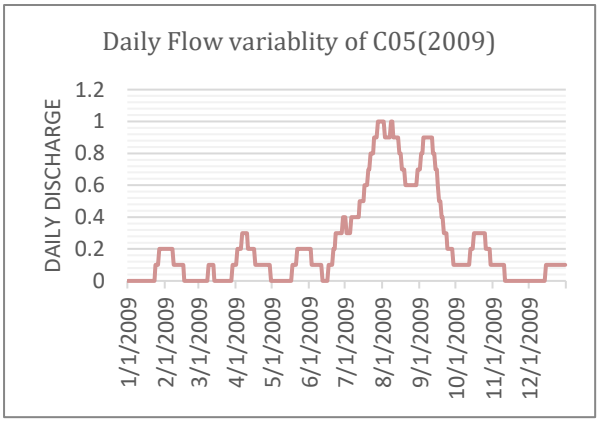
Daily Flow variablity of C05(2009)
DAILY DISCHARGE
1.2
1
0.8
0.6
0.4
0.2
0
1/1/2009
2/1/2009
3/1/2009
4/1/2009
5/1/2009
6/1/2009
7/1/2009
8/1/2009
9/1/2009
10/1/2009
11/1/2009
12/1/2009

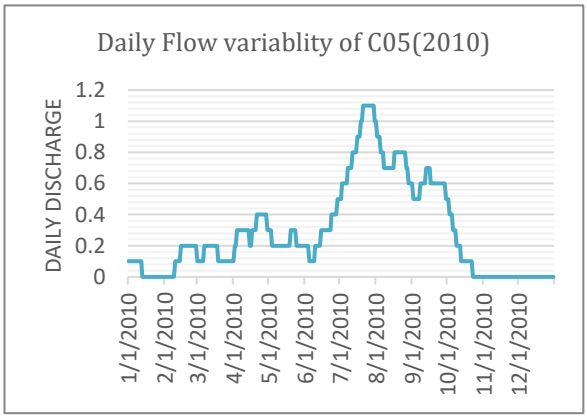
Daily Flow variablity of C05(2010)
DAILY DISCHARGE
1.2
1
0.8
0.6
0.4
0.2
0
1/1/2010
2/1/2010
3/1/2010
4/1/2010
5/1/2010
6/1/2010
7/1/2010
8/1/2010
9/1/2010
10/1/2010
11/1/2010
12/1/2010

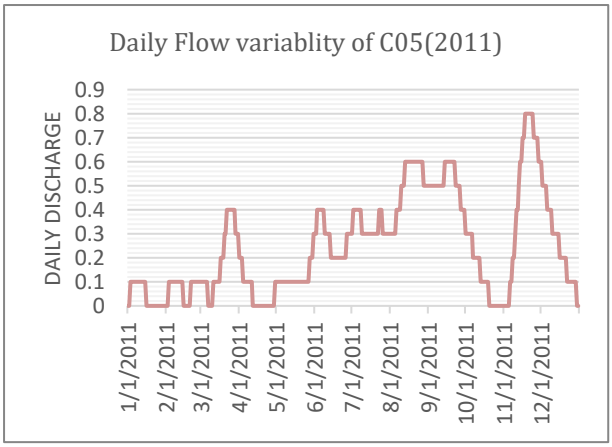
Daily Flow variablity of C05(2011)
DAILY DISCHARGE
0.9
0.8
0.7
0.6
0.5
0.4
0.3
0.2
0.1
0
1/1/2011
2/1/2011
3/1/2011
4/1/2011
5/1/2011
6/1/2011
7/1/2011
8/1/2011
9/1/2011
10/1/2011
11/1/2011
12/1/2011

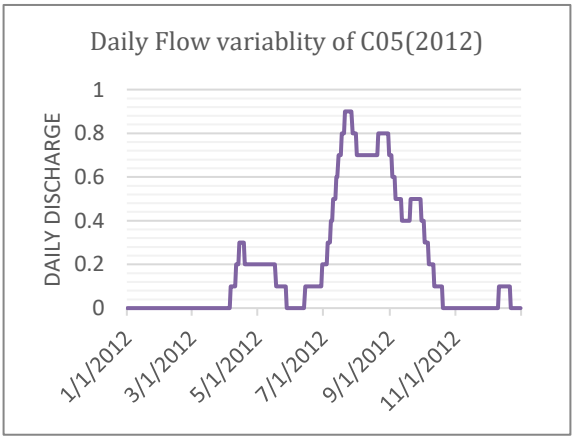
Daily Flow variablity of C05(2012)
DAILY DISCHARGE
1
0.8
0.6
0.4
0.2
0
1/1/2012
3/1/2012
5/1/2012
7/1/2012
9/1/2012
11/1/2012

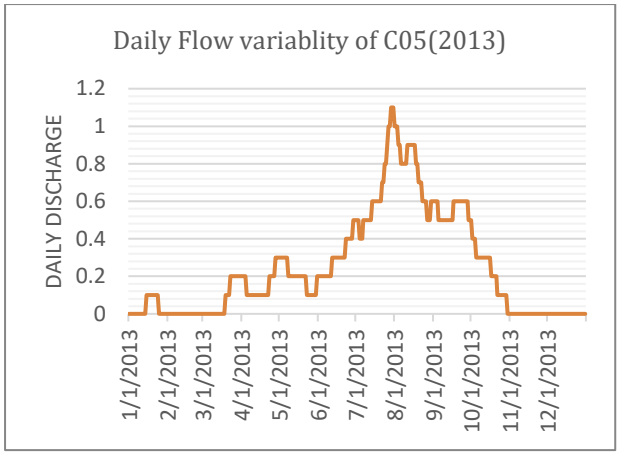
Daily Flow variablity of C05(2013)
DAILY DISCHARGE
1.2
1
0.8
0.6
0.4
0.2
0
1/1/2013
2/1/2013
3/1/2013
4/1/2013
5/1/2013
6/1/2013
7/1/2013
8/1/2013
9/1/2013
10/1/2013
11/1/2013
12/1/2013

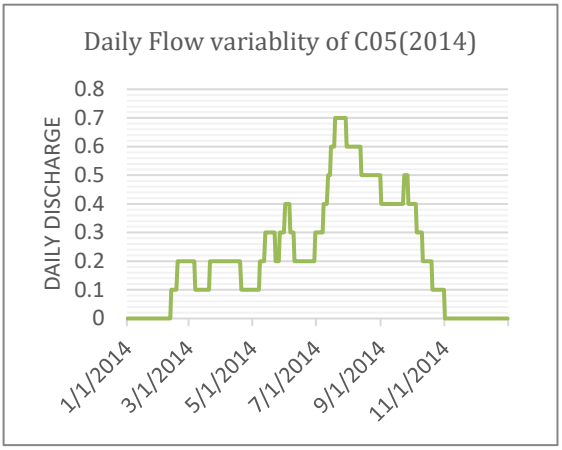
Daily Flow variablity of C05(2014)
DAILY DISCHARGE
0.8
0.7
0.6
0.5
0.4
0.3
0.2
0.1
0
1/1/2014
3/1/2014
5/1/2014
7/1/2014
9/1/2014
11/1/2014

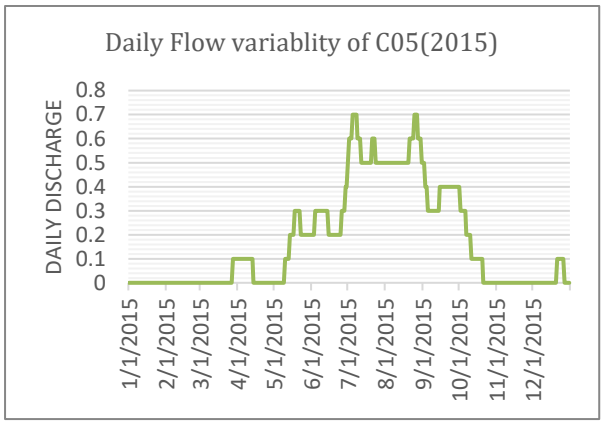
Daily Flow variablity of C05(2015)
DAILY DISCHARGE
0.8
0.7
0.6
0.5
0.4
0.3
0.2
0.1
0
1/1/2015
2/1/2015
3/1/2015
4/1/2015
5/1/2015
6/1/2015
7/1/2015
8/1/2015
9/1/2015
10/1/2015
11/1/2015
12/1/2015

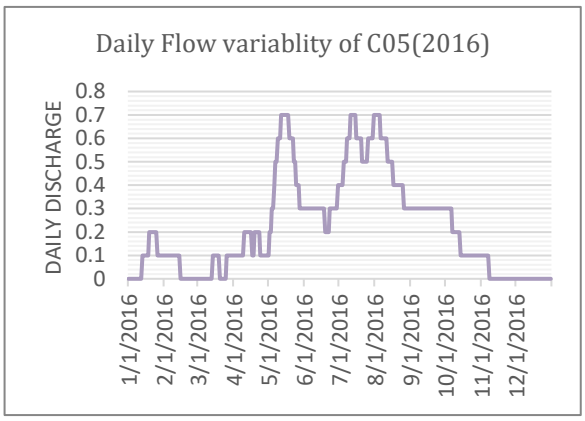
Daily Flow variablity of C05(2016)
DAILY DISCHARGE
0.8
0.7
0.6
0.5
0.4
0.3
0.2
0.1
0
1/1/2016
2/1/2016
3/1/2016
4/1/2016
5/1/2016
6/1/2016
7/1/2016
8/1/2016
9/1/2016
10/1/2016
11/1/2016
12/1/2016

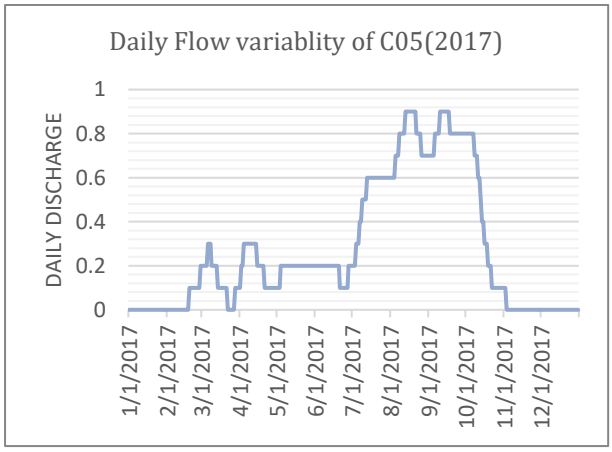
Daily Flow variablity of C05(2017)
DAILY DISCHARGE
1
0.8
0.6
0.4
0.2
0
1/1/2017
2/1/2017
3/1/2017
4/1/2017
5/1/2017
6/1/2017
7/1/2017
8/1/2017
9/1/2017
10/1/2017
11/1/2017
12/1/2017

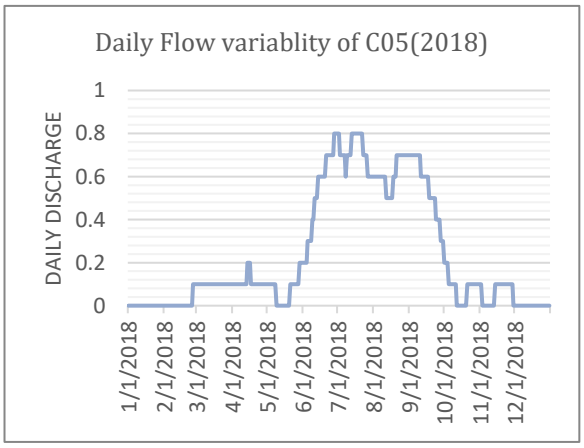
Daily Flow variablity of C05(2018)
DAILY DISCHARGE
1
0.8
0.6
0.4
0.2
0
1/1/2018
2/1/2018
3/1/2018
4/1/2018
5/1/2018
6/1/2018
7/1/2018
8/1/2018
9/1/2018
10/1/2018
11/1/2018
12/1/2018

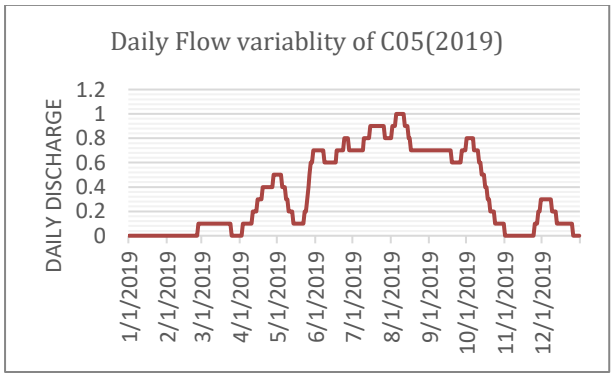
Daily Flow variablity of C05(2019)
DAILY DISCHARGE
1.2
1
0.8
0.6
0.4
0.2
0
1/1/2019
2/1/2019
3/1/2019
4/1/2019
5/1/2019
6/1/2019
7/1/2019
8/1/2019
9/1/2019
10/1/2019
11/1/2019
12/1/2019

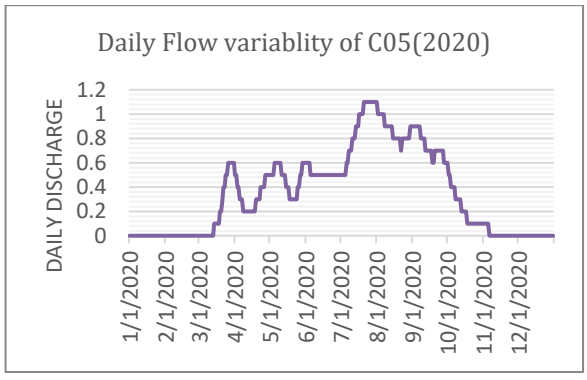
Daily Flow variablity of C05(2020)
DAILY DISCHARGE
1.2
1
0.8
0.6
0.4
0.2
0
1/1/2020
2/1/2020
3/1/2020
4/1/2020
5/1/2020
6/1/2020
7/1/2020
8/1/2020
9/1/2020
10/1/2020
11/1/2020
12/1/2020

- C15 (Double Box culvert with 4m span by 2.5m height)

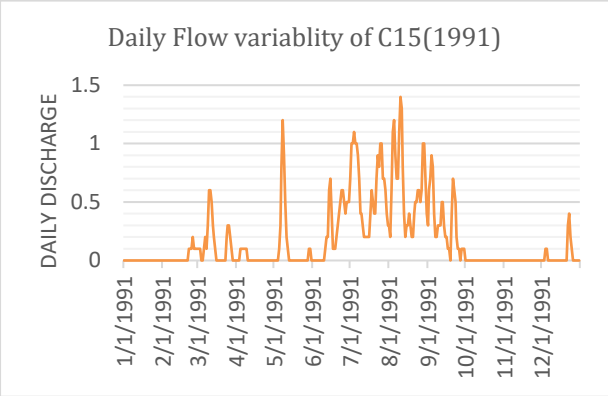


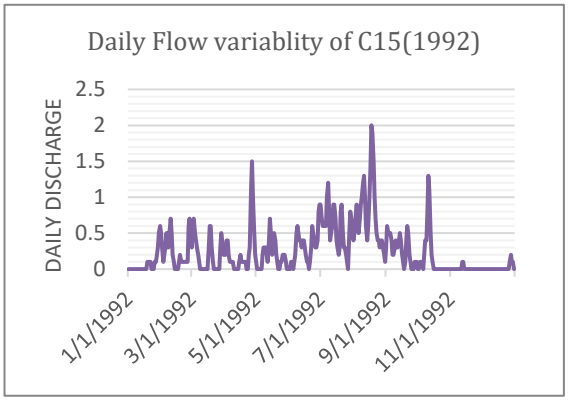


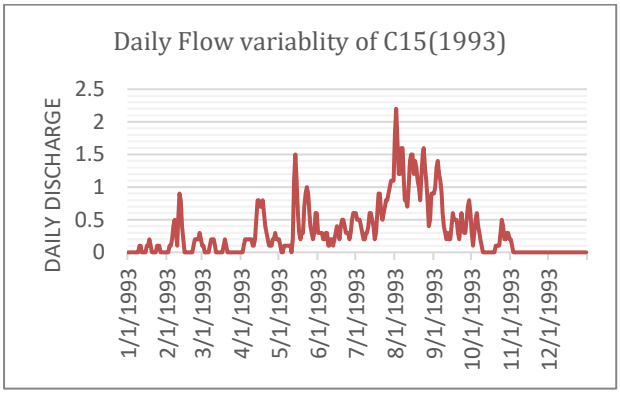


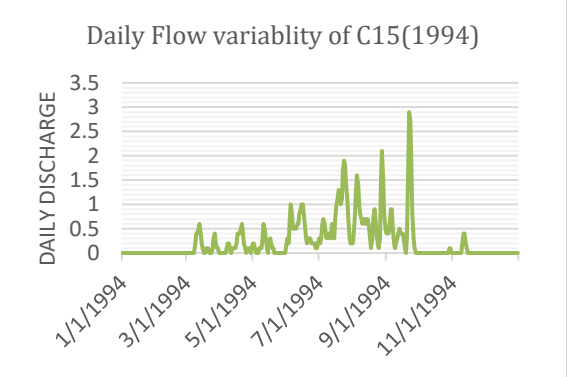


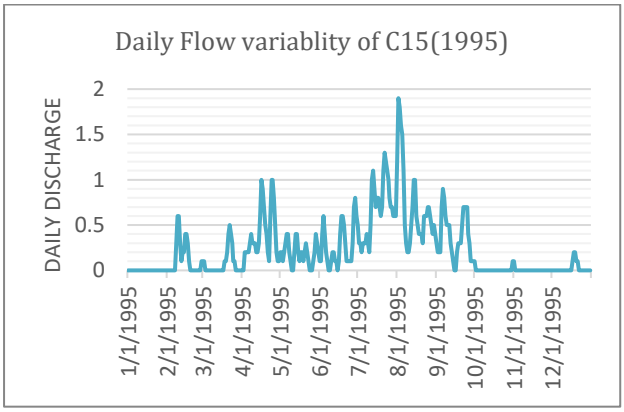


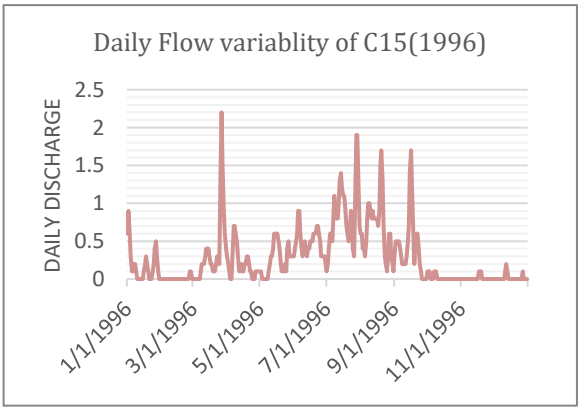


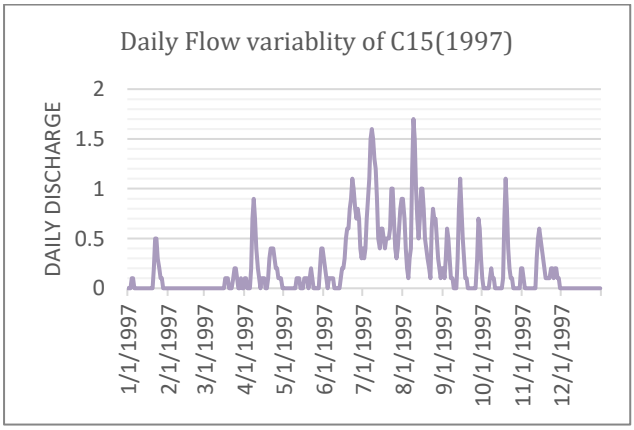


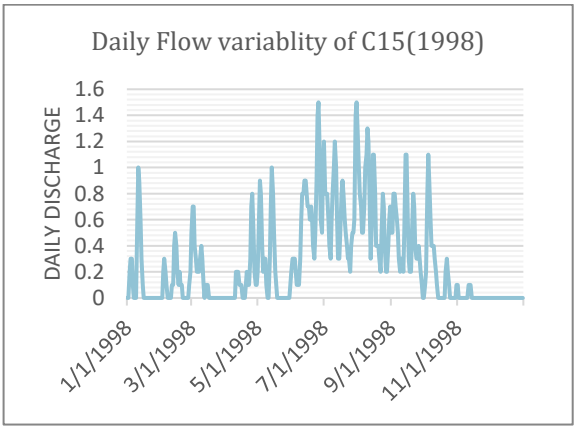

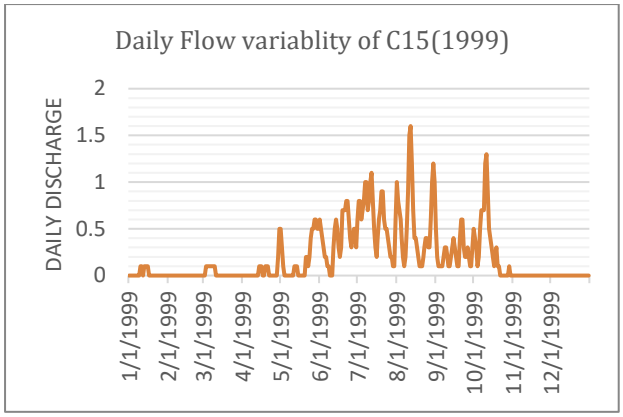
Daily Flow variablity of C15(1999)
DAILY DISCHARGE
2
1.5
1
0.5
0
1/1/1999
2/1/1999
3/1/1999
4/1/1999
5/1/1999
6/1/1999
7/1/1999
8/1/1999
9/1/1999
10/1/1999
11/1/1999
12/1/1999

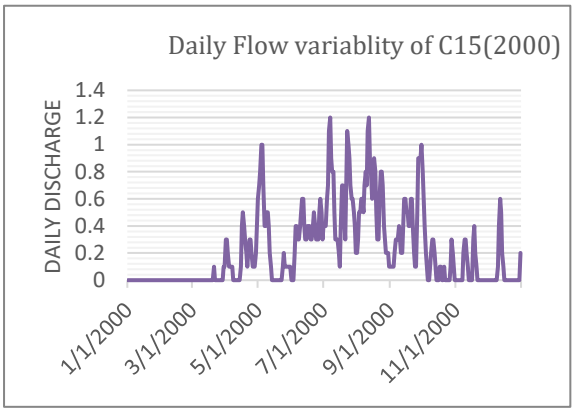
Daily Flow variablity of C15(2000)
DAILY DISCHARGE
1.4
1.2
1
0.8
0.6
0.4
0.2
0
1/1/2000
3/1/2000
5/1/2000
7/1/2000
9/1/2000
11/1/2000

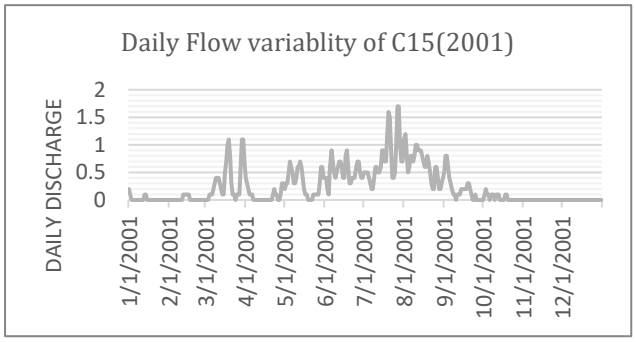
Daily Flow variablity of C15(2001)
DAILY DISCHARGE
2
1.5
1
0.5
0
1/1/2001
2/1/2001
3/1/2001
4/1/2001
5/1/2001
6/1/2001
7/1/2001
8/1/2001
9/1/2001
10/1/2001
11/1/2001
12/1/2001

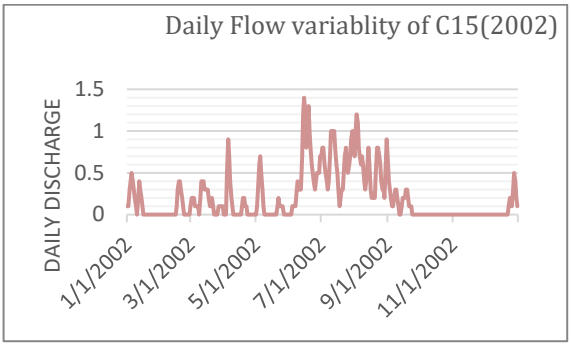
Daily Flow variablity of C15(2002)
DAILY DISCHARGE
1.5
1
0.5
0
1/1/2002
3/1/2002
5/1/2002
7/1/2002
9/1/2002
11/1/2002

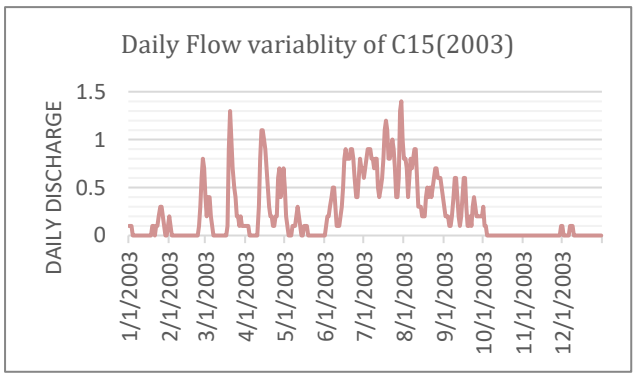
Daily Flow variablity of C15(2003)
DAILY DISCHARGE
1.5
1
0.5
0
1/1/2003
2/1/2003
3/1/2003
4/1/2003
5/1/2003
6/1/2003
7/1/2003
8/1/2003
9/1/2003
10/1/2003
11/1/2003
12/1/2003

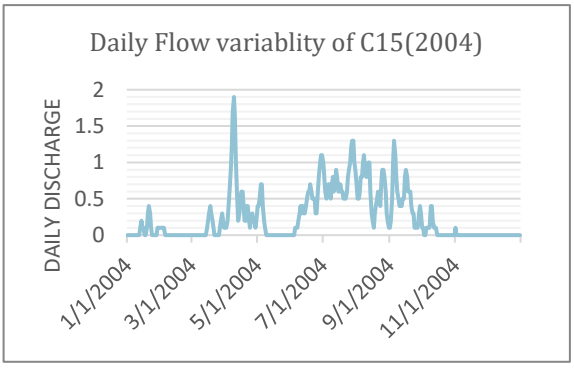
Daily Flow variablity of C15(2004)
DAILY DISCHARGE
2
1.5
1
0.5
0
1/1/2004
3/1/2004
5/1/2004
7/1/2004
9/1/2004
11/1/2004

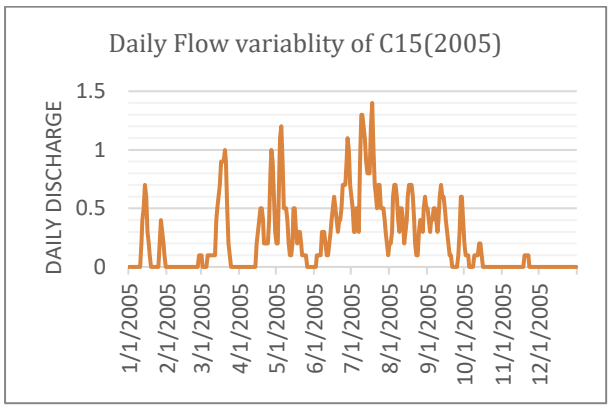
Daily Flow variablity of C15(2005)
DAILY DISCHARGE
1.5
1
0.5
0
1/1/2005
2/1/2005
3/1/2005
4/1/2005
5/1/2005
6/1/2005
7/1/2005
8/1/2005
9/1/2005
10/1/2005
11/1/2005
12/1/2005

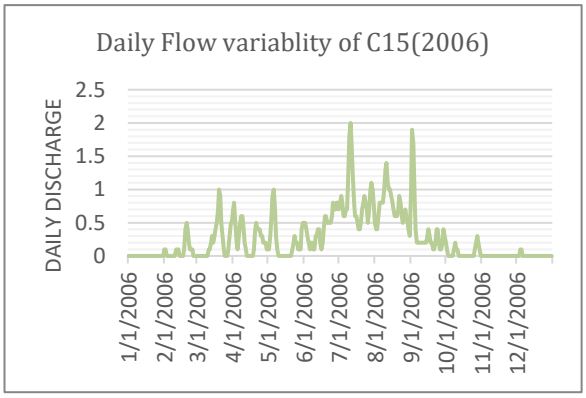
Daily Flow variablity of C15(2006)
DAILY DISCHARGE
2.5
2
1.5
1
0.5
0
1/1/2006
2/1/2006
3/1/2006
4/1/2006
5/1/2006
6/1/2006
7/1/2006
8/1/2006
9/1/2006
10/1/2006
11/1/2006
12/1/2006

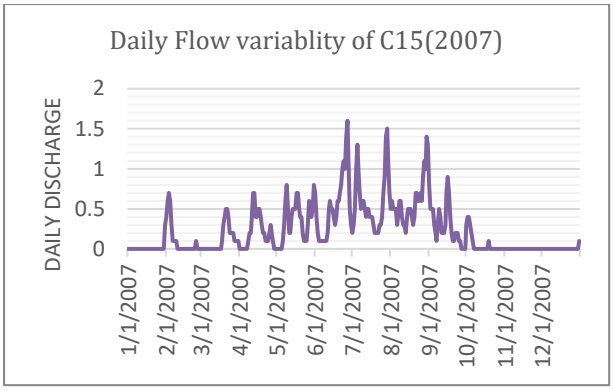
Daily Flow variablity of C15(2007)
DAILY DISCHARGE
2
1.5
1
0.5
0
1/1/2007
2/1/2007
3/1/2007
4/1/2007
5/1/2007
6/1/2007
7/1/2007
8/1/2007
9/1/2007
10/1/2007
11/1/2007
12/1/2007

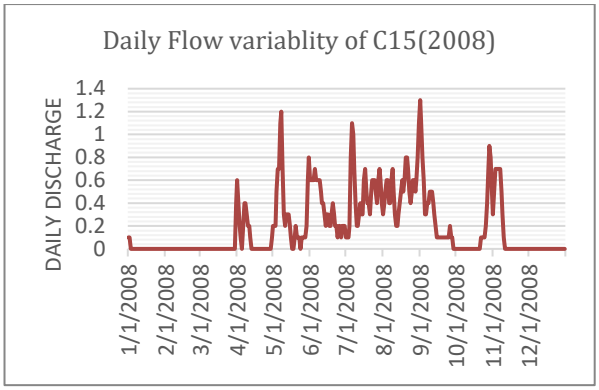
Daily Flow variablity of C15(2008)
DAILY DISCHARGE
1.4
1.2
1
0.8
0.6
0.4
0.2
0
1/1/2008
2/1/2008
3/1/2008
4/1/2008
5/1/2008
6/1/2008
7/1/2008
8/1/2008
9/1/2008
10/1/2008
11/1/2008
12/1/2008

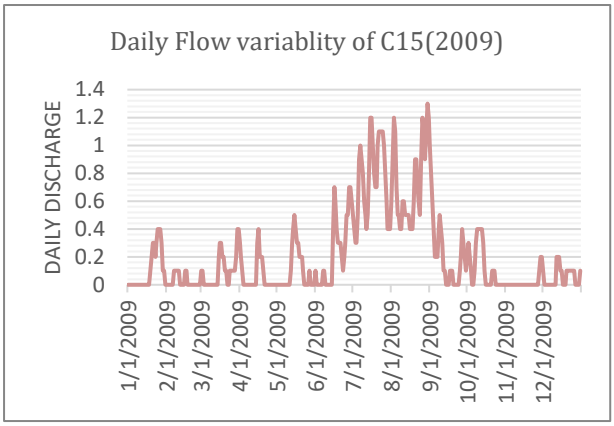
Daily Flow variablity of C15(2009)
DAILY DISCHARGE
1.4
1.2
1
0.8
0.6
0.4
0.2
0
1/1/2009
2/1/2009
3/1/2009
4/1/2009
5/1/2009
6/1/2009
7/1/2009
8/1/2009
9/1/2009
10/1/2009
11/1/2009
12/1/2009

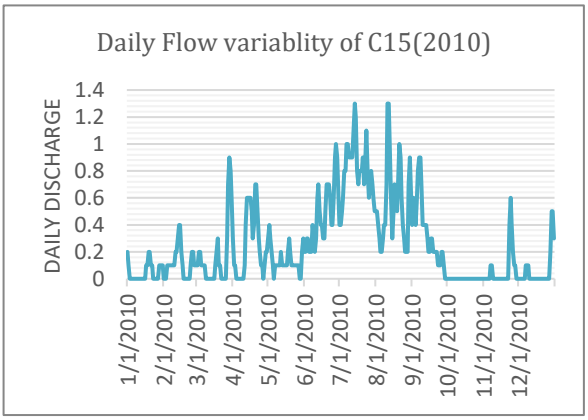
Daily Flow variablity of C15(2010)
DAILY DISCHARGE
1.4
1.2
1
0.8
0.6
0.4
0.2
0
1/1/2010
2/1/2010
3/1/2010
4/1/2010
5/1/2010
6/1/2010
7/1/2010
8/1/2010
9/1/2010
10/1/2010
11/1/2010
12/1/2010

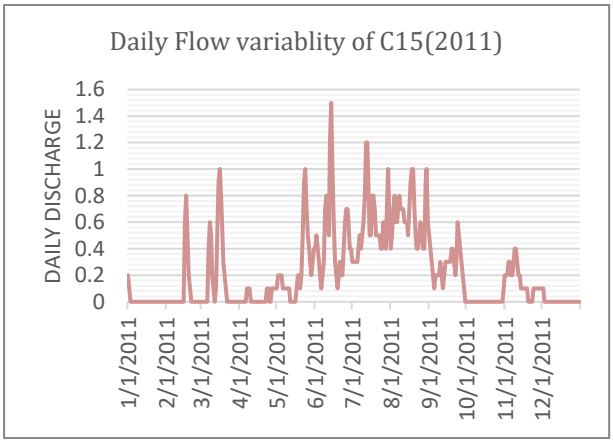
Daily Flow variablity of C15(2011)
DAILY DISCHARGE
1.6
1.4
1.2
1
0.8
0.6
0.4
0.2
0
1/1/2011
2/1/2011
3/1/2011
4/1/2011
5/1/2011
6/1/2011
7/1/2011
8/1/2011
9/1/2011
10/1/2011
11/1/2011
12/1/2011

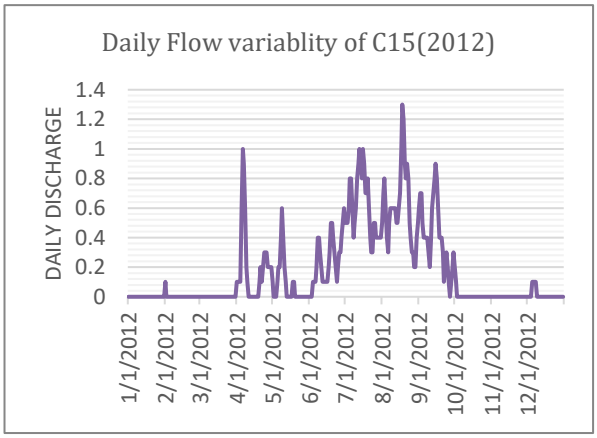
Daily Flow variablity of C15(2012)
DAILY DISCHARGE
1.4
1.2
1
0.8
0.6
0.4
0.2
0
1/1/2012
2/1/2012
3/1/2012
4/1/2012
5/1/2012
6/1/2012
7/1/2012
8/1/2012
9/1/2012
10/1/2012
11/1/2012
12/1/2012

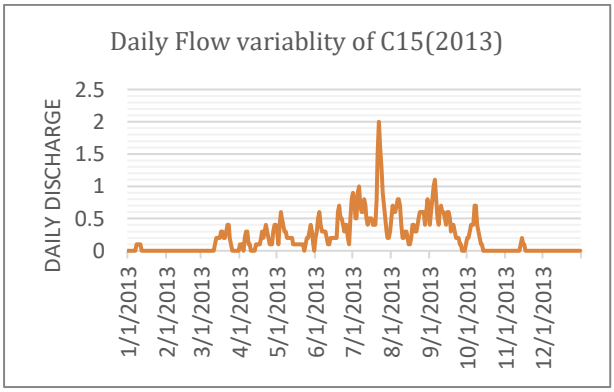
Daily Flow variablity of C15(2013)
DAILY DISCHARGE
2.5
2
1.5
1
0.5
0
1/1/2013
2/1/2013
3/1/2013
4/1/2013
5/1/2013
6/1/2013
7/1/2013
8/1/2013
9/1/2013
10/1/2013
11/1/2013
12/1/2013

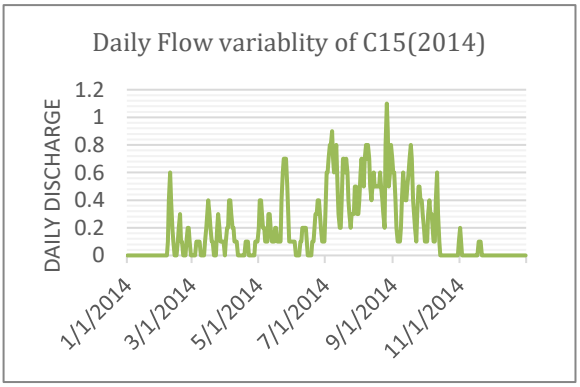
Daily Flow variablity of C15(2014)
DAILY DISCHARGE
1.2
1
0.8
0.6
0.4
0.2
0
1/1/2014
3/1/2014
5/1/2014
7/1/2014
9/1/2014
11/1/2014

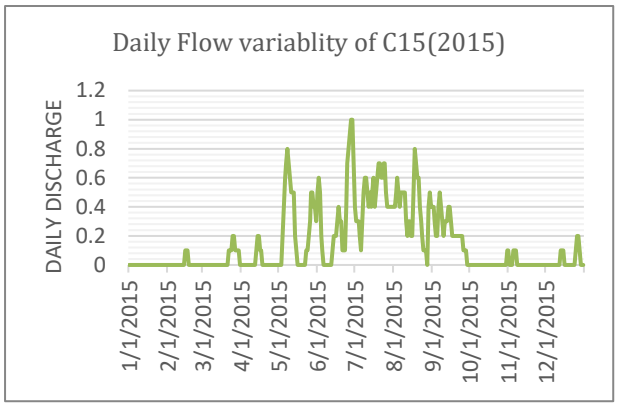


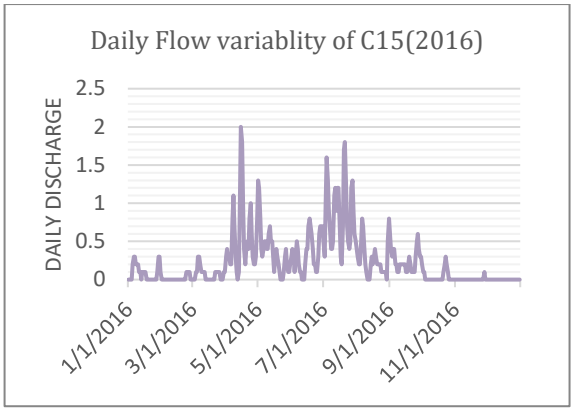


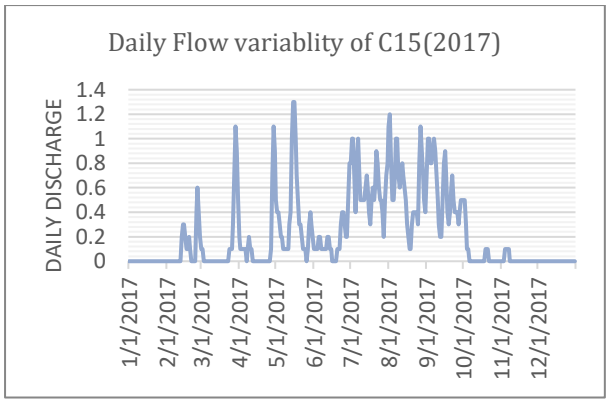


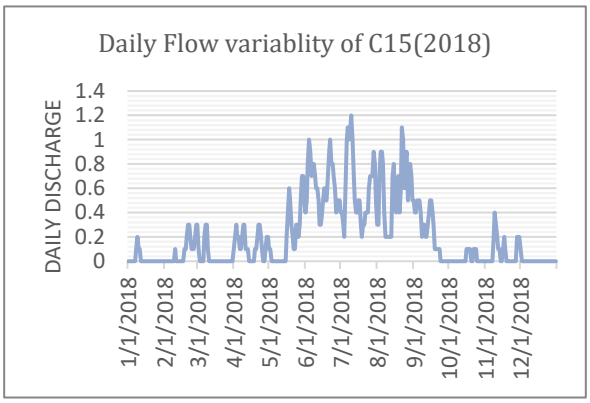


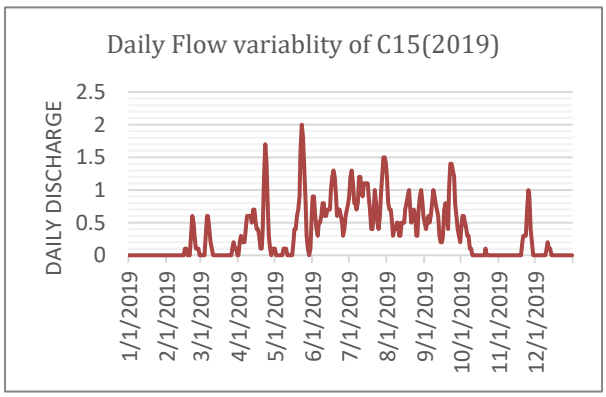


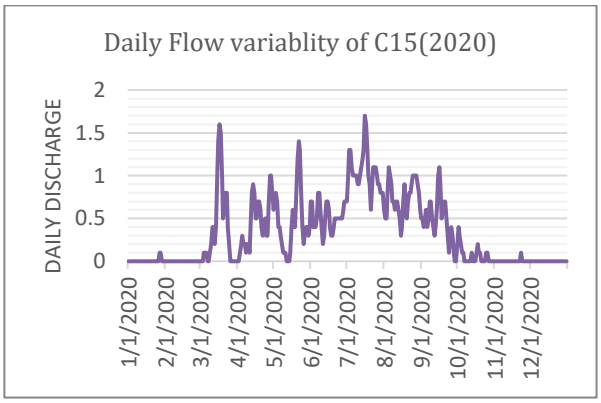


- C56 Reinforced Deck Girder Bridge (27m span with 6m height)

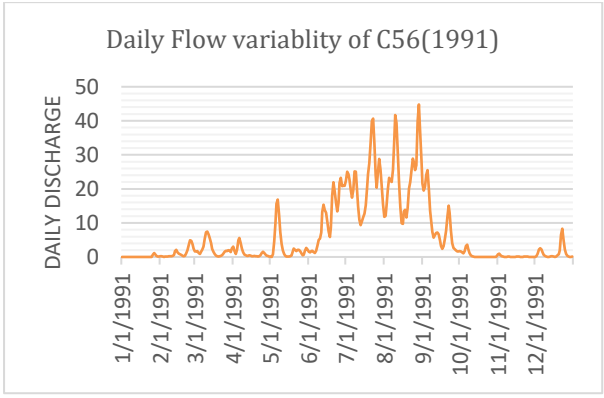


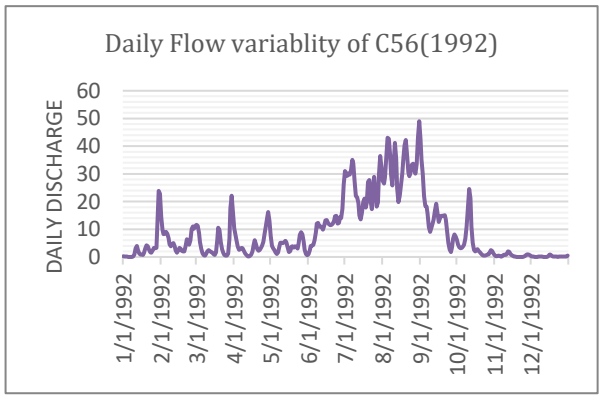

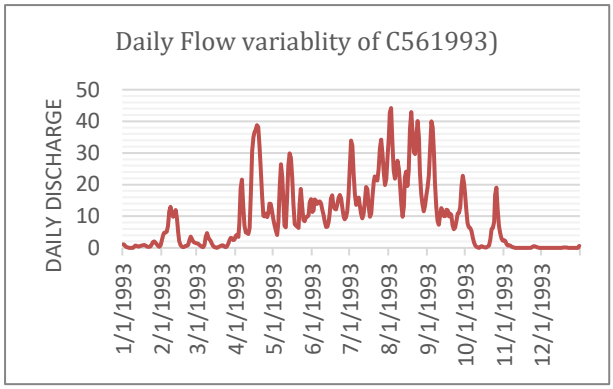
Daily Flow variablity of C561993)
DAILY DISCHARGE
50
40
30
20
10
0
1/1/1993
2/1/1993
3/1/1993
4/1/1993
5/1/1993
6/1/1993
7/1/1993
8/1/1993
9/1/1993
10/1/1993
11/1/1993
12/1/1993

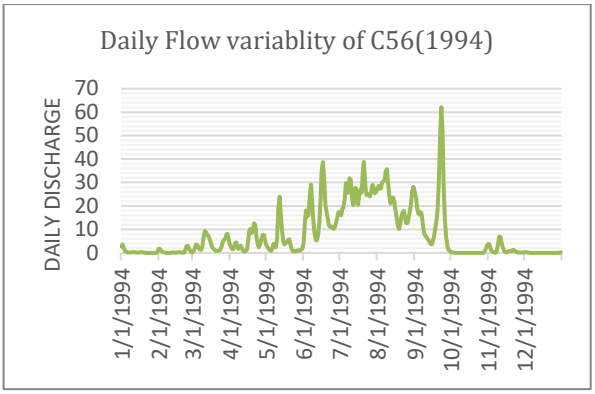
Daily Flow variablity of C56(1994)
DAILY DISCHARGE
70
60
50
40
30
20
10
0
1/1/1994
2/1/1994
3/1/1994
4/1/1994
5/1/1994
6/1/1994
7/1/1994
8/1/1994
9/1/1994
10/1/1994
11/1/1994
12/1/1994

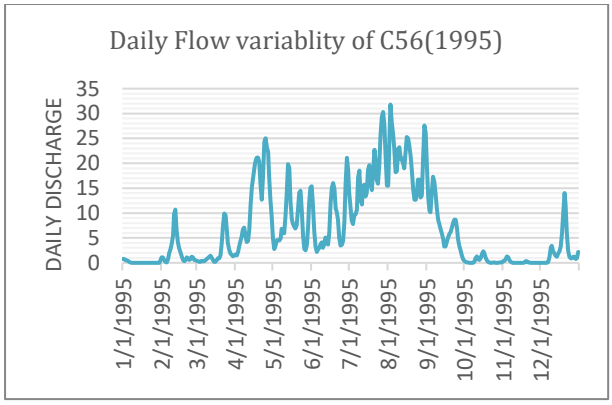
Daily Flow variablity of C56(1995)
DAILY DISCHARGE
35
30
25
20
15
10
5
0
1/1/1995
2/1/1995
3/1/1995
4/1/1995
5/1/1995
6/1/1995
7/1/1995
8/1/1995
9/1/1995
10/1/1995
11/1/1995
12/1/1995

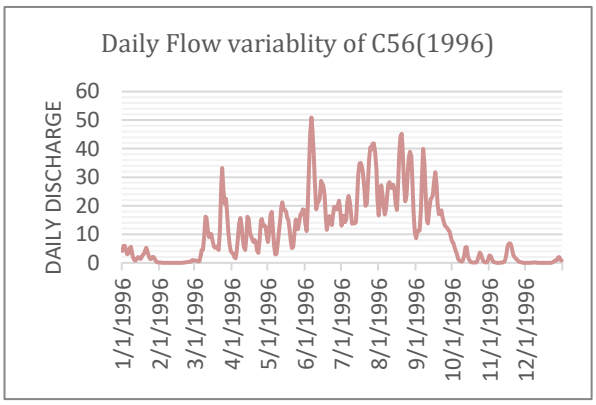
Daily Flow variablity of C56(1996)
DAILY DISCHARGE
60
50
40
30
20
10
0
1/1/1996
2/1/1996
3/1/1996
4/1/1996
5/1/1996
6/1/1996
7/1/1996
8/1/1996
9/1/1996
10/1/1996
11/1/1996
12/1/1996

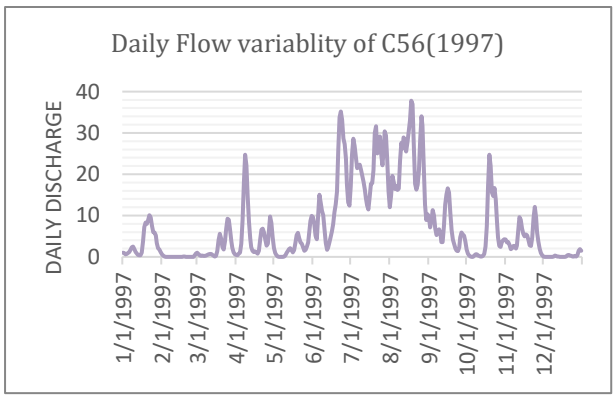
Daily Flow variablity of C56(1997)
DAILY DISCHARGE
40
30
20
10
0
1/1/1997
2/1/1997
3/1/1997
4/1/1997
5/1/1997
6/1/1997
7/1/1997
8/1/1997
9/1/1997
10/1/1997
11/1/1997
12/1/1997

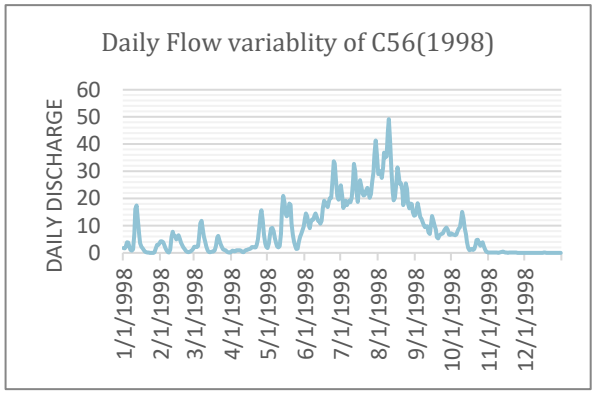
Daily Flow variablity of C56(1998)
DAILY DISCHARGE
60
50
40
30
20
10
0
1/1/1998
2/1/1998
3/1/1998
4/1/1998
5/1/1998
6/1/1998
7/1/1998
8/1/1998
9/1/1998
10/1/1998
11/1/1998
12/1/1998

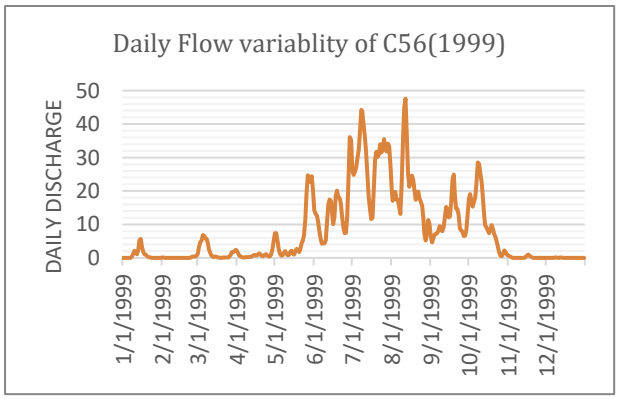
Daily Flow variablity of C56(1999)
DAILY DISCHARGE
50
40
30
20
10
0
1/1/1999
2/1/1999
3/1/1999
4/1/1999
5/1/1999
6/1/1999
7/1/1999
8/1/1999
9/1/1999
10/1/1999
11/1/1999
12/1/1999

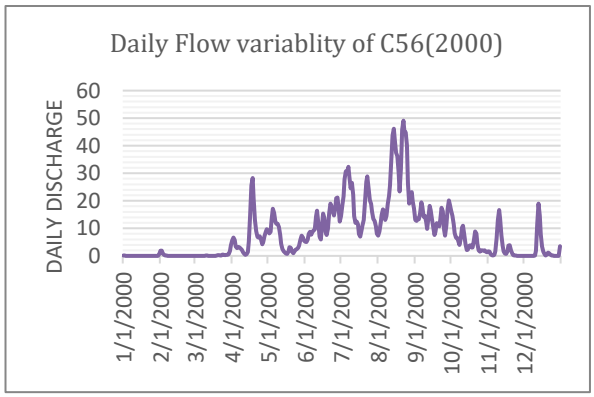
Daily Flow variablity of C56(2000)
DAILY DISCHARGE
60
50
40
30
20
10
0
1/1/2000
2/1/2000
3/1/2000
4/1/2000
5/1/2000
6/1/2000
7/1/2000
8/1/2000
9/1/2000
10/1/2000
11/1/2000
12/1/2000

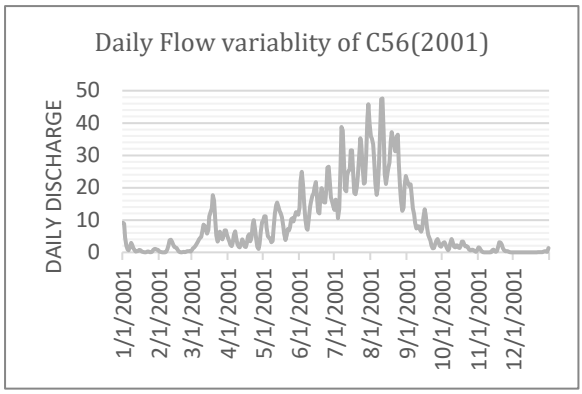
Daily Flow variablity of C56(2001)
DAILY DISCHARGE
0
10
20
30
40
50
1/1/2001
2/1/2001
3/1/2001
4/1/2001
5/1/2001
6/1/2001
7/1/2001
8/1/2001
9/1/2001
10/1/2001
11/1/2001
12/1/2001

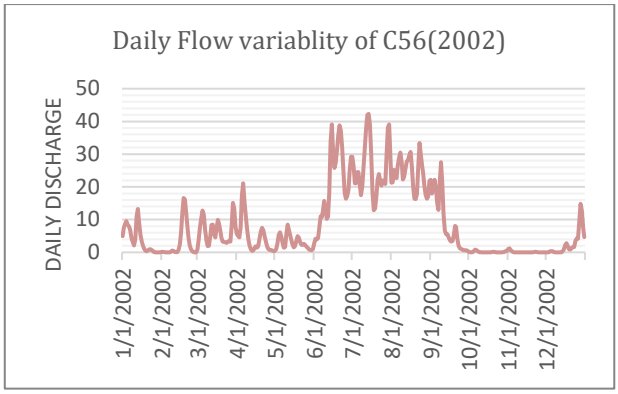
Daily Flow variablity of C56(2002)
DAILY DISCHARGE
0
10
20
30
40
50
1/1/2002
2/1/2002
3/1/2002
4/1/2002
5/1/2002
6/1/2002
7/1/2002
8/1/2002
9/1/2002
10/1/2002
11/1/2002
12/1/2002

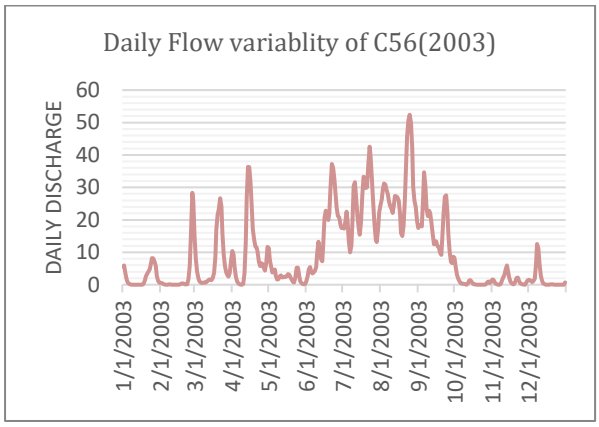
Daily Flow variablity of C56(2003)
DAILY DISCHARGE
0
10
20
30
40
50
60
1/1/2003
2/1/2003
3/1/2003
4/1/2003
5/1/2003
6/1/2003
7/1/2003
8/1/2003
9/1/2003
10/1/2003
11/1/2003
12/1/2003

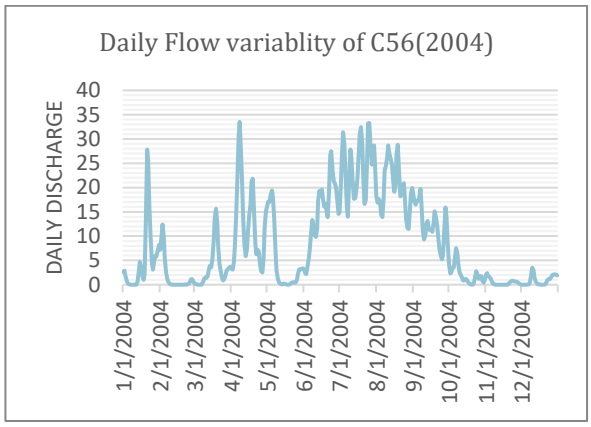
Daily Flow variablity of C56(2004)
DAILY DISCHARGE
0
5
10
15
20
25
30
35
40
1/1/2004
2/1/2004
3/1/2004
4/1/2004
5/1/2004
6/1/2004
7/1/2004
8/1/2004
9/1/2004
10/1/2004
11/1/2004
12/1/2004

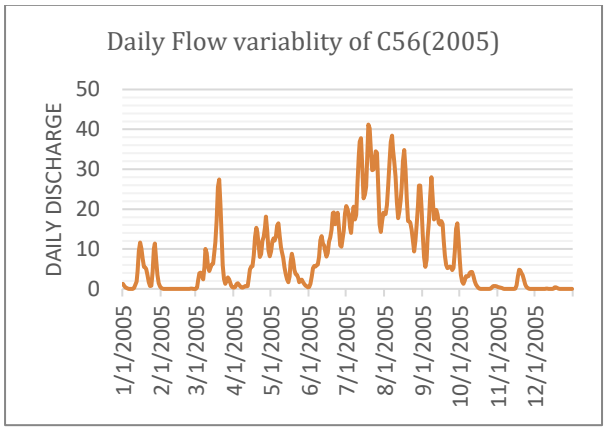
Daily Flow variablity of C56(2005)
DAILY DISCHARGE
0
10
20
30
40
50
1/1/2005
2/1/2005
3/1/2005
4/1/2005
5/1/2005
6/1/2005
7/1/2005
8/1/2005
9/1/2005
10/1/2005
11/1/2005
12/1/2005

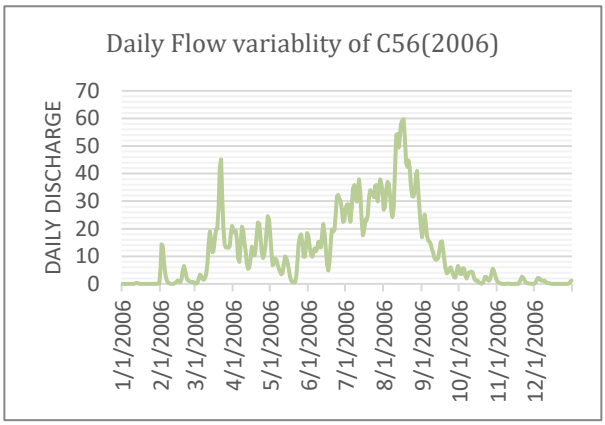
Daily Flow variablity of C56(2006)
DAILY DISCHARGE
0
10
20
30
40
50
60
70
1/1/2006
2/1/2006
3/1/2006
4/1/2006
5/1/2006
6/1/2006
7/1/2006
8/1/2006
9/1/2006
10/1/2006
11/1/2006
12/1/2006

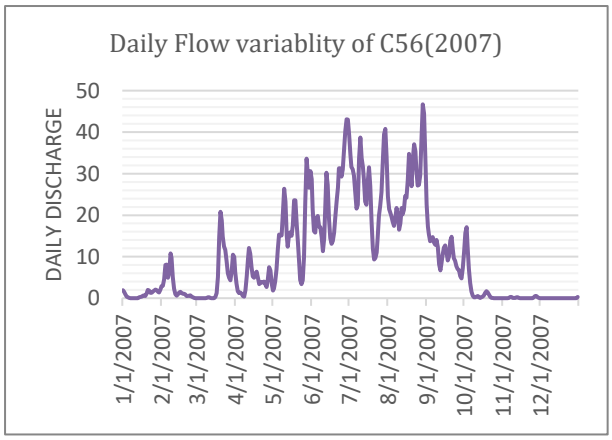
Daily Flow variablity of C56(2007)
DAILY DISCHARGE
0
10
20
30
40
50
1/1/2007
2/1/2007
3/1/2007
4/1/2007
5/1/2007
6/1/2007
7/1/2007
8/1/2007
9/1/2007
10/1/2007
11/1/2007
12/1/2007

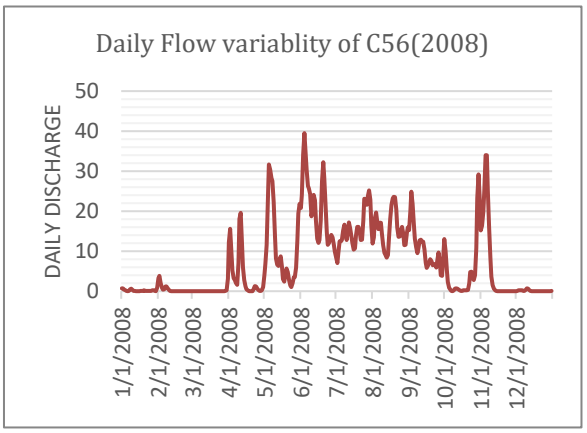
Daily Flow variablity of C56(2008)
DAILY DISCHARGE
0
10
20
30
40
50
1/1/2008
2/1/2008
3/1/2008
4/1/2008
5/1/2008
6/1/2008
7/1/2008
8/1/2008
9/1/2008
10/1/2008
11/1/2008
12/1/2008

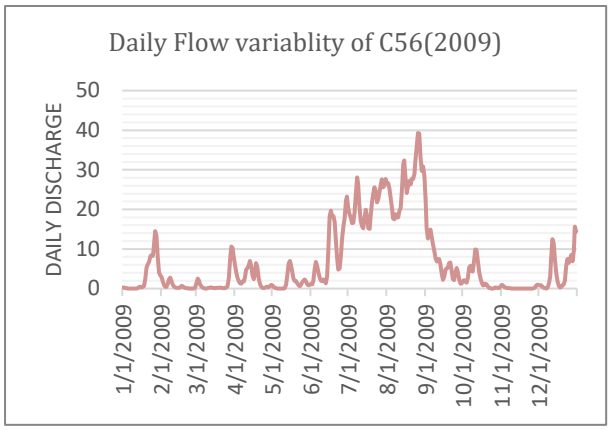
Daily Flow variablity of C56(2009)
DAILY DISCHARGE
0
10
20
30
40
50
1/1/2009
2/1/2009
3/1/2009
4/1/2009
5/1/2009
6/1/2009
7/1/2009
8/1/2009
9/1/2009
10/1/2009
11/1/2009
12/1/2009

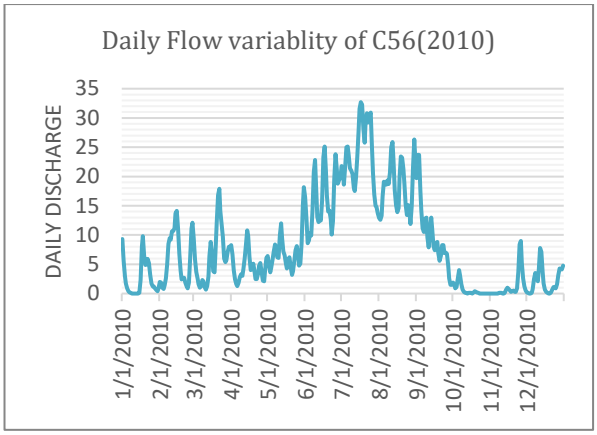
Daily Flow variablity of C56(2010)
DAILY DISCHARGE
0
5
10
15
20
25
30
35
1/1/2010
2/1/2010
3/1/2010
4/1/2010
5/1/2010
6/1/2010
7/1/2010
8/1/2010
9/1/2010
10/1/2010
11/1/2010
12/1/2010

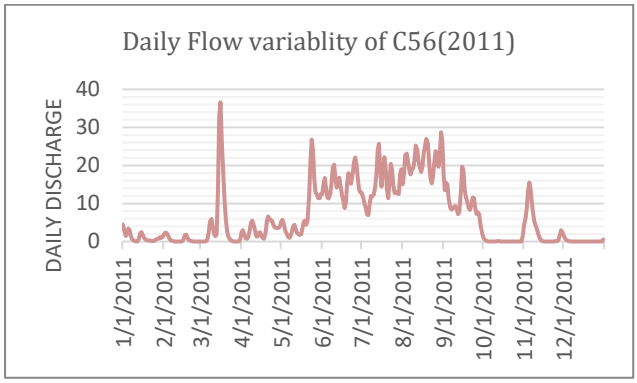
Daily Flow variablity of C56(2011)
DAILY DISCHARGE
0
10
20
30
40
1/1/2011
2/1/2011
3/1/2011
4/1/2011
5/1/2011
6/1/2011
7/1/2011
8/1/2011
9/1/2011
10/1/2011
11/1/2011
12/1/2011

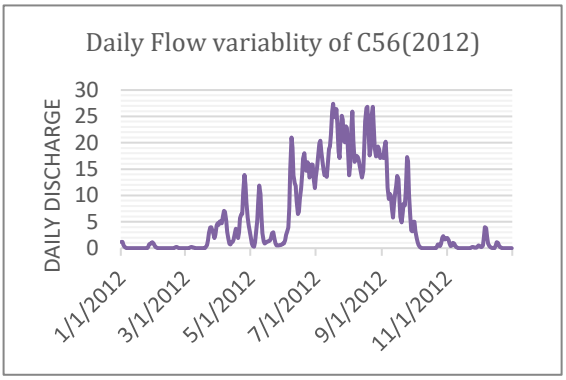
Daily Flow variablity of C56(2012)
DAILY DISCHARGE
0
5
10
15
20
25
30
1/1/2012
3/1/2012
5/1/2012
7/1/2012
9/1/2012
11/1/2012

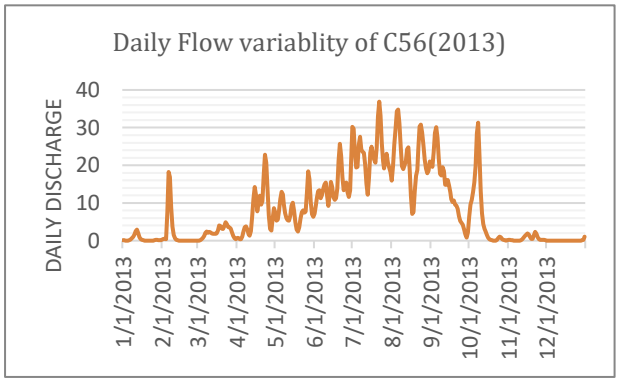
Daily Flow variablity of C56(2013)
DAILY DISCHARGE
0
10
20
30
40
1/1/2013
2/1/2013
3/1/2013
4/1/2013
5/1/2013
6/1/2013
7/1/2013
8/1/2013
9/1/2013
10/1/2013
11/1/2013
12/1/2013

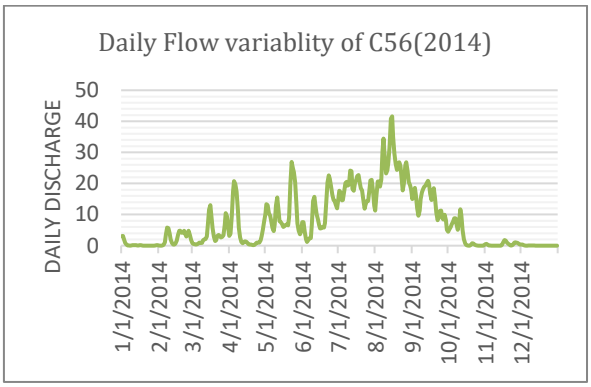
Daily Flow variablity of C56(2014)
DAILY DISCHARGE
0
10
20
30
40
50
1/1/2014
2/1/2014
3/1/2014
4/1/2014
5/1/2014
6/1/2014
7/1/2014
8/1/2014
9/1/2014
10/1/2014
11/1/2014
12/1/2014

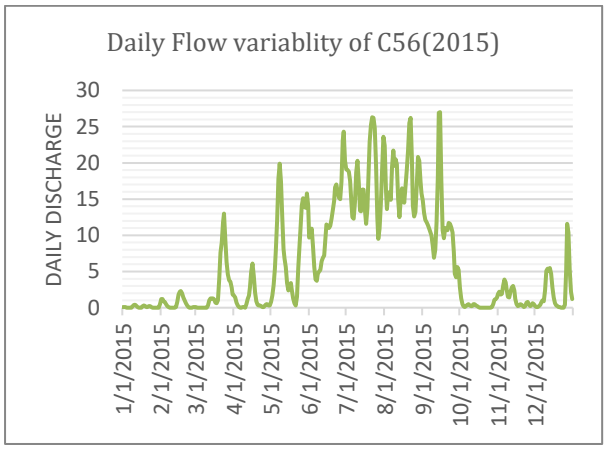
Daily Flow variablity of C56(2015)
DAILY DISCHARGE
0
5
10
15
20
25
30
1/1/2015
2/1/2015
3/1/2015
4/1/2015
5/1/2015
6/1/2015
7/1/2015
8/1/2015
9/1/2015
10/1/2015
11/1/2015
12/1/2015

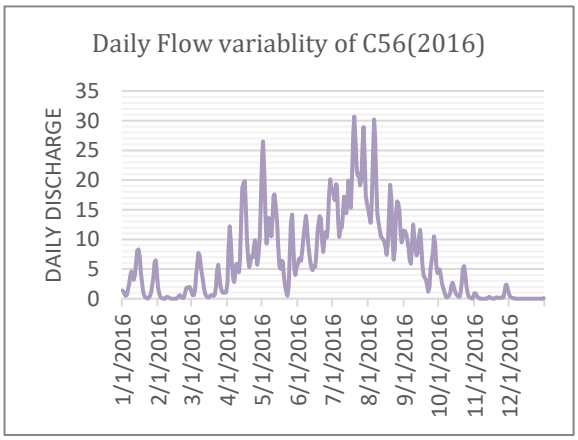
Daily Flow variablity of C56(2016)
DAILY DISCHARGE
0
5
10
15
20
25
30
35
1/1/2016
2/1/2016
3/1/2016
4/1/2016
5/1/2016
6/1/2016
7/1/2016
8/1/2016
9/1/2016
10/1/2016
11/1/2016
12/1/2016

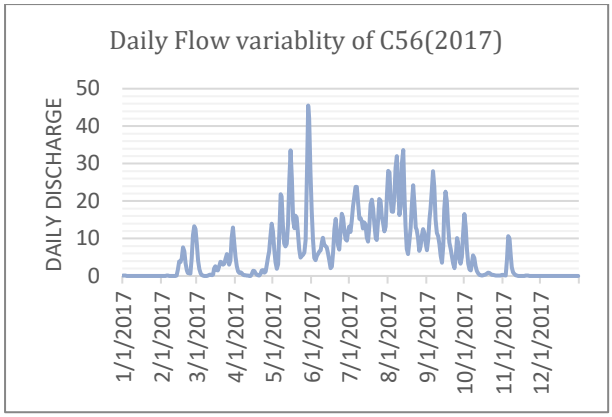
Daily Flow variablity of C56(2017)
DAILY DISCHARGE
50
40
30
20
10
0
1/1/2017
2/1/2017
3/1/2017
4/1/2017
5/1/2017
6/1/2017
7/1/2017
8/1/2017
9/1/2017
10/1/2017
11/1/2017
12/1/2017

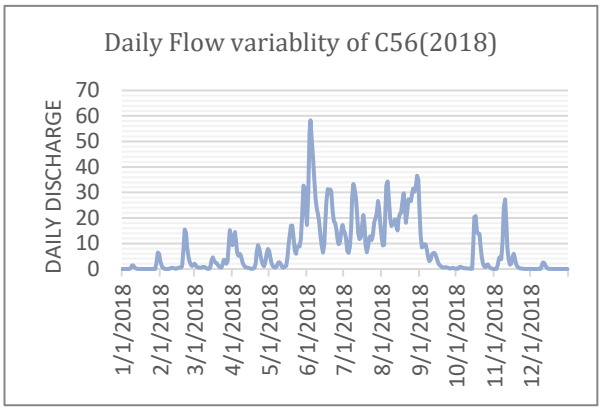
Daily Flow variablity of C56(2018)
DAILY DISCHARGE
70
60
50
40
30
20
10
0
1/1/2018
2/1/2018
3/1/2018
4/1/2018
5/1/2018
6/1/2018
7/1/2018
8/1/2018
9/1/2018
10/1/2018
11/1/2018
12/1/2018

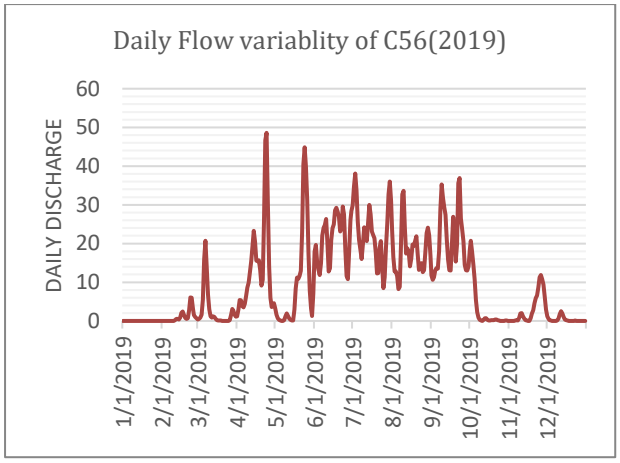
Daily Flow variablity of C56(2019)
DAILY DISCHARGE
60
50
40
30
20
10
0
1/1/2019
2/1/2019
3/1/2019
4/1/2019
5/1/2019
6/1/2019
7/1/2019
8/1/2019
9/1/2019
10/1/2019
11/1/2019
12/1/2019

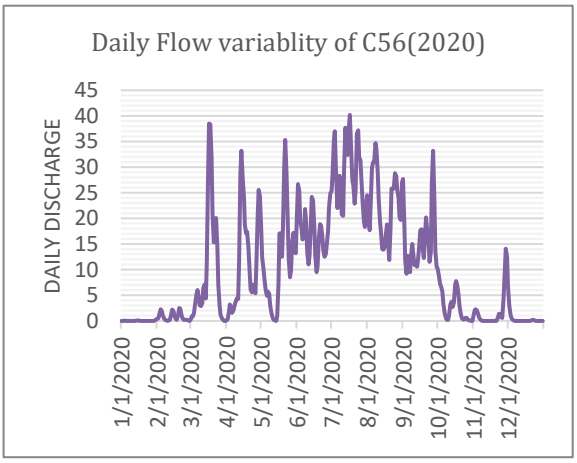
Daily Flow variablity of C56(2020)
DAILY DISCHARGE
45
40
35
30
25
20
15
10
5
0
1/1/2020
2/1/2020
3/1/2020
4/1/2020
5/1/2020
6/1/2020
7/1/2020
8/1/2020
9/1/2020
10/1/2020
11/1/2020
12/1/2020

**Appendix 3:** Drainage structure Opening size and type (on site measurement) along study area

| ID | Type of structure | Number of barrel | Width | Height | Diameter |
|---|---|---|---|---|---|
| C1 | PC | 2 | | | 1.06 |
| C2 | PC | 2 | | | 1.06 |
| C4 | PC | 1 | | | 0.9 |
| C5 | SC | 1 | 3 | 3 | |
| C6 | SPC | 1 | | | 1.22 |
| C7 | SPC | 1 | | | 1.22 |
| C9 | BR | 1 | 14 | 8 | |
| C10 | BC | 3 | 4 | 2.7 | |
| C11 | BR | 1 | 6 | 6 | |
| C12 | BC | 2 | 4 | 2 | |
| C13 | BR | 1 | 7 | 3 | |
| C14 | PC | 1 | | | 0.9 |
| C15 | BC | 2 | 4 | 2.5 | |
| C16 | BR | 1 | 10 | 7 | |
| C19 | BR | 1 | 12 | 8 | |
| C20 | PC | 1 | | | 1.06 |
| C21 | SPC | 2 | | | 1.22 |
| C22 | BR | 1 | 5 | 3 | |
| C23 | BR | 1 | 4.5 | 4 | |
| C24 | BR | 1 | 6 | 3 | |
| C25 | BR | 1 | 10 | 3 | |
| C28 | BR | 1 | 7 | 3 | |
| C30 | BR | 1 | 14 | 7 | |
| C33 | BR | 1 | 12 | 4.5 | |
| C37 | BC | 1 | 2 | 1.5 | |
| C39 | BR | 1 | 4 | 1.5 | |
| C40 | BR | 1 | 4 | 2 | |
| C41 | BR | 1 | 15 | 7.5 | |
| C42 | CBR | 1 | 20 | 8 | |
| C43 | BR | 1 | 4 | 2.2 | |
| C44 | BR | 1 | 4 | 4 | |
| C45 | BR | 1 | 6 | 4 | |
| C46 | BR | 1 | 9 | 5 | |
| C47 | BR | 1 | 4 | 4 | |
| C48 | BR | 1 | 10 | 7 | |
| C50 | BR | 1 | 4 | 3 | |
| C51 | SC | 1 | 4 | 2 | |
| C53 | BR | 1 | 4 | 3.4 | |
| C54 | SC | 1 | 2.5 | 2 | |
| C56 | BR | 1 | 27 | 6 | |

*PC: Reinforced pipe culvert* *BC: Box culvert*
*SPC: Corrugated steel pipe* *BR: Bridge*
*SC: Slab culvert* *CBR-Steel girder/Composite bridge*

**Appendix 4:** Sample Drainage structure pictures along Holeta to Ambo road

C10

C19

C21

C23

C25

C39

| | |
|---|---|
|  |  |
| C41 | C46 |
|  |  |
| C48 | C54 |

**Appendix 5:** Simulated run result of Estimated Peak Discharge on selected drainage structures

- C05 (Slab culvert with 3m span by 3m height)

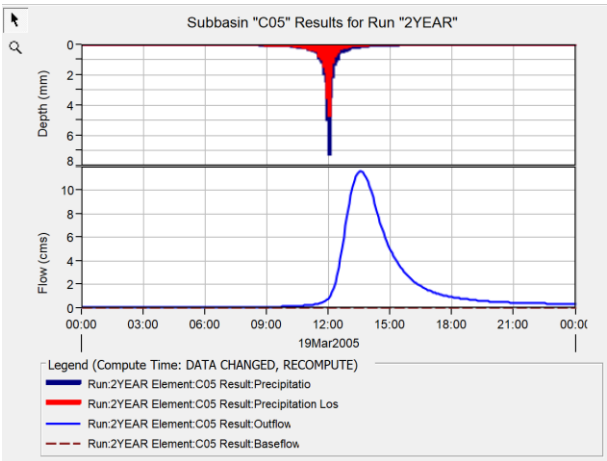


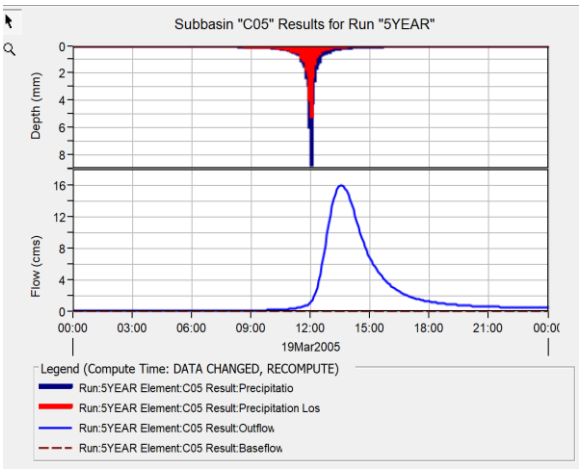


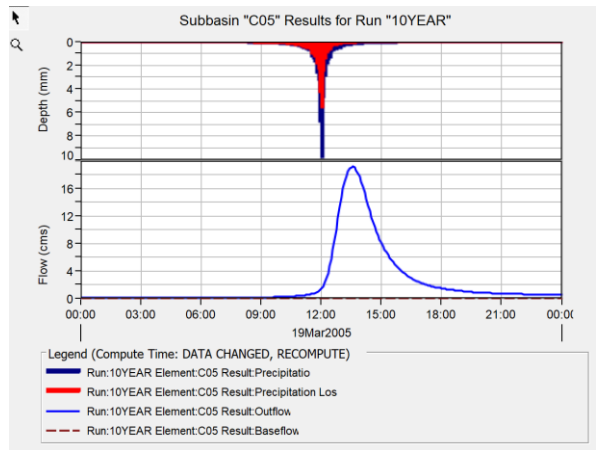


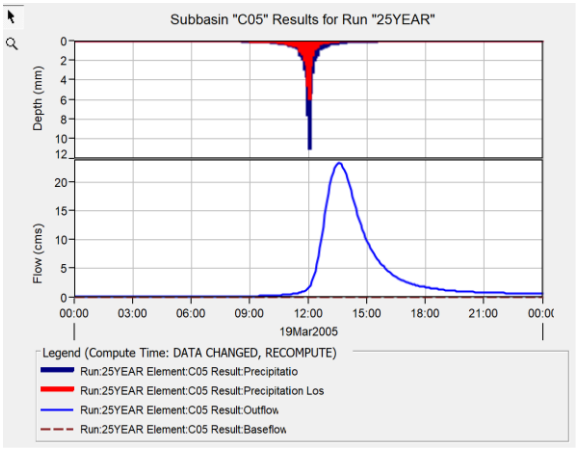


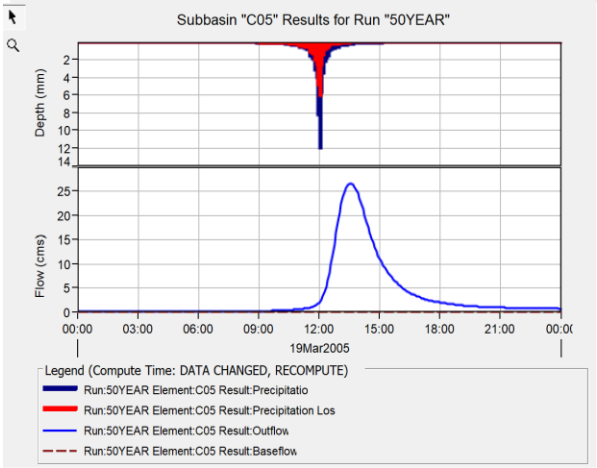


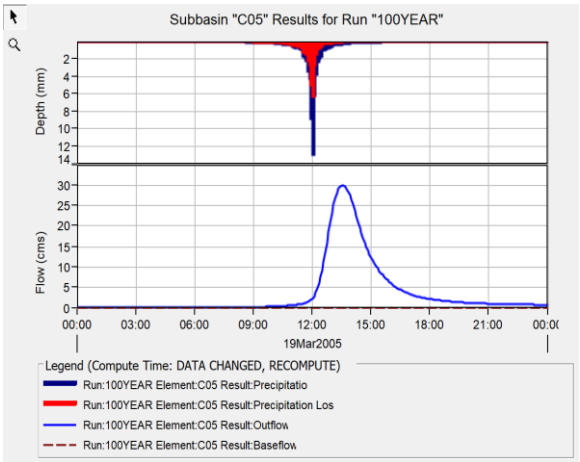

- C15 (Double Box culvert with 4m span by 2.5m height)

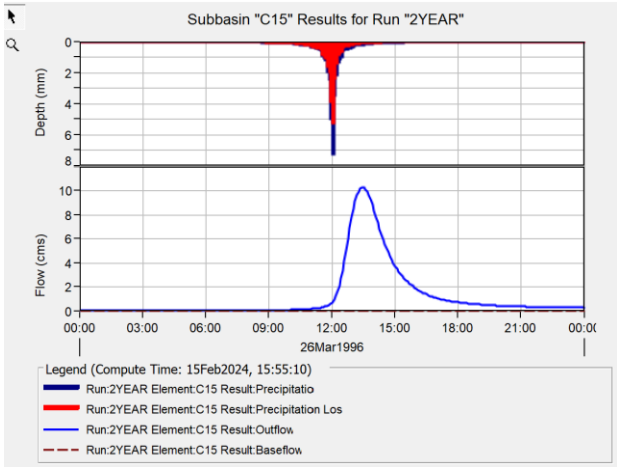


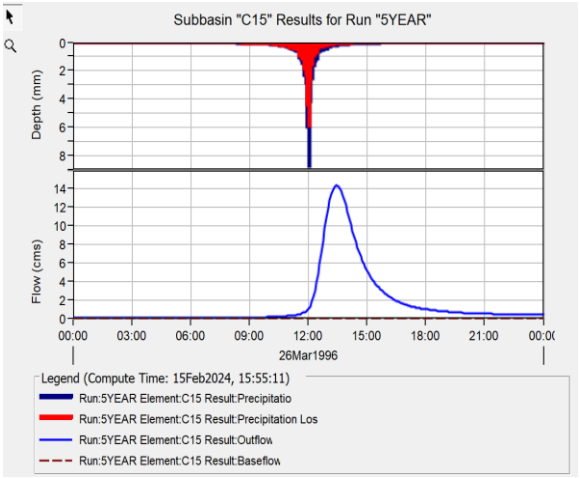


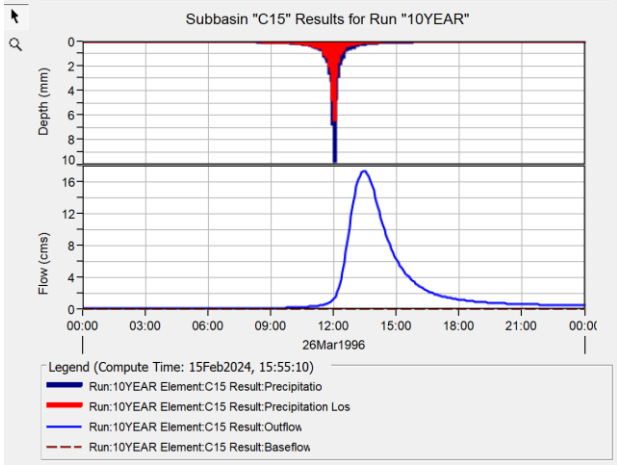


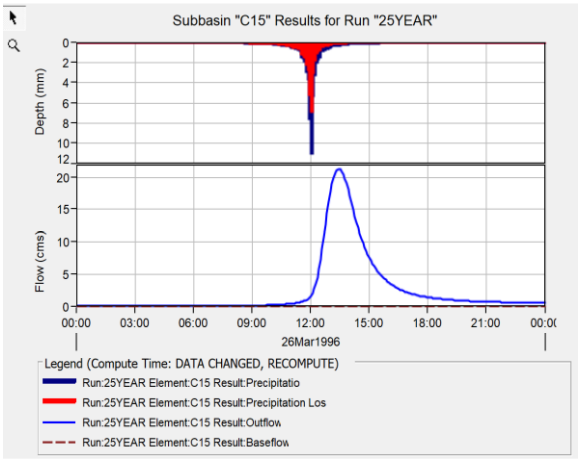


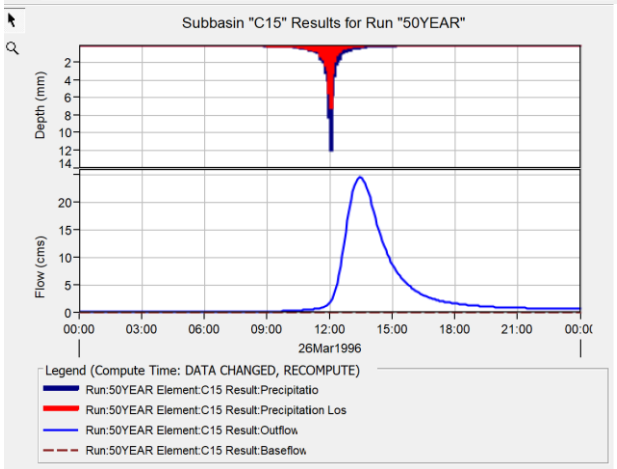


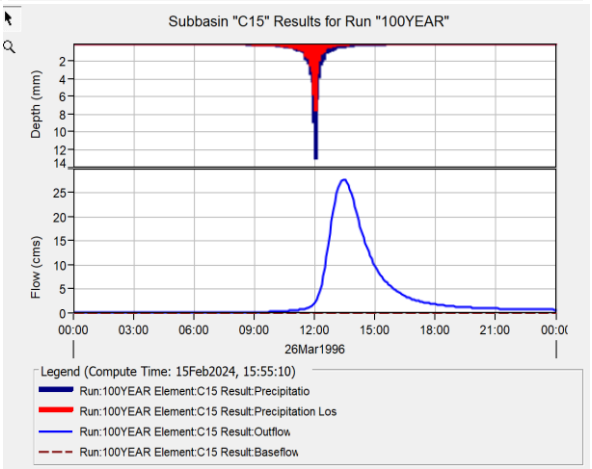

- C56 Reinforced Deck Girder Bridge (27m span with 6m height)

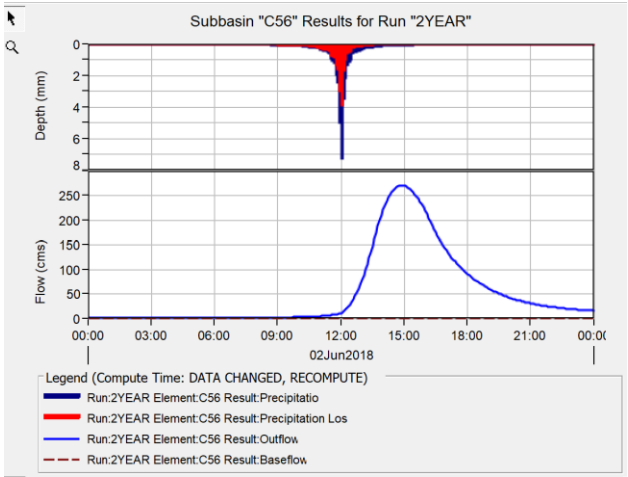


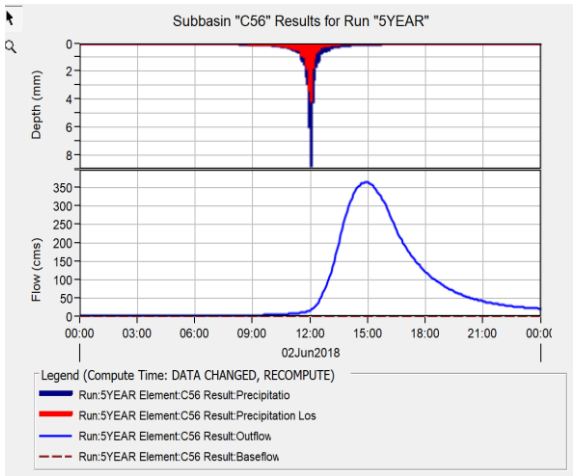


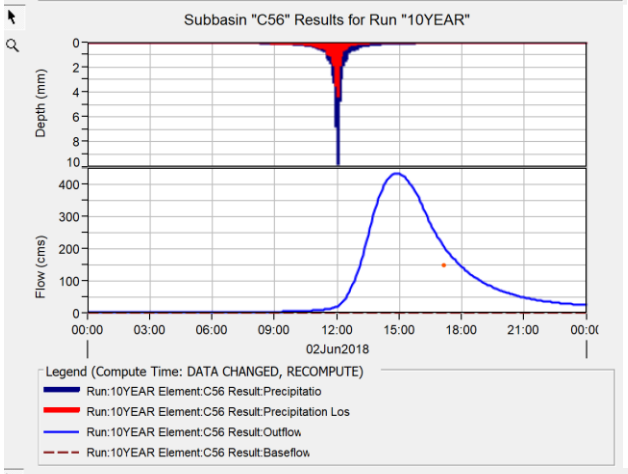


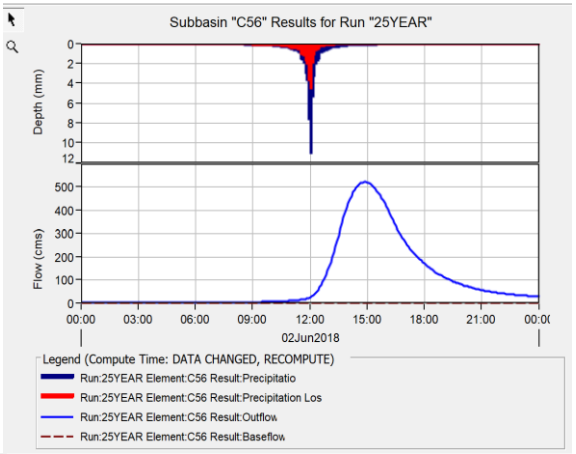


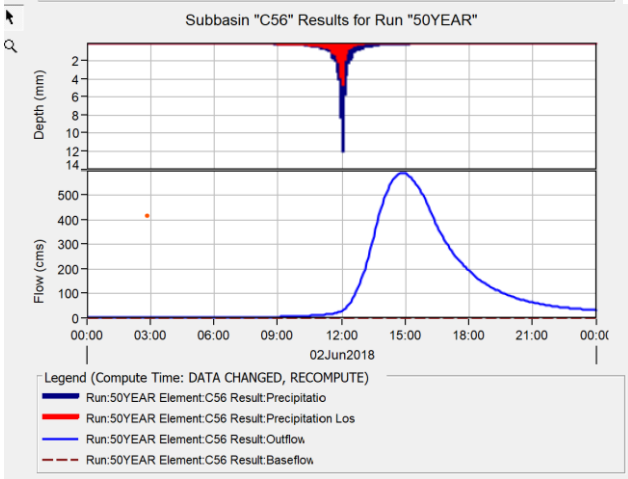


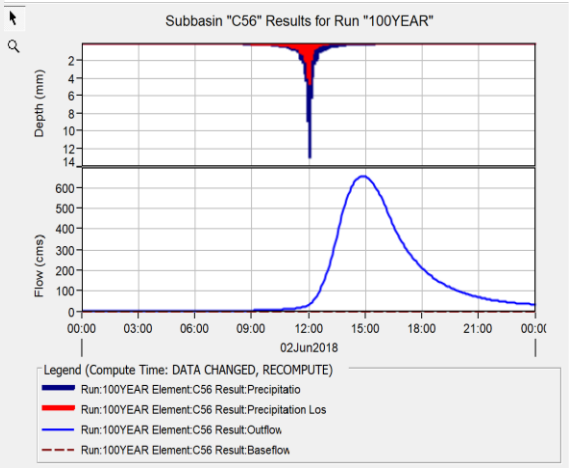

**Appendix 6:** The delineated watershed area of 56 drainage structure